

HOW TO COMBINE ENERGY MODELING TOOLS AND NET MODELING INTO ONE COMBINED TOOL



Figure 1: [Euroheat, 2016]

Authors

Kevin Skov Petersen & Michael Skyum



Title	How to combine energy modeling tools and net modeling into one combined tool
Semester theme	Master Thesis
Semester	4 th - Master's Program in Urban, Energy and Environmental Planning with Specialisation in Sustainable Energy Planning and Management
Faculty	The Technical Faculty of IT and Design
Department	Department of Planning
Project period	3 rd of February 2020 to 4 th of June 2020
ECTS	30
Supervisor	Anders N. Andersen
Authors	Kevin Skov Petersen & Michael Skyum
Pages, total	82
Appendix	3
Supplements	1

Abstract

This thesis investigates the limitations of some of the current energy modeling tools and how the individual strength potentially can be combined into one tool. This is done due to the energy plan projection towards 2030, which predicts an increase in renewable energy sources and some degree of electrification of the heating sector in other words sector coupling. The fluctuating nature of the renewable energy sources in combination with the electrification can put a lot of stress on the energy system. The future energy system therefore needs to be managed properly and the tools modeling the new energy system needs to be prepared for the challenges of the future energy system. This is why both different thermal energy storage concepts are investigated in order to supply the energy system with the needed flexibility as well as strength and limitations of selected energy modeling tools are analysed. This thesis want to demonstrate how the strength of the individual tools can be combined into one tool in order to be better suited for the future challenges of the energy system.

The challenges identified in the problem analysis are the challenges of seasonal storage, specifically pit thermal energy storage, and which of these challenges that needs to be corrected in order to operate ideally. Furthermore the limitations and strengths of TERMIS and energyPRO are identified and the potential to combine the strength of the two modeling tools into one is investigated in the analysis.

The research question is answered through the results from the two sub-questions. The first sub-question focuses on how to calculate the multiple temperature levels that are inside a thermal energy storage and what optimisations benefits, accessing these temperature will have when modeling an energy system. The other sub-question focuses on recreating the results from a chosen pipeline network in TERMIS in a Excel model. Thereby laying the foundation of how it can be combined with the modeling of a energy system.

As a result of the analysis it can be concluded that the development in the temperature levels can be calculated both for a isolated perspective and in a charging situation. By being able to implement this form of calculation in an energy modeling tool, would make it possible to further optimise the energy system as well as change the operation strategy, and give more flexibility when considering booster options. The results of the analysis further indicates that it is possible to recreate the results from TERMIS, although not all of the calculated results were equally close to the TERMIS values, it is still deemed to be possible if the correct way of calculating for example the heat loss and pressure gradient for the pipes is used. The final result demonstrates that it is possible to establish a energy system where the flows in the pipeline network dictates the production flow in the heat pump and to the thermal energy storage.

The thesis demonstrates the potential of combining the strengths of TERMIS and energyPRO into one tool, in order to be better suited for the challenges of the future energy system.

Preface

This thesis have been composed by a project group on the 4th semester of the master's program 'Sustainable Energy Planning and Management' at Aalborg University. The semester project is also the Master Thesis for this master program, which is the semester theme. The project period for the Master Thesis is from the 3rd of February to the 4th of June. The students would like to thank Laurits Tækkemand Nissen at Aalborg Forsyning and Aalborg Forsyning for making it possible to use the energy modeling tool TERMIS and helping in retrieving the data used for this thesis.

A special thanks should be directed to our supervisor Anders N. Andersen who have provided this thesis with critical information regarding the Excel models for both net modeling and temperature development. His invested time and advice has helped in the work done in this thesis.

For this thesis the Harvard method have been used when inserting the reference. The Harvard method states the author and year of publishing, every time a source have been cited and used. The projects bibliography holds all the sources that have been used or cited throughout the thesis, along with additional information for the sources.

The technical data used for the pipeline network model, have been extracted from TERMIS and have been the point of reference for the pipeline model made in Excel.

All calculations made regrading the pipeline network model and the temperature levels inside of the thermal energy storage in Excel will be attached as a ZIP file.

Nomenclature

Units

A	Area [m ²]
$A_{c,i}$	Cross-sectional area of a node [m ²]
$A_{s,i}$	Surface area of a node [m ²]
$A_{c,wall}$	Cross-sectional area of the tank wall [m ²]
$A_{s,wall}$	Surface area of the tank wall [m ²]
C_p	Heat capacity of water [J/kg*K]
D_{pipe}	Diameter of district heating pipe [m]
f	friction factor [-]
i	Node index. $i=N$ is the bottom node, $i=1$ is the top node
k	Tank fluid thermal conductivity [kW/m*K]
Δk	De-stratification conductivity [kW/m*K]
k_{wall}	Heat exchanger wall conductivity [kW/m*K]
\dot{m}	Mass flow [kg/s]
\dot{m}_{1in}	Mass flow rate entering fluid one [kg/s]
\dot{m}_{1out}	Mass flow rate exiting fluid one [kg/s]
\dot{m}_{down}	Fluid flow rate down the tank [kg/s]
\dot{m}_{up}	Fluid flow rate up the tank [kg/s]
M_i	Mass of node i [kg]
N	Number of nodes [-]
P	pressure [kPa]
Q_{HC}	Heat consumption [W]
Re	Reynolds number [-]
T_{1in}	Temperature of entering fluid one [°C]
T_{i-1}	Temperature of the node above node i [°C]
T_i	Temperature for the each node i [°C]
T_{i+1}	Temperature of the node below node i [°C]
T_{env}	Temperature of environment [°C]
T_{Return}	Return temperature to the district heating [°C]
T_{supply}	Supply temperature from the district heating [°C]
U_{tank}	Overall tank loss coefficient per unit area [kW/m ² *K]
U_i	Heat loss coefficient per unit area of node i [kW/m ² *K]
v_{avg}	Average velocity [m/s]
v_{flow}	Flow velocity [m/s]
$\Delta x_{i-1 \rightarrow i}$	Center-to-center distance between node i and the node above it [m]
$\Delta x_{i+1 \rightarrow i}$	Center-to-center distance between node i and the node below it [m]
Δz	Change in elevation [m]
ϵ	Roughness [-]
μ	Dynamic viscosity [kg/m*s]
ρ_{water}	Density of water [kg/m ³]
π	Pi [-]

Contents

Abstract	iii
Chapter 1 Introduction	1
Chapter 2 Problem analysis	3
2.1 The 2030 goals for the district heating sector	3
2.2 Thermal energy storage concepts	8
2.3 Energy Modeling tools	19
Chapter 3 Research question	23
3.1 Delimitations	24
3.2 Research Design	25
Chapter 4 Methodological framework	27
4.1 Case study	27
4.2 Data collection	28
Chapter 5 Theories	29
5.1 Temperature levels	29
5.2 District heating network	35
Chapter 6 Analysis	43
6.1 Temperature levels inside a thermal energy storage	43
6.2 Pipeline network	48
6.3 A combination of the Excel models	59
Chapter 7 Discussion	63
Chapter 8 Conclusion	69
Chapter 9 Future research	71
Bibliography	73
Appendix A Appendix	77
A.1 Appendix A.1	77
A.2 Appendix A.2	78
A.3 Appendix A.3	80

Introduction

1

The increased capacity of renewable energy sources such as wind and solar that comes with the energy plan projection towards 2030, poses as a challenge to the existing and future energy system. The fluctuating nature of these energy sources demands an energy system that can manage the intermittency in the energy production. Central heating power plants are compelled to change their production primarily from coal to another energy source such as heat pumps, which are more in line with the energy plan projection. This could mean a higher degree of sector coupling between the electricity sector and heating sector. With some parts of the heating sector getting electrified, the energy system will be much more complex. This is due to the electrified part of the heating production in most cases will be dependent on the electricity spot market prices. This dependency will more likely than not demand that heat must be produced when the electricity price is low even though the heat demand is satisfied. In other words, flexibility in energy production is needed.

One way to ensure flexibility in the energy production is by implementing energy storage. With this development of the energy system, the existing energy modeling tools needs to be developed as well. With the complex nature of the future energy system, switching between energy modeling tools as one performs different simulations could prove to be a disadvantages, since valuable data or information could get lost when switching between them. This thesis will describe the equation behind the net modeling of TERMIS as well as the equation of how multiple temperature levels can be calculated in a thermal energy storage, and its advantages compared to only using a top and bottom temperature. The purpose is to demonstrate how a energy modeling tool could benefit from being able to perform energy system analysis and have more optimisation possibilities with a better utilisation of the thermal energy storage in combination with net modeling.

Problem analysis 2

2.1 The 2030 goals for the district heating sector

In 2014 the head of state and government decided on a set of rules and regulations for the politics regarding climate and energy towards 2030. It was agreed that within EU, the CO₂-emissions should be lowered by 40% by 2030 compared to the CO₂-emission levels of 1990. Within this goal another goal was set, the goal was that the countries in EU should be covered with 27% renewable energy. The Danish government set an even more ambitious goal for Denmark, which was that the energy demand should be covered by 55% renewable energy by 2030. This agreement was set in 2018. [Klima, n.d.]

As part of the agreement made by the Danish politicians in 2018, an energy agreement was made. The agreement enacts that the electricity must be covered entirely by renewable energy in 2030, mainly by expanding the amount of offshore wind turbines [Klima, n.d.]. The agreement contains that the prices on electricity for the consumers will get cheaper towards 2021 and that there should be invested more in effective use of energy as well as investing more in energy technologies [Klima, n.d.]. Regarding the heat production and usage, the energy agreement enacts that the district heating companies are more free to choose which renewable technology to use for their energy production. The energy agreement states that there is a need for change in the heat production area. Renewable technologies will be more promoted in order to ensure more flexibility in the heat production area. To ensure this, the mandatory connection to the district heating network in some areas is removed, this empowers the consumers in choosing where they want to get their heat from. The most interesting point in the energy agreement is that the district heating plants is now free to choose how they want to produce heat and with which technology. This should help the district heating companies to choose a more renewable and sustainable technology for the future, as of right now the obvious choice seems to be technologies like biomass, big heat pumps or geothermal energy [Klima, n.d.].

The Danish government has also set a goal of reducing the CO₂-emission by 70% by 2030 compared to the 1990-levels as one of the climate goals for Denmark. One of the main focus points of reaching that goal is the heating sector. By converting the district heating sector to become 100% renewable by 2030 will aid the process of reaching a 44% CO₂ reduction, which will be more than half of the way towards the energy goal [Fjernvarme, 2020].

2.1.1 Energy plan projections towards 2030

As mentioned in the paragraph above, the trajectory towards 2030 predict a near complete transition of the district heating and power supply to renewable energy sources [Energistyrelsen, 2019]. This is contingent on the central and decentralised coal and gas fired combined heat and power plants (CHP) phases out [Energistyrelsen, 2019]. Due to the phasing out of these units the consumption of natural gas, coal and oil is expected to reduce by 86% in 2030 compared to 2017 values [Energistyrelsen, 2019]. The phasing out of these central and decentralised production units can be seen on figure 2.1.

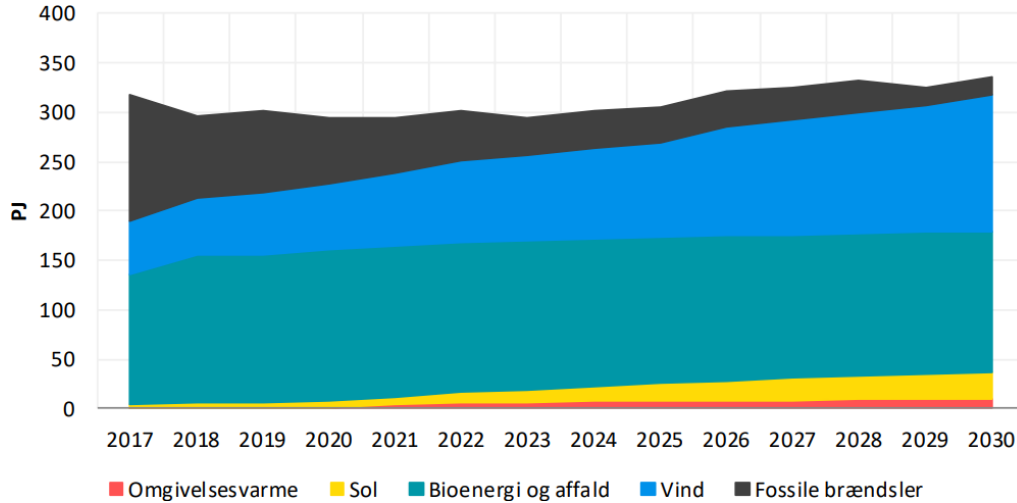


Figure 2.1: The development of district heating and electricity production towards 2030 [Energistyrelsen, 2019].

Coal and gas consumption

The energy projection towards 2030 predict a reduction to 17 PJ in the consumption of fossil fuels for district heating and electricity production. According to 2017 values, this corresponds to a reduction of 85% [Energistyrelsen, 2019]. In this context the coal and natural gas consumption is reduced by 92% and 80%, respectively, and the consumption from 2030 will account for 7 PJ and 8 PJ, respectively [Energistyrelsen, 2019]. This reduction is a result from the anticipated cease of operation on coal by the central coal fired power plants [Energistyrelsen, 2019]. The reduction during the projection period can be seen on figure 2.2.

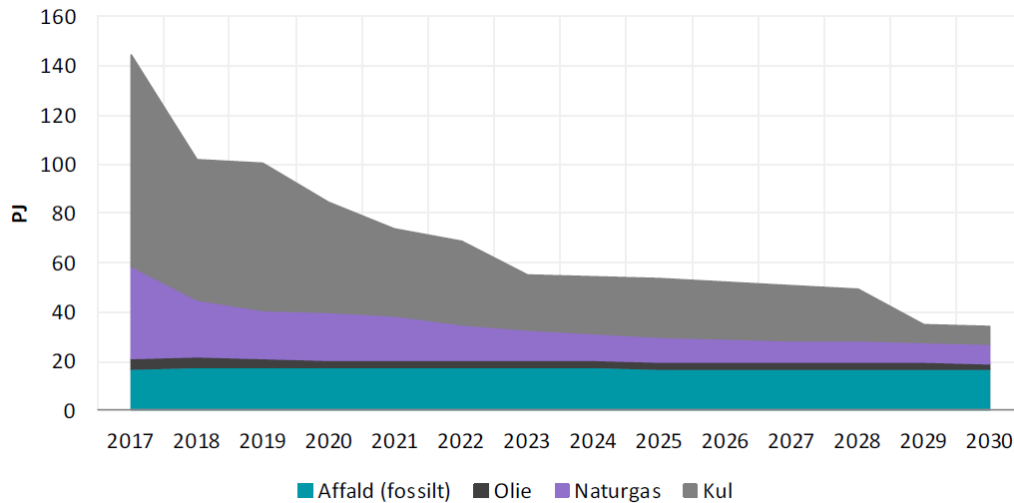


Figure 2.2: The Electricity and district heating sectors consumption of fossil fuels [Energistyrelsen, 2019].

The selected central coal fired power plants ceases their operation on coal by the latest of 2030 and many of them before that. This is mainly the reason behind the big reduction of coal consumption. Figure 2.3 illustrates the cease of operation of the selected coal fired power plants in the projection period [Energistyrelsen, 2019]. There are different parameters coming into play when the central coal fired power plant decide when they cease their operation. For example 'Avedøreværket' and 'Studstrupværket' ceases their operation based on coal in 2023 [Energistyrelsen, 2019]. The reason for this is due to the expected increase of CO₂-quota prices which would no longer make it feasible [Energistyrelsen, 2019].

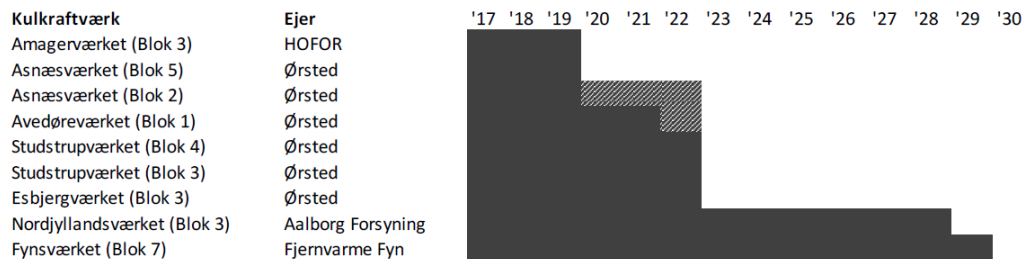


Figure 2.3: The coal fired power plants cease of operation. The grey area means that the power plant operation will be limited in the given time period [Energistyrelsen, 2019].

The availability of utilising condensing mode in central heating power plants (CHP) is reduced due to the reduction in consumption of coal and natural gas [Energistyrelsen, 2019]. This have a direct effect on the CHP share of electricity production, which reduces from 44% in 2017 to 17% in 2030 [Energistyrelsen, 2019]. Meaning a reduced percentage share of the produced electricity will come from CHP plants, this is due to a change of operation strategy by the decentralised CHP plants [Energistyrelsen, 2019]. The decentralised CHP plants will implement a higher capacity of electric boilers as well as heat pumps [Energistyrelsen, 2019]. The change in electricity production during the projection period can be seen on figure 2.4.

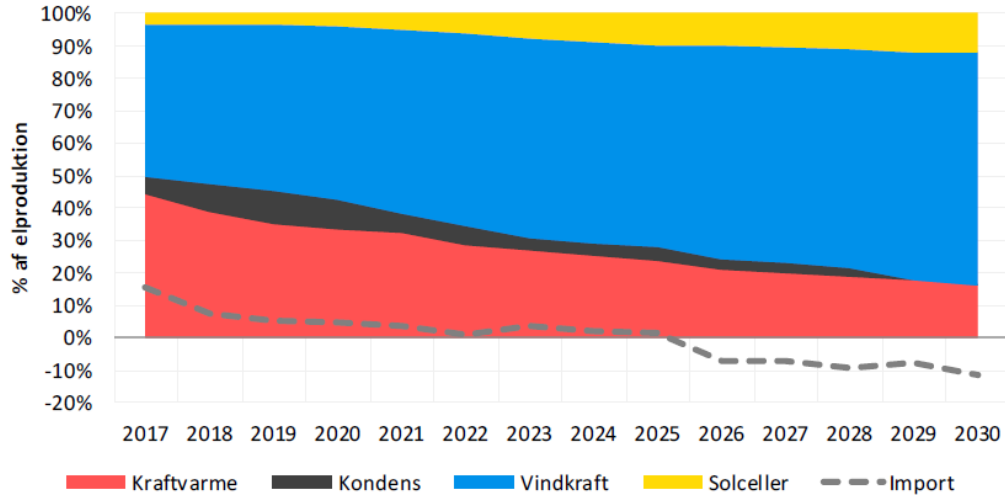


Figure 2.4: The electricity production divided among the different types of production [Energistyrelsen, 2019].

Renewable energy share in electricity production

The renewable energy share of the electricity consumption is expected to exceed 100% in 2028 and by 2030 reach 109% [Energistyrelsen, 2019]. This development is however contingent on substitution of older wind turbines, expansion on commercial solar power facilities as well as the establishment of new offshore wind turbines and substitution of older wind turbines [Energistyrelsen, 2019].

Figure 2.5 illustrates the allocation of the different renewable energy sources and their percentage share of the electricity consumption. When the domestic electricity production exceeds the domestic electricity consumption, as expected from 2026, Denmark will increasingly be a net exporter of electricity [Energistyrelsen, 2019].

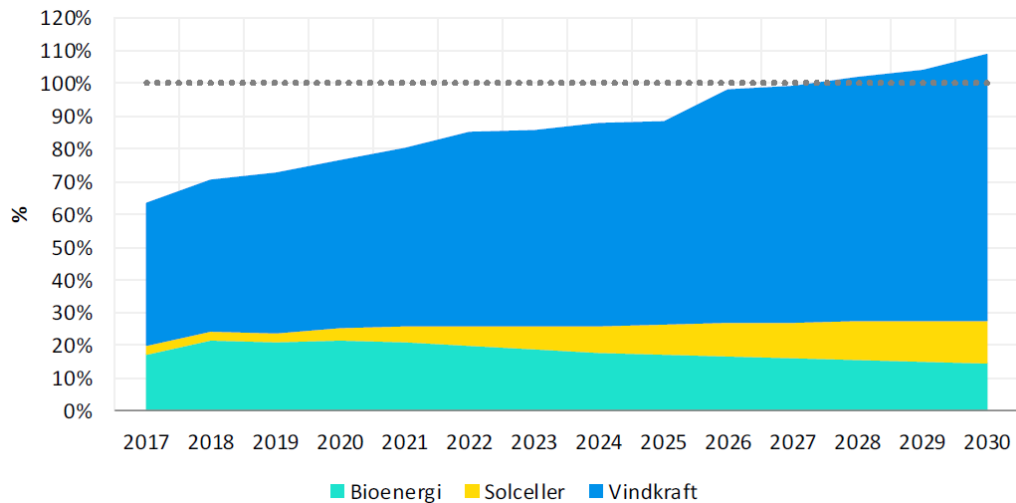


Figure 2.5: Renewable energy share of the electricity consumption [Energistyrelsen, 2019].

Renewable energy share in the district heating system

The energy plan projection towards 2030 in regards to the district heating system is in the first couple of years dominated by the emphasis on biomass utilisation. From 2017 to 2020

the biomass consumption steadily increases with 10% on an annual basis [Energistyrelsen, 2019]. Thus suppressing the consumption of natural gas and coal [Energistyrelsen, 2019]. This results in an annual decrease in natural gas consumption by 10% during the whole projection period [Energistyrelsen, 2019]. The consumption of coal have an annual reduction towards 2020 by 30%, this reduction then reduces to an annually reduction of 10% for the remainder of the projection period [Energistyrelsen, 2019]. This development can be seen on figure 2.6

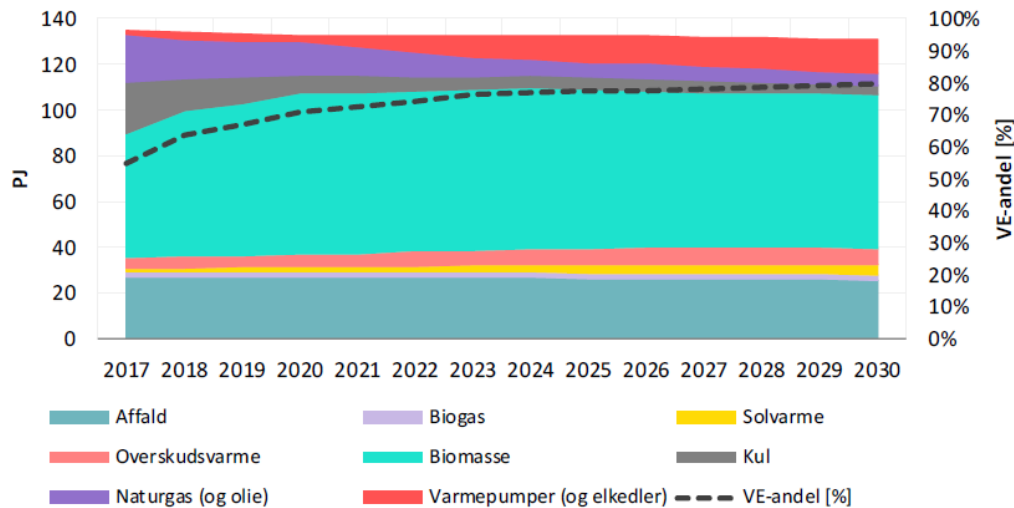


Figure 2.6: The district heating production allocated by different energy sources [Energistyrelsen, 2019].

It is important to note that after the government have chosen to phase out the PSO-tariff as well as adjust the electric heating tax. This results in an annual increase of 15% in district heating production from electric boilers and heat pumps [Energistyrelsen, 2019]. By the end of the energy plan projection period by 2030, electric boilers and heat pumps will supply up to 10% of the total district heating production [Energistyrelsen, 2019]. This development can be seen on figure 2.6. Furthermore a development of industrial excess heat, solar heat can be seen, whereas waste and biogas are utilised at a constant level. Industrial excess heat experiences an increase of 3% and solar heat increases by 10% on an annual basis [Energistyrelsen, 2019].

Due to the described developments it is expected that the share of renewable energy in the district heating sector will increase from 55% in 2017 to 76% in 2023, and by the end of the projection period in 2030 reach 80% [Energistyrelsen, 2019]. One of the main reasons for the share of renewable energy not reaching a higher level is due to the utilisation of waste incineration as well as non biological degradable materials [Energistyrelsen, 2019].

The energy plan projection towards 2030 predicts an increased capacity of fluctuating electricity production such as photovoltaic systems and wind turbines as well as sector coupling between the electricity sector and heating sector. In order to handle this increase in fluctuating energy production, storage concepts that enables flexibility and sector coupling in the energy system must be one of the leading priorities. The focus for determining a storage solution will in this thesis be in the context of a seasonal storage. The reason for this focus is due to the seasonal storage enables the two previously mentioned

parameters, flexibility and sector coupling.

2.2 Thermal energy storage concepts

With the projected increase in renewable energy sources, a better and more optimised control of the energy system is needed. One of the biggest challenges when working with fluctuating energy sources is its intermittency in production. The fluctuation in the energy production varies throughout the day, a month, a year as well as on a seasonal basis. The uncertainty of not knowing the production pattern for the next day or even for the next hours poses as a challenge, and the future energy system needs to be able to handle these kinds of challenges. If the development of the energy system follows the energy plan projection made by Energistyrelsen [2019], different energy sectors will experience an increase of renewable energy and thereby experience an increased intermittency in energy production. Due to the higher capacity of fluctuating energy sources, periods with a surplus of energy and periods with insufficient energy will be more common. The mismatch between energy demand and energy supply in on and off peak hours requires a more intelligent and flexible energy system in order to handle these challenges.

Possibly one of the biggest mismatch between the production of energy from renewable sources and the energy demand is the availability of solar heat in the summer period and the high energy demand of space heating in the winter period [Abdulrahman Dahash, 2019].

In order to handle the intermittency of renewable energy sources like for example solar, storage solution would be an ideal technology. In this context, thermal energy storage (TES) are one of the premiere alternatives in order to handle the intermittency as well as the challenge of solar availability in the summer period when the heat demand is low [Abdulrahman Dahash, 2019]. The seasonal TES allows for storing of the thermal energy produced by fluctuating energy sources, for example solar collectors. The excess production of heat in the summer period, can be stored independently of the heat demand [Christoph Bott, 2019]. The TES thereby makes it possible to 'convert' temporary energy in the form of fluctuating energy into permanent energy that can be accessed at all times and on-demand [Christoph Bott, 2019]. This means in hours with peak load it is possible to shave off the peak load with the TES instead of using other cost-intensive energy production units to cover the peak load [Christoph Bott, 2019]. TES can be split up into two different concepts, where the first concept is short term storage and the second being long term storage or seasonal storage. The function of the short term storage is to utilise the storage as much as possible, meaning having as many charge and discharge cycles as possible on a yearly basis, whereas the long term storage or seasonal storage only will have a couple of charge and discharge cycles [Arcon-Sunmark, 2019]. As mentioned in the beginning of this paragraph it would be beneficial to combine solar power with TES, as these two technologies compliments each other, since seasonal thermal energy storage solutions (STES) ensures that the abundance of solar heat in the summer period can be stored for space heating for the winter period for example. In a district heating context this symbiosis ensures an efficient utilisation of renewable energy [Abdulrahman Dahash, 2019]. There are however other storage technologies alternatives to STES such as hydro storage, gas storage and power to heat but it is important to note that

these storage technologies are challenged on an economical level when compared to STES in a district heating context [Abdulrahman Dahash, 2019]. Power to heat has a more obvious symbiosis in district heating applications due to the interconnection between the heating network and power grid [Abdulrahman Dahash, 2019]. One example is that it exploits the hours with surplus electricity production to produce heat with high share of renewable energy, thereby empowering both the heating network and power grid with flexibility [Abdulrahman Dahash, 2019]. Power to heat would seem as an obvious choice in the future energy system where one of the main challenges seems to be sector coupling and flexibility. Just as TES plays a vital part of exploiting the abundance of solar heat in the summer, TES will most likely be a main beneficiary in the context of power to heat. Furthermore TES provides the energy system with support and resilience [Abdulrahman Dahash, 2019]. Resilience, flexibility and sector coupling are all important keywords that need to be implemented in the future energy system in order to achieve a smarter and more optimised energy system.

In order to visualise the effectiveness of a given energy system and the utilisation of for example STES, an example with solar heating will be used. The effectiveness of pairing solar heat with a STES can be seen on figure 2.7. The discrepancy between the abundance of solar heat in the summer period and the space heat demand in winter is especially evident as well as the potential to "move" the solar heat from summer to winter. It is however important to note that STES is not without its challenges. The challenges originate from the technical aspect of the technology. A couple of the challenges are for example: geological conditions in the terms of the ground water and bedrock, the volume required for the seasonal storage, 'handling of rainwater' dependent on the storage type, leakage [Abdulrahman Dahash, 2019], [Arcon-Sunmark, 2019].

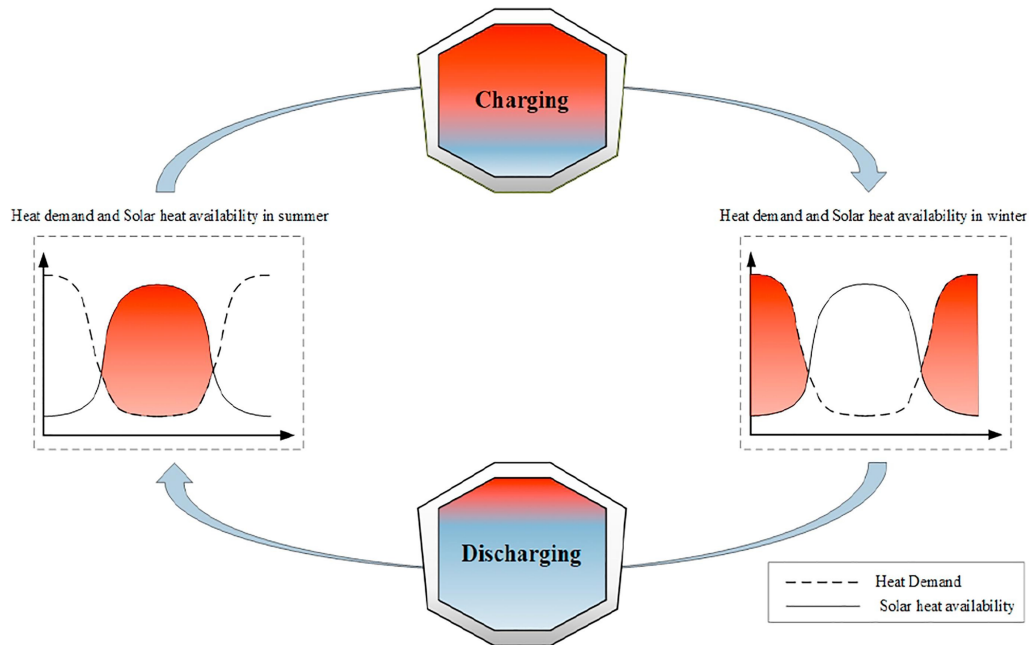


Figure 2.7: Illustration of an annual load duration curve in a solar powered district heating system as well as the cycle of the seasonal thermal energy storage [Abdulrahman Dahash, 2019].

Due to the relatively big volume needed for a STES it is often either fully or partially buried under ground [Abdulrahman Dahash, 2019]. There are multiple storage concepts that uses this form of approach, these storage concepts are for example: borehole thermal energy storage (BTES), aquifer thermal energy storage (ATES), tank thermal energy storage (TTES) and pit thermal energy storage (PTES) [Abdulrahman Dahash, 2019]. The advantage as well as the disadvantage of these four storage technologies is described in table 2.1 [Abdulrahman Dahash, 2019]. Both the advantage and the disadvantage is described from a isolated perspective. This means that the connected energy system as well as the operation parameters are not taken into consideration [Abdulrahman Dahash, 2019]. Table 2.2 [Abdulrahman Dahash, 2019], shows the energy density and the storage medium for the four storage technologies. Table 2.2 shows that the storage medium for PTES is 'gravel-water' and therefore have a lower energy density than TTES. This is however not true for all cases of PTES, in Denmark the storage medium are usually PH treated water and not 'gravel-water' as stated in the table [Arcon-Sunmark, 2019]. Therefore the PTES are assumed to have the same energy density value as the TTES.

Storage technology	Pros	Cons
ATES	Medium thermal capacity. Very low construction costs.	No thermal insulation possible. Relatively high thermal losses. Operation characteristics. Very limited choice of location.
BTES	Easily extendable. Low construction costs.	Low thermal capacity No thermal insulation are possible at side and bottom. Maintenance repair difficult/not possible. Operation characteristics. Limited choice of location.
PTES	Medium (gravel - water) to high (water) thermal capacity. Reasonable construction costs. Operation characteristics. Nearly unlimited store dimensions.	Limited freedom of design (slope angle). Complex and costly cover (in case of water). Maintenance repair difficult/not possible.
TTES	High thermal capacity (water). Freedom of design (geometry). Good operation characteristics. Maintenance/repair.	Primary energy demand. High construction costs. Limited size ($<100,000 \text{ m}^3$).

Table 2.1: Advantage as well as the disadvantage of the four storage technologies [Abdulrahman Dahash, 2019].

Storage technology	Storage medium	Energy density [kWh/m ³]	Storage volume for 1 m ³ water equivalent
ATES	Sand-water	30 - 40	2 - 3 m ³
BTES	Soil	15 - 30	3 - 5 m ³
PTES	Gravel-water	30 - 50	1.3 - 2 m ³
TTES	Water	60 - 80	1 m ³

Table 2.2: Storage medium and energy density for the four storage technologies [Abdulrahman Dahash, 2019].

2.2.1 Review of the four storage concepts

Aquifer thermal energy storage

ATES functions as a underground water reservoir and is therefore really dependent on soil conditions. It is evident from table 2.2 that the storage medium is a mixture of sand and water, since the collected heat are stored in the underground layers. In these underground layers, a few wells are drilled, some cold and some hot, in order to circulate the water and thereby inject and extract the heated water [Lee, 2010]. As stated as one of the disadvantages in table 2.1, it is not possible to insulate the storage, due to it being underground. The storage have therefore a high heat loss to its surroundings [Martin Bloemendal, 2015], [Olesen, 2012]. On the basis of the aforementioned as well as the restrictions of placement and the lower supply temperature compared to both the TTES and PTES, the ATES will not be considered any further in this thesis [Abdulrahman Dahash, 2019].

Borehole thermal energy storage

BTES share a number of similarities with ATES. Like ATES, BTES utilises the ground layers as storage medium [Abdulrahman Dahash, 2019], [Liang Zhang, 2015], whereas ATES drilled wells into the aquifer. BTES have vertical boreholes where the heat is transferred from the heat carrier to the ground surrounding the boreholes [Abdulrahman Dahash, 2019]. The similarities between the ATES and BTES is also apparent in the disadvantages. BTES has a high heat loss to the surroundings and is dependent on the soil conditions as well as when compared to TTES and PTES, the supply temperature is lower [Abdulrahman Dahash, 2019]. On the basis of the mentioned disadvantages and challenges, BTES will not be considered any further in this thesis.

Tank thermal energy storage and pit thermal energy storage

Just as the ATES and BTES share a number of similarities, the TTES and the PTES does as well. One example is in the operation of the storage, where they both utilise the stratification concept. When a storage is stratified, the hot water is at the top of the storage and the cold water is at the bottom, which is due to thermal buoyancy [Abdulrahman Dahash, 2019]. The reason behind the hot water being at the top of the storage is because it has a lower density than that of cold water, resulting in the hot water rising to the top while the cold water sinks to the bottom of the storage [Abdulrahman Dahash, 2019]. Thereby forming a thermocline region between the cold and hot region [Li, 2015], [Arcon-Sunmark, 2019]. The thermocline region acts as a dynamic natural barrier between the two regions, thereby preventing the two regions from mixing [Li, 2015], [Arcon-Sunmark, 2019]. Thus it is of significant importance that the thermocline

region is as small as possible in order to decrease the mixing effect of the hot and cold region [Abdulrahman Dahash, 2019]. By having a minimal thermocline region the thermal losses from the storage will be decreased [Abdulrahman Dahash, 2019]. The impact of the stratification levels can be seen on figure 2.8

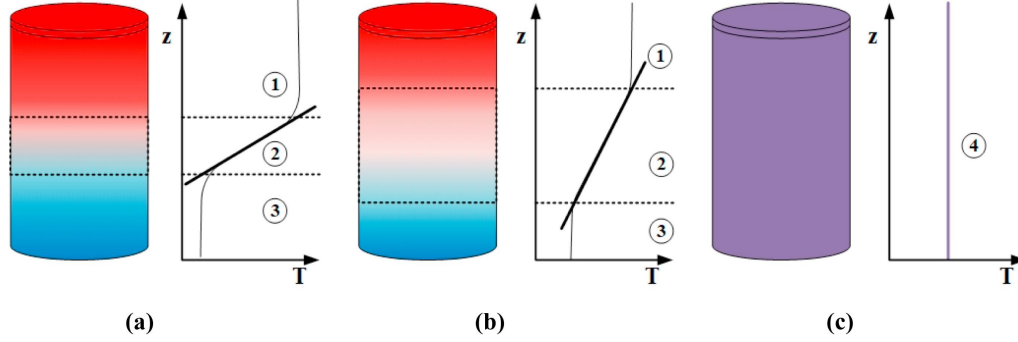


Figure 2.8: "Different levels of stratification for same amount of stored heat (a) highly stratified, (b) moderately stratified, while (c) fully mixed storage. (1) Hot region, (2) thermocline, (3) cold region, and (4) uniform temperature" [Abdulrahman Dahash, 2019].

Case (a) is highly stratified, case (b) is moderately stratified and case (c) is fully mixed. In terms of the thermocline region, case (a) have a small thermocline region, whereas case (b) has a larger thermocline region. The numbers on the figure represent: (1) hot region, (2) temperature gradient and (3) the cold region. In case (a) with the small thermocline region, the temperature gradient between (1) and (3) is high, whereas case (b) have a larger thermocline region and therefore a smaller temperature gradient. The thermocline regions does not appear in case (c) due to the uniform temperature level, this results in an unstratified storage, or in other words a fully mixed storage [Abdulrahman Dahash, 2019], [Cruickshank, 2009]. There is one deciding parameter that have a direct impact on how good the thermal stratification can be, and that is the design and location of the inlet and outlet ports [Abdulrahman Dahash, 2019], [Arcon-Sunmark, 2019]. The stratification is dependent on the design and location of these inlet and outlet ports. This is due to the local turbulence that can be created at the ports, which results in a mixing effect [Hegazy, 2007]. Turbulence within the storage would result in a less stratified storage thereby creating a larger thermocline region and with it a smaller temperature gradient. If the temperature of the water going into the storage is higher than that of the water where the inlet is located, the supplied water will start moving up due to the thermal buoyancy and start a mixing effect [Arcon-Sunmark, 2019], [Abdulrahman Dahash, 2019]. In order to minimise these effects and ensure the best settings for the stratification, both the location and design of the inlet and outlet port must be carefully considered. Figure 2.9 illustrates two examples of the inlet and outlet location. The optimal location for the inlet and outlet ports are at the top and at the bottom of the storage, respectively, as illustrated in case (b) [Abdulrahman Dahash, 2019]. When the inlet and outlet port are placed further from each other a more uniform water flow can be achieved, which empowers a smaller thermocline region, which facilitates a larger effective water volume, see the dashed area in figure 2.9.

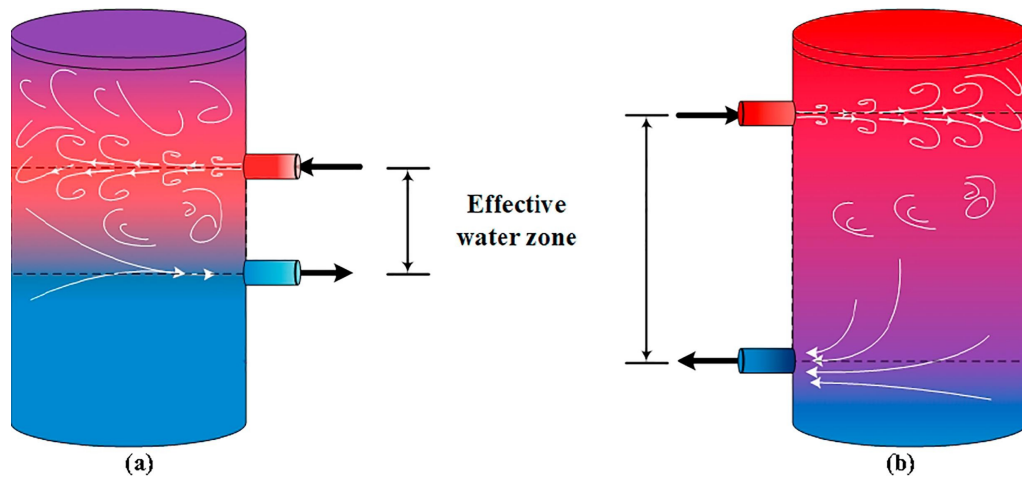


Figure 2.9: Illustration of the impact of the inlet and outlet placement as well as the effective water volume due to the placement [Abdulrahman Dahash, 2019].

The TTES and PTES shares all of these similarities even though they are different in design. Where the TTES is usually a steel tank above ground, PTES is constructed underground and with the form of an upside down truncated pyramid see figure 2.10. This design is usually used because it is the simplest excavation shape [Jensen, 2014].

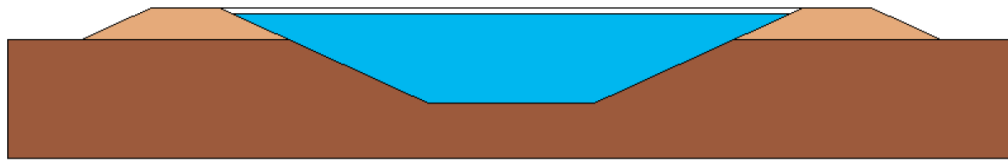


Figure 2.10: Cross section sketch of a PTES [Jensen, 2014].

One of the main disadvantages of the TTES is the 'limited' storage capacity and the high construction cost [Abdulrahman Dahash, 2019]. When planning for a larger and more combined energy system the TTES falls short due to storage sizes above 10,000 - 20,000 m³ is too expensive, when the storage size is above this, then it would be more cost-effective to build a PTES [Arcon-Sunmark, 2019].

2.2.2 Pit thermal energy storage

Design

The structure design of a PTES is rather simple, as mentioned before the excavation shape of a PTES is that of an upside down truncated pyramid and the cover consists of a water tight liner [Jensen, 2014]. An important aspect to keep in mind when dimensioning the PTES, is soil balance. Soil balance is the balance between the excavated soil versus the needed soil for the embankments, the light brown area in figure 2.10. When dimensioning a PTES, soil balance should be aimed to be as closely to zero as possible. By doing so, the cost associated with handling and transporting the excavated soil can be minimised, and the need for new soil can be completely removed [Jensen, 2014].

Insulation

When building a PTES there are primarily two aspects that take priority, an appropriate

heat insulation and ensuring no to minimal water leakage. This is obtained by using different kinds of liner material. The liners primary job is to function as a water tightener at the sides and at the bottom of the PTES, see figure 2.11. The liner are furthermore used as a floating liner at the top of the storage in order to keep the cover afloat [Arcon-Sunmark, 2019].

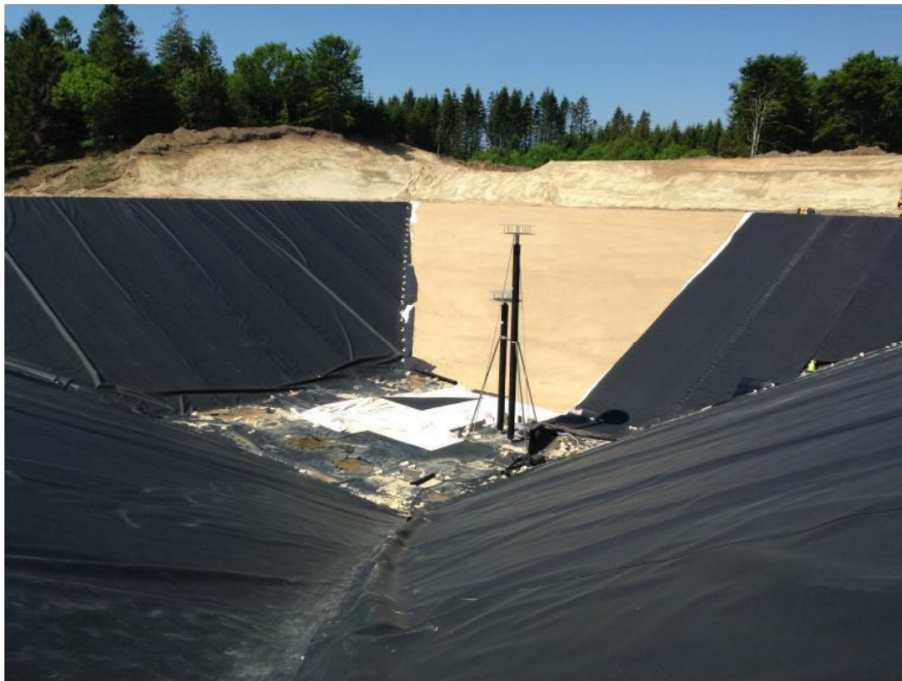


Figure 2.11: Side and bottom liner protection as well as the inlet and outlet ports [Jensen, 2014].

Even though the two most important aspects when building a PTES is heat insulation and ensuring no water leakage, no further measures of heat insulation is done at the bottom and sides of the PTES despite the limited heat insulation of the liner material [Arcon-Sunmark, 2019]. This is because of the greatest amount of heat loss happens at the top of the storage, at the cover, partly due to the large surface area of the cover. There are different materials used as liners such as: polymer liners, metal liners etc. Polymer liners have a well documented welding and testing techniques on top of being relatively cheap and easy to install, whereas the material cost as well as the installation cost for metal liners are considerably higher [Jensen, 2014]. Metal liners main advantage over polymer liners are that they are water vapour tight and can withstand high temperatures, whereas the water vapour permeability for polymer liners is strongly temperature dependent [Jensen, 2014]. Due to the relatively low material cost as well as the well documented welding techniques polymer liners are generally the preferred choice as the geomembranes [Jensen, 2014]. Out of the other geomembranes high density polyethylene (HDPE) liners have the lowest water vapour permeability [Jensen, 2014]. As mentioned before the water vapour permeability is strongly temperature dependent and it increases exponentially with the temperature, see figure 2.12. The lifetime of the polymer liners are also dependent on the temperature. With a constant temperature exposure of 90°C the expected lifetime of some of the best tested HDPE liners is at most three years [Jensen, 2014]. Compare

this to a typical temperature profile of a PTES in combination with a solar plant, the lifetime of the liner is then expected to be more than 20 years [Jensen, 2014]. Under the same circumstances another polymer liner would have an expected life time of less than six years [Jensen, 2014]. It is therefore extremely important to carefully select the correct liner material. These are the two main factors that should be taken into consideration when choosing the liner material. When choosing the liner material for the floating liner, the water vapour permeability is perhaps the most important factor of the two. This is due to the risk of decomposing, this happens if the insulation inside of the cover becomes moist [Jensen, 2014], [Arcon-Sunmark, 2019]. As mentioned in the beginning of this paragraph, metal liners could be used as the liner material instead of HDPE liners and thereby avoid some of these challenges but at the cost of other challenges such as corrosion, but probably the most important of all, at a much higher price. A project sponsored by the Danish district heating organisation was carried out by Marstal District heating company, The Danish Technological Institute, PlanEnergi and Force Technology. They estimated that for the given project the material cost for a metal liner solution, aluminium liner or a stainless steel liner, would be approximately three times higher than that of a HDPE liner solution, as well as the installation cost would be twice as high [Jensen, 2014].

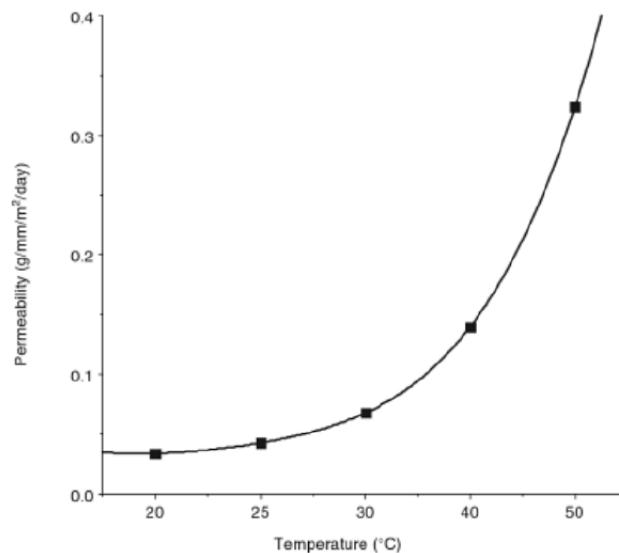


Figure 2.12: "Water vapour permeability as a function of temperature for a typical HDPE liner" [Jensen, 2014].

On top of the floating liner is the insulated floating cover, which is the most expensive part of the PTES [Jensen, 2014]. A lot of research have therefore gone into investigating the best solution [Jensen, 2014]. In short the overall designs of the cover can primarily be divided into three cover designs: [Jensen, 2014]

1. Cover based on flexible insulation mats
2. Cover based on stiff insulation elements
3. Cover based on bulk insulation

The three cover designs will not be investigated in further details due to they all share some of the same challenges. The main challenges they all share are handling of the water

vapour through the floating liner and cover coming from the storage, as well as handling of rainwater [Jensen, 2014], [Arcon-Sunmark, 2019]. If the water vapour from the storage inside the cover is not ventilated away, the insulation material will start to get moist and start to decompose. None of the above mentioned cover designs offers an optimal way of dealing with rainwater which accumulates into relatively large pockets of water on top of the cover. One common way to deal with the rain water is by placing weight pipes on top of the cover. By increasing the diameter of the weight pipes towards the center of the storage, a small inclination towards the center of the storage is created, see figure 2.13. The idea behind this is that the rainwater will be lead to the weight pipes and from there on follow the inclination made by the weight pipes towards the center of the storage, where a pump will pump the rainwater away [Jensen, 2014], [Arcon-Sunmark, 2019]. The weight pipes serves another purpose than just trying to handle the rainwater. The inclination created by the weight pipes should also guide the air bobbles beneath the cover towards the edges of the storage in order to ventilate the air bubbles out through the soil [Jensen, 2014], [Arcon-Sunmark, 2019].

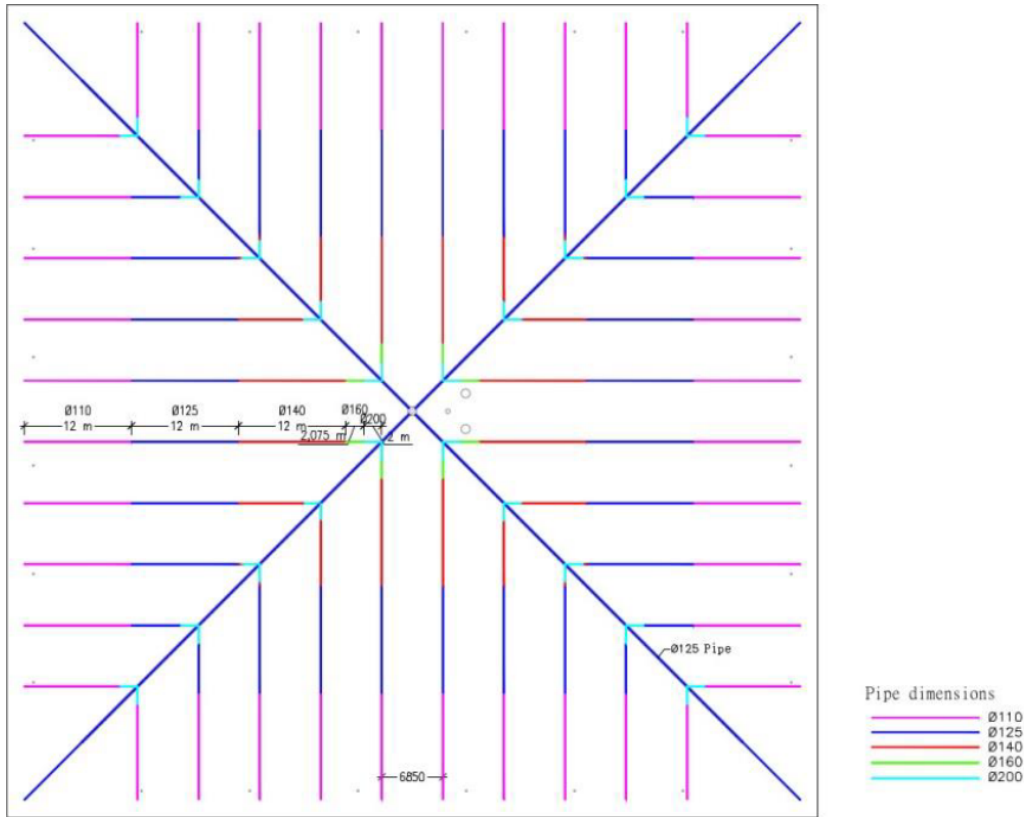


Figure 2.13: An example of how the weight pipes can be arranged on top of the cover [Jensen, 2014].

A ventilation gap between the floating liner and insulation is made in order to vent away the moisture that can come inside of the cover insulation layers [Jensen, 2014]. There are several reasons for why there can come moisture inside the cover insulation layers. The moisture can be a effect of a floating liner or top liner that was damaged during the implementation phase, or if the floating liner or top liner was not kept dry during the implementation phase [Jensen, 2014]. As mentioned before the HDPE liners are

not completely vapour tight and therefore the moisture can also be a result from vapour penetration [Jensen, 2014]. The amount of vapour penetration is dependent on the material and temperature as illustrated in figure 2.12. If the moisture inside the cover insulation layers are not ventilated away, the insulation material will start to degrade. The ventilation gap that separates the insulation and floating liner consist of a small gap between 3 - 6 mm. This small gap allows a flow of air to ventilate the liner and insulation material. The material that creates this small gap can for example be made of geonet, see figure 2.14 [Jensen, 2014].

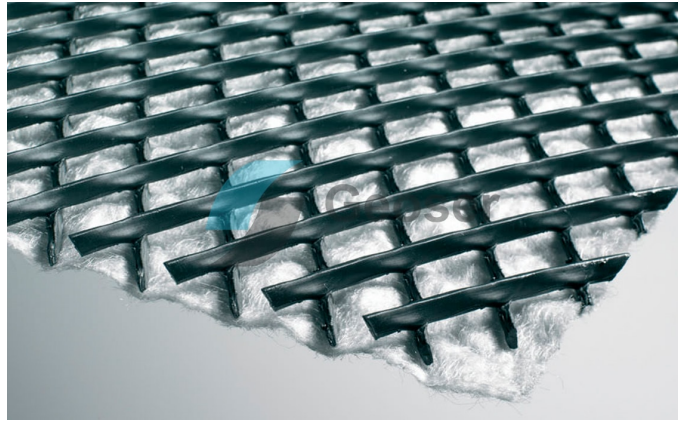


Figure 2.14: Geonet used to separate the insulation and liner [Geoser, 2019].

Another ventilation gap is made between the insulation and top liner in order to ventilate the water vapour inside the cover away. This is done by installing vacuum vents alongside the edges of the PTES [Jensen, 2014]. The function of the vacuum vents are to only allow air to flow out of the cover and not in, but some vacuum vents are modified in order to allow air to flow into the cover as well, see figure 2.15 [Jensen, 2014]. The reason for this modification is to allow the cold outside air to be drawn into the cover where it will be heated by the warmer atmosphere inside of the cover meanwhile absorbing the moisture inside as well [Jensen, 2014]. If the moisture level inside the cover is too high, the ventilation process can be accelerated mechanically by connecting a suction blower [Jensen, 2014].

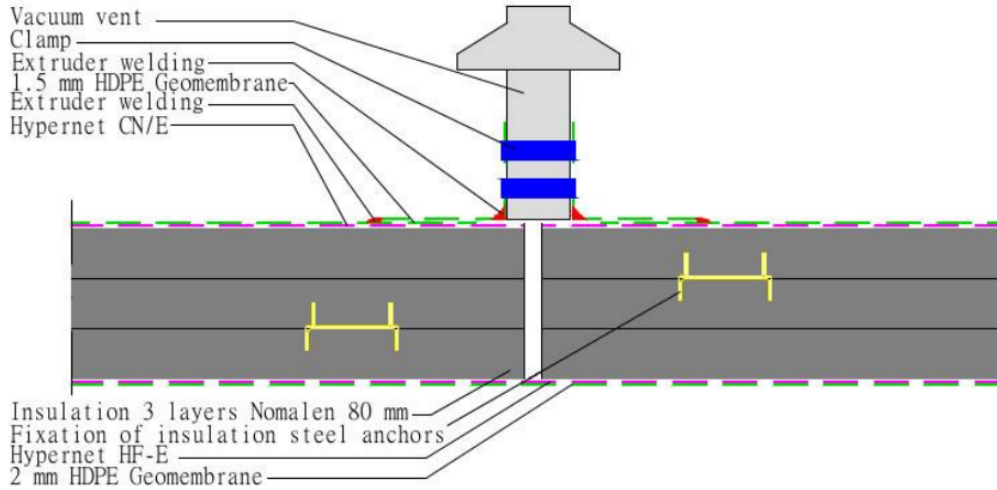


Figure 2.15: Cross section view of the cover [Jensen, 2014].

2.2.3 An excerpt of PTES in Denmark

Marstal

Back in 2010 Marstal District Heating received funds from EU's 7th framework program in order to expand their energy production plant. Half of the heat demand would be covered by a wood chip fired co-generation plant and the other half of the heat demand would be covered by solar collectors [Jensen, 2014]. In order to do so, a PTES with a capacity of 75,000 m³ was implemented in combination with a heat pump of 1.5 MW_{heat} and the existing solar field was expanded to 33,000 m² [Jensen, 2014]. The SUNSTORE 4, 2011-2012, project would develop on the previous constructed PTES from the SUNSTORE 2 project back in 2003 [Jensen, 2014]. Apart from expanding the PTES, the project would try to amend some of the challenges the existing PTES experienced. The problems were described by Jensen [2014] as: Accumulation of air pockets beneath the cover due to air being freed from heating the water. Water pockets on top of the cover due to rain. A leak at the manhole was found two years into the operation of the storage, the leak was most likely a result of using the wrong HDPE liner material, the leak caused the insulation material to be filled with water and made the insulation capacity virtually zero. After further cutting in the cover it was discovered that the materials used as the vapor barrier was not intact and the solutions in the future will not implement it.

After the completion of the SUNSTORE 4 project, the PTES was monitored from 2012 - 2017 but even though the system worked well it was still deemed that the heat losses exceeded acceptable limits, according to [Abdulrahman Dahash, 2019]. The reason for this could be that there still was no optimal way of handling the rain water on top of the storage as well as ventilating the water vapor away from the insulation thereby keeping it dry [Arcon-Sunmark, 2019]. Which is one of the reasons for the cover being replaced in the first quarter of 2020 by Arcon-Sunmark. Arcon-Sunmark have patented a new cover design and are in the process of a Lloyd's certification [Arcon-Sunmark, 2019]. The PTES in Marstal will therefore also serve as a test pilot for the new cover design, which believes to have solved the challenges regarding handling of air pockets, rain water and keeping the insulation dry [Arcon-Sunmark, 2019].

Dronninglund

In 2009 Dronninglund District Heating was granted support from 'Energiteknologiske Udviklings- og Demonstrationsprogram' (EUDP) to install 35,000 m² solar collectors, a 3 MW_{heat} heat pump in combination with a PTES with the capacity of 60,000 m³ [Jensen, 2014]. They have a yearly heat storage capacity of 17.453 MWh and have a average heat loss of around 2.260 MWh a year in the thermal energy storage. The energy production system was constructed back in 2013 and the project was called SUNSTORE 3 [Jensen, 2014]. In order to prevent corrosion a number of precautions was taken. The construction itself was similar to the one for Marstal SUNSTORE 4 [Jensen, 2014]. Because of a similar approach, this storage shares the same challenges as the one in Marstal. When it is raining, the rainwater forms into large water pockets on top of the cover and air bubbles gathers into small air pockets beneath the cover [Arcon-Sunmark, 2019]. The district heating staff have come up with some creative and temporary solutions for dealing with the rainwater pockets and the air pockets. The district heating company invites children from preschool to a field trip where they will have the opportunity to walk on top of the storage meanwhile they are guiding the rainwater to the nearest weight pipe in order to guide the water to the center of the storage where the pump can pump the water away [Arcon-Sunmark, 2019].

Despite the challenges of the PTES in Marstal and Dronninglund, they are still considered as a successful operative example of large scale hot water pits according to Abdulrahman Dahash [2019]. Abdulrahman Dahash [2019] further states that in spite of other PTES in other parts of the world, the Danish experience is the leading one regarding large scale pits.

2.3 Energy Modeling tools

As described in section 2.1.1, the future energy system is going to get more complex with the integration of more fluctuating energy sources. Regarding the phasing out of central coal fired power plants and thereby the decentralisation of the CHP plants, the energy system needs to be more flexible. The design of the energy system should potentially be rethought in terms of the placement of certain energy producing units and thermal energy storage. It is not unthinkable that smaller buildings containing heat pumps would be constructed closer to the consumers instead of the same location as the district heating company. The same is evident with thermal energy storage. By placing heat pumps or thermal energy storage closer to the consumers it would be possible to supply the heat demand closer to the source. It should though be noted that the general directions for larger cities such as Aalborg and Odense is to centralise the thermal energy storage and thereby build a big scale thermal energy storage that serves as a seasonal storage [Aalborg Forsyning, 2019]. In order to achieve the goals for the future energy system, this way of thinking could become a necessity. If it does become a reality, it is of extreme importance that the energy modeling tools will develop with this line of thinking. Multiple flow directions and more optimised energy systems in combination with a thermal energy storage must be a higher priority in the development of the energy modeling tools, if they should have any change to succeed in modeling the future energy system.

Since the authors of this thesis have prior knowledge about TERMIS and energyPRO, they are the chosen energy modeling tools that will be focused on. TERMIS and

energyPRO excels in net modeling and in energy systems, respectively. The advantages and disadvantages for each of the chosen energy modeling tools in regards to modeling the future energy system, will be shortly described.

TERMIS

TERMIS focuses primarily on network management for heat networks. Including both design and planning of the network [Electric, 2020]. This would for example be an extension of the network because of new houses being build and added to the heat network. TERMIS can also be used as a form of maintenance tool. An example of a company that uses TERMIS as a form of maintenance tool is 'Aalborg Forsyning' [Aalborg Forsyning, 2019]. An example of this would be if a section of the pipeline should be replaced, the consumers should still have access to hot water. TERMIS would in this case suggest how the consumers would still have access to hot water but it is up to the user to check and see if the parameters for pressure drop, flow, friction gradient is not exceeding the allowed limits. TERMIS is however "limited" to only work with network management and it is not able to make energy system simulations, which is one of the limitations of the program. This means that in order for the user to model for example a new energy systems that should be connected to the existing heat network. The user have to use a minimum of two different energy modeling tools in order to create a model that would show the implication of the new energy system and how it will affect the existing heat network.

EnergyPRO

EnergyPRO can however not do network management as TERMIS but it is able to model and analyse complex energy systems, which TERMIS can not. EnergyPRO can model energy system with combined supply of thermal energy and electricity [international, 2020]. It is used to model both new and existing energy systems. One of energyPRO's advantages is that it is capable of analysing both the technical aspect of the energy system as well as the financial aspect of the energy system. Regarding energy systems in combination with a thermal energy storage, energyPRO have its limitations. It is for example only possible to use two temperatures inside of the storage, one at the top of the storage and one at the bottom of the storage. This limitations have an effect on how well the user can optimise any given energy system that uses a thermal energy storage. If it were possible to calculate with multiple temperature levels, it would be possible to optimise the operation strategy by changing the priority of the energy producing units within the energy system.

As described in the beginning of this section, the future energy system is going to be complex and it is likely that not all of the energy producing units will be placed at the same location. [Arcon-Sunmark, 2019]. With the increase of both fluctuating energy sources and an electrification of the heat sector. In order to achieve the energy goals, the future energy system needs an energy modeling tool that is capable of modeling the complex nature of the future energy system, with a better and more accurate utilisation of the thermal energy storage, in combination with network management. This coupling is necessary in order to see if the future energy system can be incorporated in the existing heat network.

One combined energy modeling tool

The goal of this thesis is to reproduce the same values for a chosen heat network made in TERMIS and thereby validate the equations used in this thesis. Furthermore the

thesis wants to demonstrate how it is possible to calculate the temperature levels inside of a thermal energy storage and thereby see how the stratification process impacts the temperature levels. The idea is to better utilise the thermal energy storage and use the accurate temperature levels. By doing so it would be possible to provide the energy system with much more flexibility and perhaps even optimise the operation strategy of the energy system. This could potentially allow some energy producing units to be considered as an booster option that previously never would have been considered as a booster option. Which can be attributed to a poor utilisation of the thermal energy storage potential.

The idea is to use energyPRO as the base of the energy modeling tool and make an Excel model that can illustrate the development of the temperature levels inside of the storage instead of only showing the energy value inside of the storage. The calculations used to verify the values of TERMIS should be implemented in order for energyPRO to be able to work with network management. If this is achieved it would lay the foundation for a way to implement the best features of TERMIS into energyPRO. This would result in an energy modeling tool much better suited for the challenges posed by the future energy system.

Research question 3

The inspiration for this thesis was to look into the issues of changing between multiple energy modeling tools which have their own area of expertise. This inspiration lead to the wondering of how to combine key features from two energy modeling tool into one. The energy modeling tool will be based on raw numbers and data from TERMIS and energyPRO and adapted in a Excel model. The idea behind the combined energy modeling tool is to be able to increase the optimisation capabilities, in order to be better suited for the challenges of the future energy system. The future energy system of Denmark are already under pressure in order to reach the energy goals by 2030. With the increase of renewable energy sources and its intermittency in energy production sets higher demands for the energy system. The future energy system must be equally as ready to react to sudden changes in demand or in supply as the old energy system based on fossil fuels was. This can be a challenge with the fluctuating nature of the renewable energy sources. This is one of the reasons why the energy modeling tools needs to be able to fully utilise thermal energy storage and use the flexibility that comes along with the storage. Which is why there is a need for improving existing energy modeling tools. Thus the research question laying the foundation for this thesis is:

"What limitations does the current energy modeling tools have, and how can the individual strength of the modeling tools be combined into one?"

The following sub-questions will aid in answering the research question:

- *How does the utilization of a thermal energy storage change when changing from two temperature inputs to multiple?*
- *How can a Excel model be made that can recreate the same results as in TERMIS, and how can it be combined with an energy system?*

The purpose of the analysis is to both calculate the development of the temperature levels inside of the storage and how it will develop in both a isolated perspective as well as in a charging situation. A model of a pipeline network is made in Excel which should recreate the results from TERMIS. The two models should then be combined into one model, thereby laying the foundation of how these areas can be combined into one energy modeling tool.

3.1 Delimitations

A number of assumptions have been made for the calculations made in the analysis. When calculating the temperature levels inside of the thermal energy storage the geometry of the storage is assumed to be a vertical cylinder and not a upside down truncated pyramid. The correct geometry, an upside down truncated pyramid, is however used when calculating the heat loss, U_{tank} . The data for calculating U_{tank} is based on the numbers from the Pit thermal energy storage in Dronninglund. But when calculating $A_{c,fluid}$ the geometry for a vertical cylinder is used.

For all the calculations made in this thesis, the water temperature was assumed to be 45°C. Meaning the density as well as the thermal conductivity of water is extracted from this temperature. The authors are aware of the values for density and thermal conductivity is changing with the temperature of the water. This assumption has been done in order to simplify the calculation process in the Excel model.

Disclaimer

The disclaimer regarding how the corona pandemic influenced the work and results of this thesis can be found in Appendix A.3

3.2 Research Design

In order to ensure a coherent thesis, a framework for the thesis have been established. The framework should ensure a correct line of information contributing in analysing the research question. To do that the research design is split up into different levels. The levels are; research question, sub-questions, theories and methods. These levels can be seen on figure 3.1. In order to answer the research question, two sub-questions have been made to guide the thesis. The sub-question is focusing on different areas within the research question. The sub-questions is then analysed through various theories and methods.

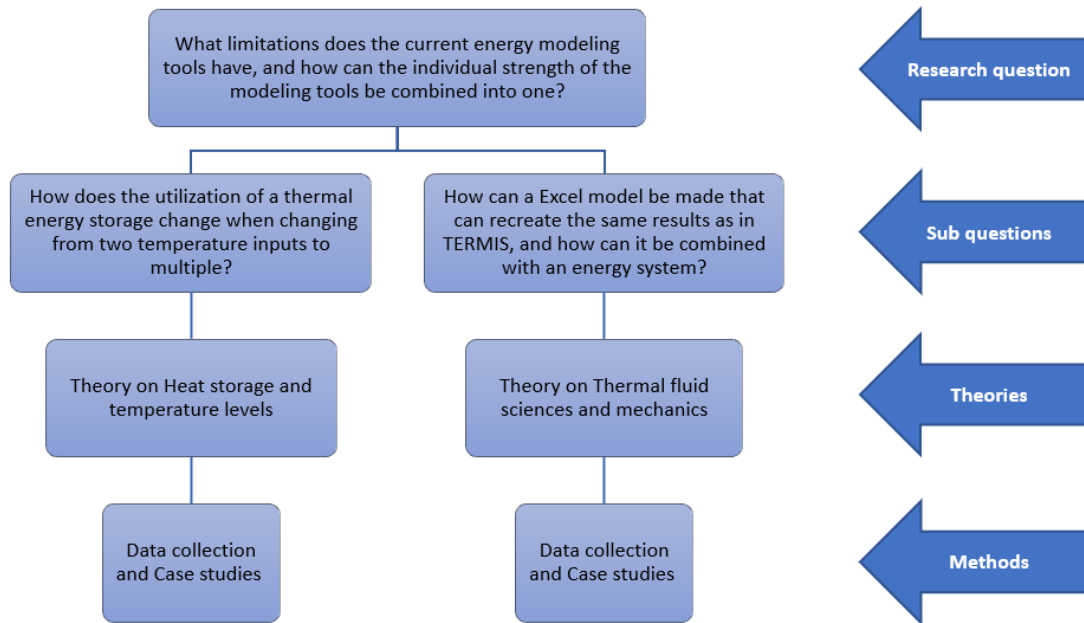


Figure 3.1: Illustrates the framework of the thesis and how the theories and methods are connected to the sub-questions.

The two sub-questions are: *'How does the utilization of a thermal energy storage change when changing from two temperature inputs to multiple?'* and *'How can a Excel model be made that can recreate the same results as in TERMIS, and how can it be combined with an energy system?'*. The sub-questions are divided so the focus on the theory and methods are more specialised to the specific area of interest. The analysis are build on the theory of each area which is primarily based on formulas. This forms the basis for building the models for each of the areas and in the end, combing them into one tool. Both models are made in Excel. The pipeline network model will be compared to the extracted results from TERMIS in order to validate the formulas used in the Excel model. The temperature level model will demonstrate the development of temperature levels both in a isolated perspective as well as in a charging situation. Both sub-question will be based on the methods of case studies and data collection, in order to acquire the needed knowledge of the area in question. The conclusion will be based on the results from the sub-questions and then conclude on the combined model and its results.

Methodological framework 4

In order to analyse the problem area and reach a valid answer to the research question, appropriate methods are used in order to ensure the interaction of the theories in the analysis. The chapter will introduce the main methodologies used for answering the two sub-questions in order to answer the research question.

4.1 Case study

To better answer the research question different methods can be taking into consideration. For this thesis one of the methods used is case study. Case study is used because the results extracted from TERMIS is based on the existing net model for Rørup to Vodskov. Furthermore a reference model for Vodskov to form the basis for the energyPRO which the temperature level model then further expands on by calculating the temperature levels inside of the storage in the chosen time period.

Case study can be divided into four different categories. The categories are; single case, multiple case. Both the single case and multiple case can be distinguished into a holistic and embedded analysis [Robert K. Yin, 2009].

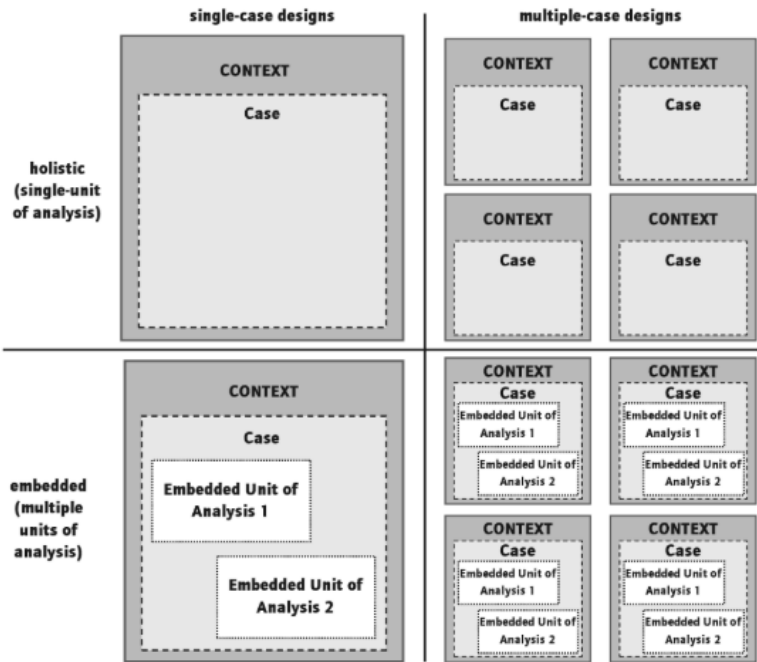


Figure 4.1: This figure shows the four different types of case studies. [Robert K. Yin, 2009]

Figure 4.1 illustrates the four different categories in which case study can be divided into. The case study used for this thesis is the single case design with an embedded analysis. This is due to the thesis investigating two different areas of interest, temperature levels inside of the storage and replicating the results from TERMIS. These two models will then be combined in the end of the analysis [Robert K. Yin, 2009]. The thesis wants to demonstrate that an energy modeling tool that can access the temperature levels inside the storage, can optimise the modelled energy system even more and then combine that with the calculations of how it will fit into the existing pipeline network. This case and its associated data will form the perimeter of the models made in Excel.

4.2 Data collection

When trying to better understand the research question, different types of data collection methods can be used. In this thesis most of the data collection have been done through literature review, but also the use of expert knowledge gathered through last semester's internships. The authors main assignment was working with TERMIS and thermal energy storage, specifically pit thermal energy storage. When gathering data the main focus is on the reliability and validity of the collected data. Datas' reliability and validity can be based on whether or not the source is trustworthy and or is peer reviewed . First hand data is preferable, this could for example be data collected from either official sites or documents, expert knowledge or information in the field of research. For a well documented thesis the collected data must be both reliable and valid [Nina Kanstrup Kjaer, 2011].

Data collection can be divided into two different categories, primary data or secondary data. Data collected by interview or other proactive ways of collecting data will be considered as primary data [Nina Kanstrup Kjaer, 2011]. The primary data for this thesis will come from the observations and knowledge gained from last semester during the internship, which aligns with the thesis' topic.

Second hand data is collected and sorted by others. This means that data that once were primary data will become secondary data for the ones who uses it. Secondary data can for example be reflection on texts, surveys or statistics [Nina Kanstrup Kjaer, 2011]. The secondary data used in this thesis will be based on the literature review of multiple reports, others thesis, PHD's and so on.

Data collection can also be divided into quantitative data and qualitative data. Quantitative data is for example data that can be measured or counted, and is easily compared with other similar data sets. In this thesis that data could come from measurement or data collected from a simulation that makes up the basis for the further analysis. The second category is the qualitative data. Qualitative data is a data set that is unique and cannot be compared to other data sets but it can be used to demonstrate a specific point of view and provide a deeper understanding or simply substantiate a certain theory. A common type of qualitative data, would be data collected during a survey or interview with open question that focuses on the individual answer. The qualitative data are a good way to answer the what, why and how question which allows the interviewed person to go deeper into a specific context [Nina Kanstrup Kjaer, 2011].

Theories 5

In this chapter the theories used to answer the research question and the two sub-question will be presented. This chapter present the needed knowledge required to make the analysis. The theories in this chapter will consist of different equations, that explains how the model can be made in each of the research areas in this thesis.

5.1 Temperature levels

As mentioned in section 2.3, energyPRO are only capable of calculating with two temperatures in the thermal energy storage. It is possible to achieve an appropriate answer by only using two temperature profiles. If energyPRO however were able to calculate with multiple temperature levels, it would be possible to further optimise the energy system and thereby give more flexibility in the operation strategy, as described in section 2.3. The aim of this section is therefore to focus on, how to calculate the temperature levels inside of a thermal energy storage.

Through the use of literature review, multiple open source reports have been investigated, in order to analyse how the temperature levels inside of a thermal energy storage can be calculated. The result of the literature review showed that a limited amount of reports actually calculated the temperature levels without the use of experimental data or the use of computer tools such as Computational Fluid Dynamics (CFD). Two reports were found where the needed information was available in order to calculate the temperature levels without the need of extensive calculating tools. The two reports is respectively a master of science thesis from Newton [1995] and a PHD thesis from Cruickshank [2009]. Cruickshank [2009] bases her temperature level calculations on the same calculation as used in Newton [1995] thesis. The literature review conducted in this thesis indicates that there are not many reports, that further explains or illustrates, by the use of equations, how to calculate the temperature levels without the use of experimental data or other computer software programs. At least for the reports that are accessible to the public. This thesis will therefore base the calculations of the temperature levels inside a thermal energy storage on the same approach as Newton [1995] and Cruickshank [2009].

The first step to be able to calculate the temperature levels within the thermal energy storage is to divide the storage into N number of node sections. This is done in order to calculate the temperature for each node N . An illustration of this can be seen on figure 5.1. The assumption is that each node is completely mixed and have a uniform temperature across the entire node [Cruickshank, 2009]. The models accuracy of the temperature levels within the storage is dependent on the number of, N , nodes [Cruickshank, 2009]. This means that increasing the number of, N , nodes within the thermal energy storage have

an significant impact of the accuracy of the modelled temperature levels [Cruickshank, 2009]. Figure 5.2 illustrates how the accuracy of the calculation of the temperature levels are dependent on the number of nodes. Figure 5.2 is from Cruickshank [2009] thesis and it illustrates how the temperature develops inside of a thermal energy storage when it is heated over a set period of time. Furthermore it illustrates the improvement in accuracy of the temperature levels inside of the storage as the number of nodes increases. The number of nodes chosen for the thermal energy storage in this project is 15. The reason behind choosing 15 nodes instead of for example 5 is because of the improved accuracy. Whereas doubling the number of nodes to a total of 30 nodes results in a smaller improvement in accuracy compared to doubling the calculations. The figure illustrates that 15 nodes is a good approximation for the accuracy of the temperature levels.

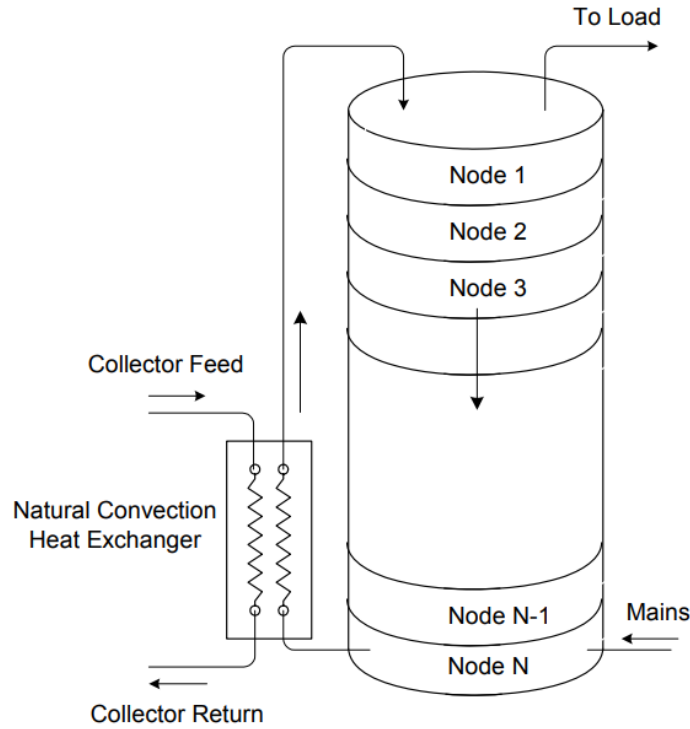


Figure 5.1: Illustration of the indexation of the thermal storage in order to calculate the stratification [Cruickshank, 2009].

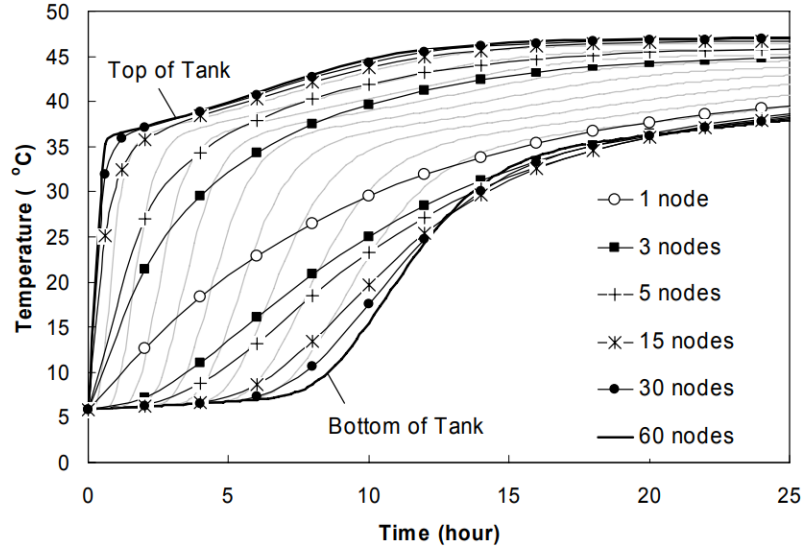


Figure 5.2: "Node sensitivity of storage model" [Cruickshank, 2009].

In order to estimate the temperature of each node section in the thermal storage an 'energy balance' equation is used. The equation takes the following into consideration when determining the energy balance: *"Thermal losses to the surroundings and the influence of the adjacent nodes (e.g., mass and energy flows, including conduction between the layers and vertical conduction through the tank walls, etc.)"* [Cruickshank, 2009]. These parameters accounts for all energy flows possible that goes into and out of the node [Newton, 1995]. This means that these are the parameters that affects the temperature of each node and should be taken into consideration for each number of, N , nodes. Figure 5.3 illustrates all of the energy flows that can occur at the same time for node i [Cruickshank, 2009], [Newton, 1995].

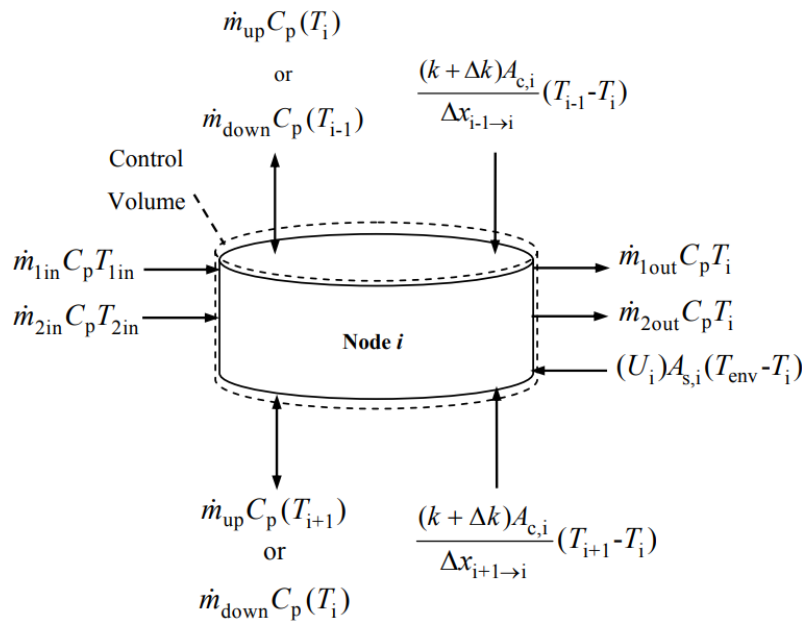


Figure 5.3: Illustration of all the parameters affecting the temperature of node i [Cruickshank, 2009].

In order to calculate the temperature levels inside the thermal storage, all of the parameters shown in figure 5.3 must be taken into consideration. Then a differential equation for each N node's energy balance can be expressed. The energy balance equation for the i^{th} node is given by: [Cruickshank, 2009], [Newton, 1995].

$$\begin{aligned}
M_i C_p \frac{dT_i}{dt} = & \frac{(k + \Delta k) A_{c,i}}{\Delta x_{i+1 \rightarrow i}} (T_{i+1} - T_i) + \frac{(k + \Delta k) A_{c,i}}{\Delta x_{i-1 \rightarrow i}} (T_{i-1} - T_i) \\
& + (U_i) A_{s,i} (T_{env} - T_i) + \dot{m}_{down} C_p (T_{i-1}) - \dot{m}_{up} C_p (T_i) - \dot{m}_{down} C_p (T_i) \\
& + \dot{m}_{up} C_p (T_{i+1}) + \dot{m}_{1in} C_p T_{1in} - \dot{m}_{1out} C_p T_i + \dot{m}_{2in} C_p T_{2in} - \dot{m}_{2out} C_p T_i \quad (5.1)
\end{aligned}$$

All of the variables and constants will now be listed:

T_i is the temperature at the given node i and it is the temperature that will be calculated. k and Δk represents the thermal conductivity of the tank fluid as well as the tank fluids de-stratification conductivity, respectively [Cruickshank, 2009], [Newton, 1995]. How to calculate the de-stratification conductivity will be explained later in this section. $A_{c,i}$ and $A_{s,i}$ represent node i 's cross-sectional area as well as the surface area, respectively [Cruickshank, 2009], [Newton, 1995]. $\Delta x_{i+1 \rightarrow i}$ and $\Delta x_{i-1 \rightarrow i}$ represents the center-to-center distance between the node below and above the given node, respectively [Cruickshank, 2009], [Newton, 1995]. U_i represents the heat loss coefficient per unit area of node i , which can also be expressed by U_{tank} . How to calculate the heat loss coefficient will be explained later in this section. T_{i+1} , T_i , T_{i-1} , T_{1in} , T_{2in} and T_{env} represents the temperature below, at and above the given node i as well as the temperature that enters and exits the node and the temperature of the environment, respectively [Cruickshank, 2009], [Newton, 1995]. \dot{m}_{up} and \dot{m}_{down} represents the flow of fluid up and down in the tank, respectively [Cruickshank, 2009], [Newton, 1995]. In other words, \dot{m}_{up} represents water that experiences an increase in temperature and therefore will rise into a hotter water layer until the temperature level equalises, whereas \dot{m}_{down} represents water that experiences a decrease in temperature and therefore will sink into a colder water layer until the temperature levels equalises. \dot{m}_{1in} , \dot{m}_{1out} , \dot{m}_{2in} and \dot{m}_{2out} represent the flow of mass entering and exiting the node, respectively [Cruickshank, 2009], [Newton, 1995]. If figure 5.1 is used as an example and looking at node 1, \dot{m}_{1in} represent the hot water supplied by the solar collectors into the tank and \dot{m}_{1out} is the outlet which takes the hot water out of the tank and sends it to the consumers. \dot{m}_{1in} and \dot{m}_{1out} varies depending on which node is calculated. Using figure 5.1 as an example again but looking at node N this time. \dot{m}_{1in} will in this case represent the cold return temperature from the city consumers, meanwhile \dot{m}_{1out} will be the cold water supplied to the solar collectors. In this case they could be labelled as \dot{m}_{Nin} and \dot{m}_{Nout} . The only time where both \dot{m}_{1in} , \dot{m}_{1out} and \dot{m}_{2in} , \dot{m}_{2out} will be included in equation 5.1 is when a node for example will be supplied by solar collectors as well as a heat pump. This node then have the possibility to be supplied by 'medium' temperature water by both the collector field and the heat pump and it can send the 'medium' temperature water out to the solar collectors provided that the sun is able to increase the temperature to the needed supply temperature, or/and send it to the heat pump for an increase in coefficient of performance (COP) factor.

The de-stratification conductivity will now be explained. A stratified tank will not stay

stratified forever [Newton, 1995]. This is due to the fact that the conduction of the fluid in the tank will force the N, numbers of nodes to reach a thermal equilibrium [Newton, 1995]. This is the result of the tank wall usually have a higher thermal conductivity than water due to the tank wall often consist of metal [Newton, 1995], [Cruickshank, 2009]. Because of the higher thermal conductivity at the tank walls, the fluid of node $i+1$ near the wall will be pushed up into node i due to the thermal buoyancy [Newton, 1995]. Meanwhile the fluid inside node i will cool down and will start to sink into node $i+1$ [Newton, 1995]. The affect of the higher thermal conductivity near the wall can be seen on figure 5.4

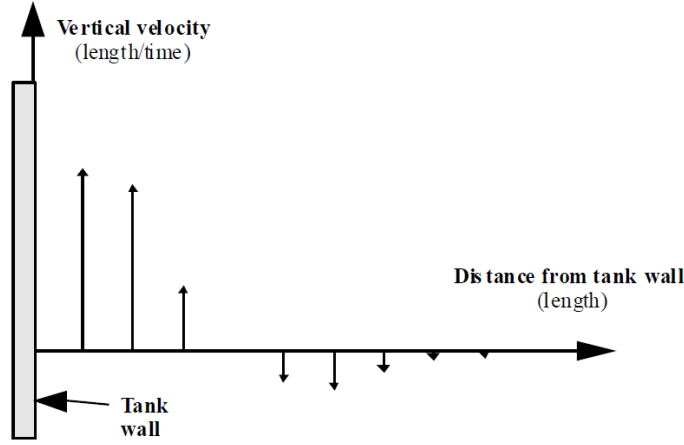


Figure 5.4: The affect of the walls higher thermal conductivity [Newton, 1995].

The heat flow from node i to node $i+1$ can according to Newton [1995] be described as follows:

$$q_{total} = q_{wall} + q_{fluid} \quad (5.2)$$

$$q_{total} = \frac{k_{wall}A_{c,wall}}{\Delta x}(T_i - T_{i+1}) + \frac{k_{fluid}A_{c,fluid}}{\Delta x}(T_i - T_{i+1}) \quad (5.3)$$

Newton [1995] then states that equation 5.3 can be rewritten to give:

$$q_{total} = \frac{k_{fluid} + \Delta k A_{c,fluid}}{\Delta x}(T_i - T_{i+1}) \quad (5.4)$$

The parameter Δk is an additional thermal conductivity, which can be described as:

$$\Delta k = k_{wall} \frac{A_{c,wall}}{A_{c,fluid}} \quad (5.5)$$

Newton [1995] states that equation 5.5 can be a good approximation but it should only be used when no experimental data is available. The approximation is used to calculate the conduction between the adjacent nodes but it have a tendency for underestimating Δk [Cruickshank, 2009], [Newton, 1995]. This tendency is caused by the approximation not considering the mixing that occurs inside the tank and the convection that this causes [Cruickshank, 2009].

The U-value can both be calculated by the area weighted average value for each node or for the overall tank: [Cruickshank, 2009].

$$U_i = \frac{Q_{loss,i}}{A_{s,i}(T_i - T_{env})} \quad (5.6)$$

$$U_{tank} = \frac{Q_{loss,tank}}{A_{s,tank}(T_{mean,tank} - T_{env})} \quad (5.7)$$

It should now be possible to calculate the temperature of each node. In order to do so, it is necessary to solve equation 5.1 simultaneously. This is because the temperature of node i , is dependent on the temperature of the environment and the temperature of the adjacent nodes [Cruickshank, 2009], [Newton, 1995]. It is however not necessary to use all of the elements in equation 5.1 when calculating the temperature for each node [Newton, 1995]. Lets use an example: if a thermal energy storage would have a inlet and outlet port placed in node 1 and 15, and a double inlet, outlet port at node 8. Equation 5.1 would look like the following for each node:

Node 1

$$\begin{aligned} M_1 C_p \frac{dT_1}{dt} = & \frac{(k + \Delta k) A_{c,1}}{\Delta x_{1+1 \rightarrow 1}} (T_{1+1} - T_1) + (U_i) A_{s,1} (T_{env} - T_1) \\ & + \dot{m}_{down} C_p (T_{1-1} - T_1) - \dot{m}_{up} C_p (T_1 - T_{1+1}) + \dot{m}_{1in} C_p T_{1in} - \dot{m}_{1out} C_p T_1 \end{aligned} \quad (5.8)$$

Because there are no temperature level above node 1, the $\frac{(k + \Delta k) A_{c,i}}{\Delta x_{i-1 \rightarrow i}} (T_{i-1} - T_i)$ can be left out of the equation for node 1.

The equation for **nodes 2 - 7 and 9 - 14** will be as follows:

$$\begin{aligned} M_i C_p \frac{dT_i}{dt} = & \frac{(k + \Delta k) A_{c,i}}{\Delta x_{i+1 \rightarrow i}} (T_{i+1} - T_i) + \frac{(k + \Delta k) A_{c,i}}{\Delta x_{i-1 \rightarrow i}} (T_{i-1} - T_i) \\ & + (U_i) A_{s,i} (T_{env} - T_i) + \dot{m}_{down} C_p (T_{i-1} - T_i) - \dot{m}_{up} C_p (T_i - T_{i+1}) \end{aligned} \quad (5.9)$$

The equation for **Node 8** with a total of 2 inlet and outlet ports will be as follows:

$$\begin{aligned}
M_8 C_p \frac{dT_8}{dt} = & \frac{(k + \Delta k) A_{c,8}}{\Delta x_{8+1 \rightarrow 8}} (T_{8+1} - T_8) + \frac{(k + \Delta k) A_{c,8}}{\Delta x_{8-1 \rightarrow 8}} (T_{8-1} - T_8) \\
& + (U_i) A_{s,8} (T_{env} - T_8) + \dot{m}_{down} C_p (T_{8-1} - T_8) - \dot{m}_{up} C_p (T_8 - T_{8+1}) \\
& + \dot{m}_{1in} C_p T_{1in} - \dot{m}_{1out} C_p T_8 + \dot{m}_{2in} C_p T_{2in} - \dot{m}_{2out} C_p T_8 \quad (5.10)
\end{aligned}$$

The equation for **node 15** is as follows:

$$\begin{aligned}
M_{15} C_p \frac{dT_{15}}{dt} = & \frac{(k + \Delta k) A_{c,15}}{\Delta x_{15-1 \rightarrow 1}} (T_{15-1} - T_{15}) + (U_i) A_{s,15} (T_{env} - T_{15}) \\
& + \dot{m}_{down} C_p (T_{15-1} - T_{15}) - \dot{m}_{up} C_p (T_{15} - T_{15+1}) + \dot{m}_{1in} C_p T_{1in} - \dot{m}_{1out} C_p T_{15} \quad (5.11)
\end{aligned}$$

Opposite of node 1, the $\frac{(k+\Delta k)A_{c,i}}{\Delta x_{i+1 \rightarrow i}} (T_{i+1} - T_i)$ can be left out of the equation due to no temperature level below node 15.

Assumptions

The accuracy of the model depends on a number of assumptions being met. These assumptions are as follows: [Cruickshank, 2009]

- *"the flow of liquid within the tank is one-dimensional;"*
- *"the temperature and density of the fluid in each node is uniform and constant over the time step;"*
- *"the fluid streams from each node are considered fully mixed before they enter an adjacent node;"*
- *"the heat loss to the exterior of the tank and conduction in the tank walls are low enough that two- or three-dimensional temperature gradients do not form, promoting convection and de-stratification; and"*
- *"the fluid velocities entering and exiting the storage tank are low enough that they do not promote extensive mixing within the storage tanks."*

Equation 5.4 and 5.5 are likewise dependent on a number of assumptions being met: [Cruickshank, 2009]

- *"the wall and fluid are assumed to be at the same temperature in each node;"*
- *"the conductivity of the fluid and wall in each node is uniform and constant over the time step; and"*
- *"the thickness of the tank wall is much less than the radius of the tank."*

5.2 District heating network

When making a net model for a district heating network for operation purposes the modeling tool that comes to mind is TERMIS. TERMIS is very good at simulating how the district heating network would react under certain conditions, like for example the coldest

hour of a year. The most extreme points like the coldest and warmest period of the year are good indicators for when the network will be most affected and pressured the most. This could for example be with the temperature or the pressure in the pipeline network of the district heating network. Danfoss is currently in the process of making a energy modeling tool that should be a close competitor to TERMIS, and one of the focus points is to make the interface more user friendly [Aalborg Forsyning, 2019]. This tool is called Energis. TERMIS has been used to model a case system, which works as the benchmark for how the pipeline network should behave when looking at flow, velocity, the temperature in supply and return, the pressure and the different losses in the network. A Excel model will be established, which should include the needed formulas in order to recreate the results from TERMIS, however the results will be without the GIS-illustrations that TERMIS also provides.

In order to make all the calculations for the case system, the Excel model will take its stating point from Rærup to Vodskov, and then use the heat consumption at the coldest hour of the year for Vodskov, which is 14.2 MW [Aalborg Forsyning, 2019]. The district heating pipeline network is set to run from an town called Rærup, where the heating facility in this case is placed, and to Vodskov and back again.

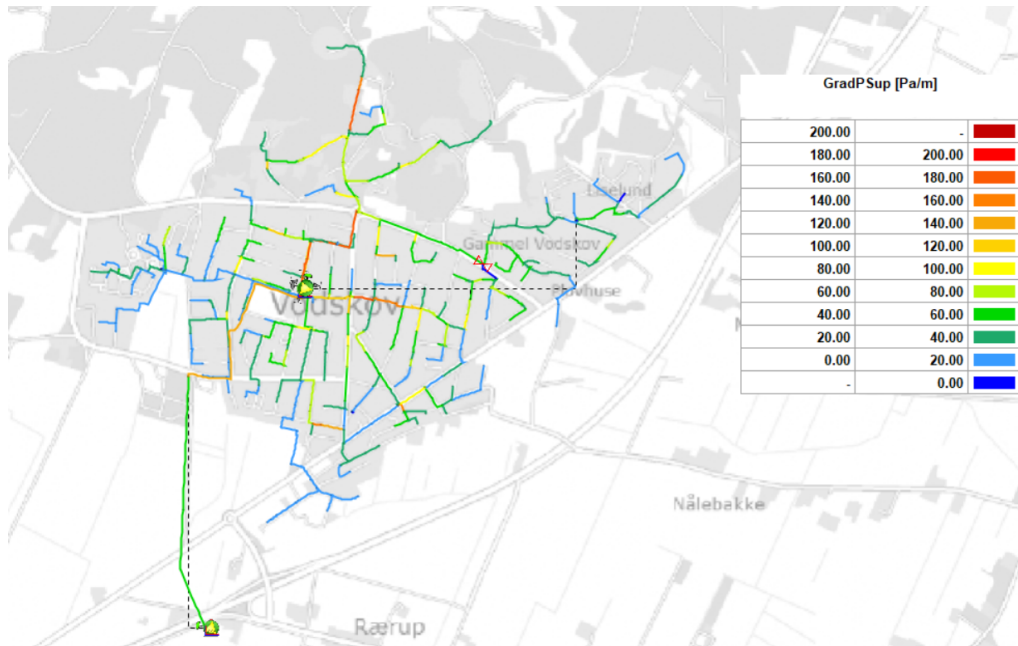


Figure 5.5: Illustration of the case system going from Rærup to Vodskov. The illustration also shows the frictional gradient in the pipeline network [Aalborg Forsyning, 2019].

The reason for starting with the heat consumption is that, it will be the basis for all of the other calculations made later. From the heat consumption the mass flow in the pipeline network can be calculated [Y. A. Cengel, 2012]:

$$\dot{m} = \frac{Q_{HC}}{C_p * \Delta T} \quad (5.12)$$

Where ΔT can be calculated as [Y. A. Cengel, 2012]:

$$\Delta T = T_{supply} - T_{return} \quad (5.13)$$

By calculating the mass flow in the pipeline network the flow velocity can then be calculated [Y. A. Cengel, 2012]

$$v_{flow} = \frac{\dot{m}}{\rho_{water} * \pi * (\frac{D_{pipe}}{2})^2} \quad (5.14)$$

Bernoulli

With v_{flow} calculated, it is possible to start calculating how the pressure changes through the pipeline network, due to the changes in the dimension of the pipe along the way from Rørup to Vodskov. To better understand this and calculate it, the equation from Bernoulli can be used [Y. A. Cengel, 2012].

$$P_1 + (\rho * g * h_1) + (\frac{1}{2} * \rho * v_1^2) = P_2 + (\rho * g * h_2) + (\frac{1}{2} * \rho * v_2^2) \quad (5.15)$$

The Bernoulli equation is about a constant energy balance. The equation 5.15 states that the change in velocity and pressure entering the pipe must be equal to the change exiting the pipe. This means that the pressure and velocity going into the pipe must equal to the energy leaving the pipe. This could for example be when there is a change in the pipe diameter, the fluid inside of the pipe will then experience a change in pressure and velocity when going out of the pipe. From this equation it is then possible to isolate and calculate any unknown variable. For this example the unknown variable is the pressure of the fluid when exiting the pipe along the pipeline string towards Vodskov. The equation can then be isolated for P_2 and compressed to [Y. A. Cengel, 2012]:

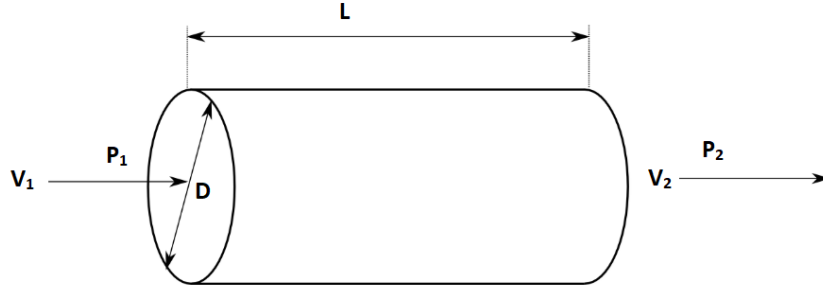


Figure 5.6: This illustrates a simple pipe with velocity and pressure going in and out of the pipe. These are the variables that are interesting for this thesis.

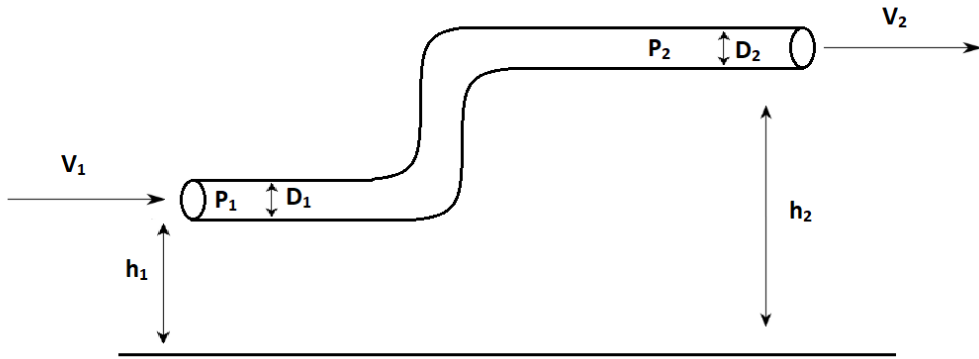


Figure 5.7: This illustration shows a pipe with the same diameter all the way, but with a change in altitude, which will have an affect on the fluid going through.

$$P_2 = P_1 + (\rho * g * (h_1 - h_2)) \quad (5.16)$$

Equation 5.16 only applies for pipes in a straight line that have the same diameter. If the diameter changes along the way, the equation would then look like [Y. A. Cengel, 2012]:

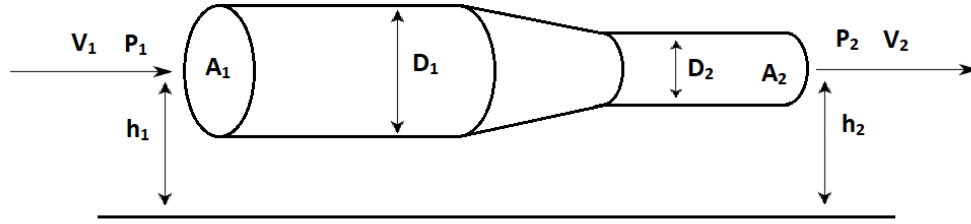


Figure 5.8: This illustration shows a pipe going from one diameter to a smaller diameter. The illustrations shows all the variables that are of interest when performing the calculation.

$$P_2 = P_1 + \left(\frac{1}{2} * \rho * (v_1^2 - v_2^2)\right) \quad (5.17)$$

If a pipe is going to split and create a Y-junction in the pipeline network, the equation 5.17 can then be altered and written as a flow continuity equation [Y. A. Cengel, 2012]:

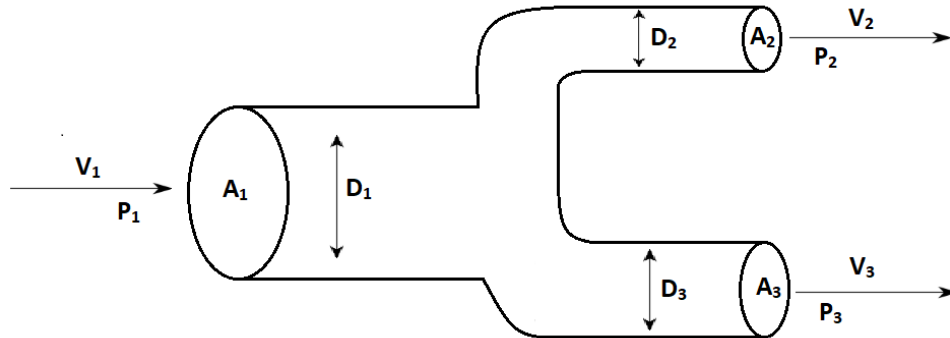


Figure 5.9: This illustration shows a pipe splitting into a Y-junction. The only variables needed for the continuity equation is the variables for the area and the velocity.

$$A_1 * v_1 = A_2 * v_2 + A_3 * v_3 \quad (5.18)$$

With this equation, the variable needed can be isolated and calculated. This equation have be used to prove the calculations of the flow velocity, compared to the diameters of the two pipe ends in the Y-junction. The Y-junction occur in right before Vodskov, where two distribution lines are split and supplies Vodskov. Vodskov have in the case system been split into a north and south distribution of heat in order to differentiate the heat consumption according to the pipeline size that are in place.

Reynolds Number

When investigating what is happening with the fluid within the pipeline network, it is interesting to see how the fluid is behaving. When looking at the flow of the fluid, it can be divided into three different kinds of motion within the pipe; laminar flow, transient flow and turbulent flow. For a Reynolds number (Re) below 2,300 the fluid will be in a laminar stage, with a Re above 3,000 the fluid will be in a turbulent stage, and in between those two numbers the fluid will be in a transient stage. The motion of the flow is important when looking at the pressure inside the pipe. Depending on the fluid being in a laminar, transient or turbulent stage, can result to a higher pressure loss through the pipeline network. The equation can be written as [Y. A. Cengel, 2012]:

$$Re = \frac{\rho * v_{avg} * D_{pipe}}{\mu} \quad (5.19)$$

By calculating the Reynolds Number it can be determined what stage the fluid is in. By calculating the Reynolds number it can then be calculated what the friction factor in the pipe will be. The variable f can be calculated by using the Colebrook equation[Y. A. Cengel, 2012]:

$$\frac{1}{\sqrt{f}} = -2.0 \log\left(\frac{\frac{\epsilon}{D_{pipe}}}{3.7} + \frac{2.51}{Re}\right) \quad (5.20)$$

Losses

With the friction factor f calculated, the pressure drop in the pipes can then be calculated. The pressure drop will have an affect on the network in relation to the power requirement that a pump in the network will use in order to maintain the flow. The pressure drop can be calculated as following [Y. A. Cengel, 2012]:

$$\Delta P_L = \rho * g * \left(\Delta z + f * \frac{L_{pipe}}{D_{pipe}} * \frac{v_{avg}^2}{2 * g}\right) \quad (5.21)$$

Equation 5.21 is also known as the Darcy-Weisbach equation. If the length is divided on both sides of the equal sign, the frictional gradient [Pa/m] can be written as [Y. A. Cengel, 2012]:

$$\frac{\Delta P_L}{L_{pipe}} = \rho * g * \left(\Delta z + f * D_{pipe} * \frac{v_{avg}^2}{2 * g}\right) \quad (5.22)$$

The frictional gradient indicates how much pressure there is on the inside of the pipe and how much it is stressed. The frictional gradient must not exceed acceptable limits, due to the stress it puts on the network. When planning to expand the district heating network with new pipes, the network is only modelled and calculated with a 200 [Pa/m] in the coldest hour of the year.

Another loss that can occur in the network, that is important to take into account, is the head loss. Head loss indicates the additional height the fluid needs to be lifted in order to overcome the frictional losses in the pipes. The head loss equation can be written as [Y. A. Cengel, 2012]:

$$H_L = f * \frac{L_{pipe}}{D_{pipe}} * \frac{v_{avg}^2}{2 * g} \quad (5.23)$$

In order to determine the temperature at the consumers, it is important to calculate the heat losses in the pipeline network along the way. Aage B. Lauritsen [2015] describes the heat losses as following, where the equation for h_s is based on Aitkaliyev [2017]:

$$Q_{hl} = q_{hl1} + q_{hl2} = 2 * q_s \quad (5.24)$$

$$q_s = (T_s - T_{env}) * 2 * \pi * \lambda_i * h_s \quad (5.25)$$

$$T_s = \frac{T_{supply} + T_{return}}{2} \quad (5.26)$$

$$h_s = \frac{1}{LN\left(\frac{r_0^2}{2 * D_{pipe} * r_i}\right) - LN\left(\frac{r_0^4}{r_0^4 - D_{pipe}^4}\right) - \frac{\left(\frac{r_i}{2 * D_{pipe}} + \frac{2 * D_{pipe}^3 * r_i}{r_0^4 - D_{pipe}^4}\right)}{1 + \left(\frac{r_i}{2 * D_{pipe}}\right)^2 - \left(\frac{2 * r_i * r_0^2 * D_{pipe}}{r_0^4 - D_{pipe}^4}\right)^2}} \quad (5.27)$$

With equation 5.24 the supply temperature can be calculated on the behalf of the heat loss,

$$T_{supply} = \frac{\left(\frac{Q_{hl} * L_{pipe}}{1000}\right)}{c_p * \dot{m}} \quad (5.28)$$

The return temperature can be calculated with this equation [Y. A. Cengel, 2012]

$$T_{return} = \frac{(\frac{T_{return,4} + T_{return,2}}{2} - T_{env}) * (\frac{L_{pipe} * \lambda_{dis}}{1000})}{c_p * \dot{m}} \quad (5.29)$$

Analysis 6

This chapter will introduce and analyse the values and numbers going into the two models made in Excel. The equations and formulas introduced in section 5.1 and 5.2 will now be calculated with the gathered data. This will form the foundation for the combined model. The calculation shown will be examples of how it has been done in Excel, but it will not contain every number calculated for the sake of simplicity for both the writers and readers. All of the calculations made can be found in the Excel files attached as ZIP-files.

6.1 Temperature levels inside a thermal energy storage

As described in section 5.1, equation 5.1 forms the basis for calculating the different temperature levels inside the storage. On basis of the information gathered through the problem analysis, PTES have been chosen as the storage technology in this thesis. A number of assumptions have been made in order to simplify the differential equation 5.1. The assumptions are as follows: when calculating the temperature level for the storage, it is assumed that the energy storage have a cylindrical shape and not a truncated pyramid placed upside down. Inside the thermal energy storage there is a conservation of mass expressed by Kirchhoff's law:

$$m_{down,i} - m_{up,i} + m_{1in,i} - m_{out,i} = 0 \quad (6.1)$$

This is also true for the adjacent nodes. The flow of mass from the node_{*i*} to node_{*i-1*} fulfills:

$$m_{down,i} = -m_{up,i-1} \quad (6.2)$$

Equation 5.1 can then be simplified to:

$$\begin{aligned} M_i C_p \frac{dT_i}{dt} = & \frac{(k + \Delta k) A_c}{\Delta x_{i+1 \rightarrow i}} (T_{i+1} - T_i) + \frac{(k + \Delta k) A_c}{\Delta x_{i-1 \rightarrow i}} (T_{i-1} - T_i) + U_{tank} A_s (T_{env} - T_i) \\ & + \dot{m}_{down,i} C_p (T_{i-1} - T_i) - \dot{m}_{up,i} C_p (T_i - T_{i+1}) + \dot{m}_{1in,i} C_p T_{1in} - \dot{m}_{1out,i} C_p T_i \end{aligned} \quad (6.3)$$

In order to calculate the temperature level in the i^{th} node, ΔT_i is isolated:

$$\begin{aligned} \Delta T_i = & \left(\frac{(k + \Delta k)A_c}{\Delta x_{i+1 \rightarrow i}} (T_{i+1} - T_i) + \frac{(k + \Delta k)A_c}{\Delta x_{i-1 \rightarrow i}} (T_{i-1} - T_i) + U_{tank} A_s (T_{env} - T_i) \right. \\ & \left. + \dot{m}_{down,i} C_p (T_{i-1} - T_i) - \dot{m}_{up,i} C_p (T_i - T_{i+1}) + \dot{m}_{1in,i} C_p T_{1in} - \dot{m}_{1out,i} C_p T_i \right) \frac{\Delta t}{M_i * C_p} \end{aligned} \quad (6.4)$$

For this example it is assumed, that there are no flows entering or exiting the thermal energy storage. Equation 6.4 can then further be reduced to:

$$\Delta T_i = \left(\frac{(k + \Delta k)A_c}{\Delta x_{i+1 \rightarrow i}} (T_{i+1} - T_i) + \frac{(k + \Delta k)A_c}{\Delta x_{i-1 \rightarrow i}} (T_{i-1} - T_i) + U_{tank} A_s (T_{env} - T_i) \right) \frac{\Delta t}{M_i * C_p} \quad (6.5)$$

This example is as mentioned earlier in the beginning of this section; a cylindrical energy storage with a conservation of mass in each node with no fluids entering or exiting the energy storage. By doing so it is investigated how the tank fluid thermal conductivity (k), the de-stratification conductivity (Δk), and how the overall heat loss tank coefficient per unit area (U_{tank}) will affect the storage. It is assumed that the storage is at half capacity, 80 °C throughout node 1 - 8 and 40 °C from node 9 - 15. This example should illustrate how the conductivity as well as heat loss, have an impact on the stratification process and how stratified the energy storage will be after a set period of time, which will be 10 days. In order to calculate the temperature in each node, equation 6.5, the values of the variables must be calculated first.

Dimensions and values

For this example, the height of the cylindrical energy storage is 35.74 [m] and the diameter is 47 [m]. The value for the thermal conductivity of water can be looked-up, and for water at 45 °C the value is 0.000638 [kW/m*K] [Toolbox, n.d.]. The reasoning for choosing waters thermal conductivity at 45 °C is due to the calculations made in section 6.2 uses the density value of water at 45 °C. This ensures when the two models are implemented together that the values for water are based on the same temperature. The de-stratification conductivity can be calculated by the use of equation 5.5.

$$\Delta k = k_{wall} \frac{A_{c,wall}}{A_{c,fluid}}$$

It is assumed that the tank wall is made out of stainless steel and therefore have a thermal conductivity, k_{wall} , of 0.017 [kW/m*K] [Toolbox, n.d.]. The cross-sectional area of a cylinder is calculated by the following equation:

$$A_{c,fluid} = \pi * r^2$$

The cross-sectional area of the fluid, $A_{c,fluid}$ is calculated to 1,735 m². The cross-sectional area of the wall, $A_{c,wall}$, is calculated by the following equation:

$$A_{c,wall} = \pi * (r_1 + x_{tank,wall})^2 - A_{c,fluid} = \pi * (23.5[m] + 0.1[m])^2 - 1735[m^2]$$

The value $x_{tank,wall}$ is the radius added with the thickness of the wall which is 10 [cm]. The cross-sectional area of the wall, $A_{c,wall}$ can then be calculated to 14.8 m². Equation 5.5, the de-stratification conductivity can now be calculated, $\Delta k = 0.000145$ [kW/m*K]. $\Delta x_{i+1 \rightarrow i}$ and $\Delta x_{i-1 \rightarrow i}$ represents the center-to-center distance between node i and the node below and the node above, respectively. The center-to-center distance equals the height of the storage divided by the number of nodes. $\Delta x_{i+1 \rightarrow i}$ and $\Delta x_{i-1 \rightarrow i}$ is calculated to 2.38 [m]. T_{i+1} and T_{i-1} represent the temperature below node i and above node i, respectively. In order to calculate the U-value an example is used. The example is based on the values from the PTES in Dronninglund. The annual heat loss from the PTES in Dronninglund is 2,260 [MWh] [Jensen, 2014]. The U-value in this report will be calculated by equation 5.7.

$$U_{tank} = \frac{Q_{loss,tank}}{A_{s,tank}(T_{mean,tank} - T_{env})}$$

Based on the annual heat loss of 2,260 [MWh], $Q_{loss,tank}$ can be calculated by converting 2,260 [MWh] to giga joule, then to joule and then it is divided by 8,760 multiplied with 3,600 in order to get the unit watt. $Q_{loss,tank}$ is calculated to 257,991 [W]. The following calculations illustrates how the surface area, $A_{s,tank}$, of the PTES is calculated. The length and width of the top of the PTES is 100 x 100 [m] which is 10,000 m² [PlanEnergi, 2011]. It was not possible to find the length and width of the bottom of the PTES, so in order to find the dimensions of the bottom of the PTES the following equation was used:

$$V = \frac{h}{3} * (G + g + \sqrt{G * g})$$

All of the parameters in this equation is known beside, g, which is the area of the bottom of the PTES, see figure 6.1. The capacity or volume, V, of the PTES in Dronninglund was described in subsection 2.2.3 to 60,000 [m³] and the height of the PTES is 16 [m] [Anlæg, 2014]. The area of the bottom g, is then calculated to 202.38 [m²] which equals 14.22 [m]. The next step is to calculate the length of the walls of the truncated pyramid. This is done by the following equation:

$$a = \sqrt{h^2 + (m1 - m2)^2}$$

m1 is the radius of the top of the PTES and m2 is the radius of the bottom of the PTES, see figure 6.1. The figure does not portray a upside down truncated pyramid which is the case for a PTES but the math is still the same.

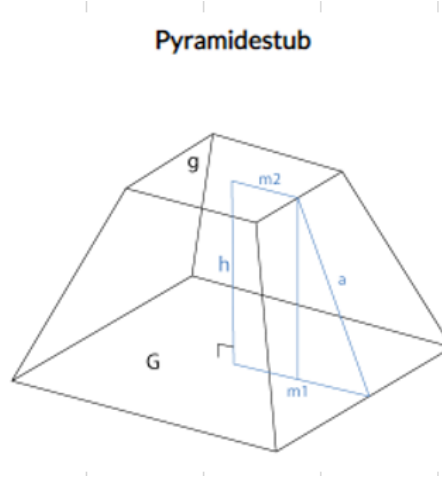


Figure 6.1: Illustration of a truncated pyramid [RegneRegler, n.d.].

The length of the truncated pyramid walls, a , are calculated to 45.77 [m]. In order to calculate the area of the truncated pyramid wall, the equation for calculating the area of a trapeze is used:

$$area = \frac{1}{2} * (a + c) * h$$

Where, a is the length of the bottom of the PTES, c is the length of the top of the PTES and h is the length of the truncated pyramid wall. The area of one wall of the truncated pyramid wall equals 2,614.34 [m²]. In order to get the surface area of the entire PTES, the 2,614.34 is multiplied by the number of walls. The surface area, $A_{s,tank}$ can then be calculated to 10,457.3 [m²]. All of the needed values for calculating equation 5.7, U_{tank} have now been accounted for. U_{tank} is calculated to 0.000486924 [kW/m²*K].

The geometry regarding the calculation of $A_{c,fluid}$ and U_{tank} does not align. $A_{c,fluid}$ is calculated as a cylinder where U_{tank} is calculated as a truncated pyramid. The authors of the thesis are aware of this contradiction in geometry but in order to simplify the calculation in terms of the development of temperature levels, the cylindrical geometry is deemed as a valid simplification. Because of the values used in calculating U_{tank} are based on real numbers from the PTES in Dronninglund, the surface area, $A_{s,tank}$ should therefore be calculated with the correct geometry. This ensures that the calculated U_{tank} have some form of validity and accuracy. Even when the $A_{c,fluid}$ is calculated for a cylindrical shape, using the U_{tank} should ensure an appropriate approximation of how the temperature levels will develop over a set period of time.

The last parameter that needs to be calculated is the mass of water in node i as well as to determine the time interval between each calculation. The mass of water in node i is calculated by multiplying the thickness of the cylindrical layers, Δx , with the cross-sectional area of node i , $A_{c,i}$ and then by 1,000 in order to get the value in kilogram. The mass of water in node $i = 275,586$ [kg]. The time interval set between each calculation is set to every 12 hour. All of the parameters have now been calculated and equation 6.5,

the temperature of node 1 after 12 hours, can now be calculated:

Node 1

$$\Delta T_i = 80 + \left(\frac{(0.000638[kW/m * K] + 0.000145[kW/m * K]) * 115.66[m^2]}{2.38[m]} \right) * (80[^\circ C] - 80[^\circ C]) + 0.000487[kW/m^2 * K] * 351.8[m^2] * (8[^\circ C] - 80[^\circ C]) * \frac{12[h] * 3600}{275586[kg] * 4.186[kJ/kg * K]} \quad (6.6)$$

As described in the last part of section 5.1, node 1 as well as node 15 can leave one additional part of the equation out due to no temperature are above or below them, respectively. The calculation shows that after 12 hours the temperature level in node 1 decreases from 80 °C to 79.5 °C. This calculation is repeated for every node until it has been made for a 10 day period, see figure 6.2.

Tidsskridt i timer	12 timer														
Temperaturlag	1	2	3	4	5	6	7	8	9	10	11	12	13	14	15
Døgn fra start															
Starttemperatur	0.0	80.0	80.0	80.0	80.0	80.0	80.0	80.0	40.0	40.0	40.0	40.0	40.0	40.0	40.0
	0.5	79.5	79.5	79.5	79.5	79.5	79.5	79.5	39.9	39.8	39.8	39.8	39.8	39.8	39.8
	1.0	79.1	79.1	79.1	79.1	79.1	79.1	79.0	39.7	39.6	39.6	39.6	39.6	39.6	39.6
	1.5	78.6	78.6	78.6	78.6	78.6	78.6	78.5	39.6	39.4	39.4	39.4	39.4	39.4	39.4
	2.0	78.2	78.2	78.2	78.2	78.2	78.2	77.9	39.4	39.2	39.2	39.2	39.2	39.2	39.2
	2.5	77.7	77.7	77.7	77.7	77.7	77.7	77.4	39.3	39.0	39.0	39.0	39.0	39.0	39.0
	3.0	77.3	77.3	77.3	77.3	77.3	77.3	76.9	39.1	38.8	38.8	38.8	38.8	38.8	38.8
	3.5	76.8	76.8	76.8	76.8	76.8	76.8	76.4	39.0	38.6	38.6	38.6	38.6	38.6	38.6
	4.0	76.4	76.4	76.4	76.4	76.4	76.4	76.0	38.8	38.4	38.4	38.4	38.4	38.4	38.4
	4.5	75.9	75.9	75.9	75.9	75.9	75.9	75.5	38.7	38.2	38.2	38.2	38.2	38.2	38.2
	5.0	75.5	75.5	75.5	75.5	75.5	75.5	75.0	38.5	38.0	38.0	38.0	38.0	38.0	38.0
	5.5	75.1	75.1	75.1	75.1	75.1	75.1	74.5	38.4	37.8	37.8	37.8	37.8	37.8	37.8
	6.0	74.6	74.6	74.6	74.6	74.6	74.6	74.0	38.2	37.6	37.6	37.6	37.6	37.6	37.6
	6.5	74.2	74.2	74.2	74.2	74.2	74.2	73.6	38.1	37.4	37.4	37.4	37.4	37.4	37.4
	7.0	73.8	73.8	73.8	73.8	73.8	73.8	73.1	38.0	37.2	37.2	37.2	37.2	37.2	37.2
	7.5	73.4	73.4	73.4	73.4	73.4	73.4	72.6	37.8	37.1	37.1	37.1	37.1	37.1	37.1
	8.0	73.0	73.0	73.0	73.0	73.0	72.9	72.2	37.7	36.9	36.9	36.9	36.9	36.9	36.9
	8.5	72.5	72.5	72.5	72.5	72.5	72.5	71.7	37.5	36.7	36.7	36.7	36.7	36.7	36.7
	9.0	72.1	72.1	72.1	72.1	72.1	72.1	71.2	37.4	36.5	36.5	36.5	36.5	36.5	36.5
	9.5	71.7	71.7	71.7	71.7	71.7	71.7	70.8	37.2	36.3	36.3	36.3	36.3	36.3	36.3
	10.0	71.3	71.3	71.3	71.3	71.3	71.3	70.3	37.1	36.1	36.1	36.1	36.1	36.1	36.1

Figure 6.2: The stratification process over a 10 day period.

Figure 6.2 illustrates how the temperature inside the storage develops over a 10 day period. The same calculation has been made for a period of half a year, in order to see how the temperature inside of the storage would develop over a longer time period. See appendix A.1 for the results of the half-yearly calculation. This calculation will help the user to understand how the temperature inside of the storage is developing over a given period. It will furthermore illustrate how the thermal- and de-stratification conductivity as well as how the overall heat loss tank coefficient per unit area, will have an effect on the stratification process inside of the energy storage. For example, if there were an inlet, outlet port in node 8, the results from performing the calculation would give the district heating company or any other user, an indication of what the temperature is at that specific layer and thereby determine if it would be more optimal to use the heat in node 8 and boost it with heat pumps. The solar collectors could also be used as a booster although it requires a warm and sunny day. By performing this calculation and thereby making the district heating company aware of this possibility, would open up for new ways to optimise their production. As of right now the energy production unit that is chosen is mostly based

on fuel prices and electricity prices. Adding this option would make the decision making much more flexible for the production companies when choosing the operation strategy. This is however entirely dependent on the capacity of the energy storage and on both the market prices for fuel and electricity as well as how much the sun is shining. An example of the possibilities and the flexibility in production will be described in the following:

High gas price, low electricity price. Energy storage at 50%

For this example, the gas price is high but the electricity price is low. This means that it would not be optimal to use gas motors or gas boilers in order to produce heat. With the low electricity price it would be most optimal to use a heat pump or an electric boiler. If this example would be used in an energy modeling tool such as energyPRO, the storage would only have two temperatures, one at the top and one at the bottom. This means that in this example the heat pump or electric boiler would use the cold water at the bottom of the storage. But by implementing the calculations of the temperature levels makes it possible to know what the temperature levels are inside of the storage, and if it were to be implemented in an energy modeling tool, it would make it possible to optimise the energy production even more. The reason for this is because it enables the modeling tool to use the temperature in the middle of the storage as long as there are an inlet and outlet port in the middle of the storage, thus improving the coefficient of performance (COP) factor of the heat pump due to the use of water with a higher temperature. It could even calculate if the solar collectors would be capable of increasing the temperature in the middle of the storage to the supply temperature send out to the consumers. This kind of calculation would enable energy modeling tools to optimise the energy production even more, and give the energy system that is being modelled much more flexibility in terms of what type of energy production units should be producing at the specific hour.

6.2 Pipeline network

The equations described in section 5.2 regarding the fluid in the pipes will be explained in more detail and with examples of what they calculate and the answers. When performing the calculations of what happens inside the pipes, it is assumed that the pipes in the ground is set to be Twin pipes where the supply and return pipe will be in the same overall pipe.

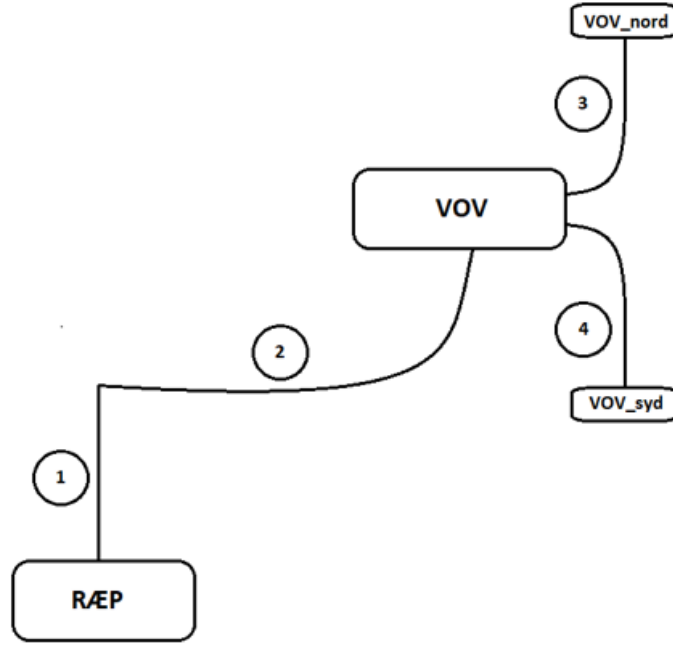


Figure 6.3: Overview of the 4 pipes that are calculated in the Excel model.

One of the four pipe sections will be used as an example of how the equations in section 5.2 can be used in practice. The example will be based on pipe number four as shown in figure 6.3, as in the Excel model will be the pipe that supplies the southern part of Vodskov.

As mentioned in the methodology chapter to start the calculation on the pipes, the mass flow rate is the first thing that needs to be calculated in order to calculate the velocity of the flow. To do this the equation 5.12 will be used.

$$\dot{m} = \frac{8,506.70[kW]}{4.17[kJ/kg/K] * (74.96 - 35)[K]} = 51.056[kg/s] \quad (6.7)$$

By having calculated the mass flow it is now possible to calculate the velocity of the flow. The velocity is necessary to know in order to calculate the Reynolds number as well as the pressure and overall losses in the system later on. The velocity can be calculated by using equation 5.14 as described in section 5.2.

$$v_{flow} = \frac{51.056[kg/s]}{990.1[kg/m^3] * \pi * (\frac{0.273[m]}{2})^2} = 0.88[m/s] \quad (6.8)$$

In all the calculations where ρ is being used, it is decided that the value for ρ is set to be 990.1 [kg/m³] which is the density of water at 45°C. This is done to make the model a little more simple instead of having a changing density with the changing temperature.

The next step in making the calculation for pipe four, is to calculate the pressure change in the pipe along the way in the system. To do this the Bernoulli equation is used. As mention in section 5.2, the Bernoulli equation is about an equilibrium, what goes into the pipe must be equal as to what comes out of the pipe, as expressed in equation 5.15. In order to calculate pipe four it is necessary to take pipe two and pipe three into account as well. In the pipeline network, pipe four is a part of a Y-junction where pipe two is split into pipe three and four, see figure 5.9. The equation used here is the flow continuity equation 5.18. What is interesting for using this equation, is that it also provides a way for calculating the velocity in the pipe, as all the areas should be known variables. Due to the velocity was calculated earlier the continuity equation has become rather irrelevant in the calculations of pipe four. The pressure in pipe four is a unknown factor that needs to be calculated. This can be done by the Bernoulli equation 5.17 which is for pipe contraction. It is assumed that the pressure in pipe two is already calculated and known in order to calculate the pressure in pipe four.

$$P_4 = 7.0597 * 10^5 [Pa] + \left(\frac{1}{2} * 990.1 [kg/m^3] * (1.47^2 - 0.88^2 [m/s])\right) = 7.0664 * 10^5 [Pa] \quad (6.9)$$

The reason for the change in pressure and even an increase in the pipe, is due to the pipe is splitting into two pipes meanwhile the dimensions of pipe four stays the same whereas the velocity changes according to the change in mass flow. By looking at the change in elevation it makes good sense that there is an increase in pressure due to the small drop in height, the higher the water travel the lower the pressure becomes, and vice versa.

Reynolds equation is used in order to calculate the flow in pipe four. The Reynolds equation is followed by the Colebrook equation which gives an indication of how much friction that occurs inside the pipe due to the type of flow.

The Reynolds number is calculated by using equation 5.19 and substituted with the needed numbers for the calculation.

$$Re = \frac{990.1 [kg/m^3] * 0.88 [m/s] * 0.273 [m]}{0.000378} = 629,945.40 \quad (6.10)$$

This calculated Reynolds number is above 3,000 and the flow inside the pipe is therefore a turbulent flow. As mentioned earlier the calculated Reynolds number will be used in the Colebrook equation 5.20. The Colebrook equation is a iterative method for finding the friction factor f . The way of finding the friction factor is to use a moody diagram to establish a initial guess and then do the calculation. This will give a new and more precise friction factor, and this value can then again be used in the equation. This method can be repeated over and over until the friction factor is only changing by a very little amount. Another way of using this equation is to use a computer based solver, that will solve for f and give a friction factor that can be used right away. By using the equation iterative, will initially give a more precise number to work with, but by solving for f will give a

number right away and the answer will in the end only vary very little. In the Excel model for the pipeline network the solving method of using the equation has been chosen. The solving method in Excel have been found as a preamble and just used directly in the model [calculation blogspot, 2013]. The equation is used like the following.

$$\frac{1}{\sqrt{f}} = -2.0 \log\left(\frac{\frac{2 \cdot 10^{-6}}{0.273[m]}}{3.7} + \frac{2.51}{629,945.40}\right) \rightarrow \text{solving} \rightarrow f = 0.0127[-] \quad (6.11)$$

Having calculated the friction factor it is now possible to calculate the different losses in the network. The most interesting losses are the pressure loss or drop and the head loss. The pressure drop demonstrate have the pressure is behaving through the pipe. This is necessary to know in order to know how big a pump would be needed in order to overcome the loss. The head loss indicates the loss in height which is necessary to know in order to know what kind of pump should be installed in the system. To calculate the pressure loss the equation 5.21 will be used.

$$\begin{aligned} \Delta P_L = 990.1[kg/m^3] * 9.81[m/s^2] * ((13.45 - 13.61[m]) + 0.0127[-] \\ * \frac{34.47[m]}{0.273[m]} * \frac{0.88[m/s]^2}{2 * 9.81[m/s^2]}) = 3,046.57[Pa] \end{aligned} \quad (6.12)$$

$$H_L = 0.0127[-] * \frac{34.47[m]}{0.273[m]} * \frac{0.88[m/s]^2}{2 * 9.81[m/s^2]} = 0.06[m] \quad (6.13)$$

The pressure loses 3,046.57 [Pa] through the pipe and will lose 0.06 [m] in height through pipe four. This means that if necessary, a pump must be installed in order to overcome the loss in pressure and height by lifting the water earlier so it can reach its destination. There where no pump connected to the pipeline network in the Excel model. It is assumed that there is a pump directly after the heat plant that will lift the water in the same amount as the lift made in TERMIS. This is also how the Bernoulli equation can be used to calculate the pressure points before and after each pipe through out the pipeline network. The first pressure point P_1 is assumed to be the same as the pressure point in TERMIS. By using the same point of origin as TERMIS makes it easier to compare the rest of the results from TERMIS with the numbers calculated in the Excel model. The pressure loss equation can also be rewritten so the frictional gradient can be found. This is a very good indicator of how much stress the pipe is under due to the amount of water going through. In order to compare the results from the Excel model with the results from TERMIS the frictional gradient is necessary to calculate. The equation will be calculated as follows:

$$\frac{\Delta P_L}{L_{pipe}} = \frac{3,046.57[Pa]}{34.47[m]} = 17.94[Pa/m] \quad (6.14)$$

As mention in section 5.2, the frictional gradient may not exceed 200 [Pa/m] which is a preset defined in TERMIS[Aalborg Forsyning, 2019]. Any number below that limit is of no concern.

The last form of loss in the pipeline network that needs to be calculated, is the heat loss of the fluid to the pipe and the surroundings. The equation used was also mentioned in section 5.2, and to keep it as simple as possible the equation shown here will only be equation 5.24.

$$Q_{hl} = 2 * 9.38[W/m] = 18.77[W/m] \quad (6.15)$$

From the heat loss calculation 6.15 it is now possible to calculate what the temperature drop in pipe four will be. To do this, equation 5.28 will be used.

$$T_{supply} = \frac{(\frac{18.77[W/m]*34.47[m]}{1,000})}{4.17[kJ/kg/K] * 51.056[kg/s]} = 0.0026^{\circ}C \quad (6.16)$$

The last thing that needs to be calculated is the return temperature, With the heat loss, it can be calculate what the supply temperature is going to be with a heat loss of 28.47 [W/m] in pipe four. The return temperature loss will be calculated by using equation 5.29.

$$T_{return} = \frac{(\frac{35^{\circ}C+35^{\circ}C}{2} - 8^{\circ}C) * (\frac{34.47[m]*0.025[W/m*K]}{1,000})}{4.17[kJ/kg/K] * 51.056[kg/s]} = 0.00011^{\circ}C \quad (6.17)$$

With all these calculations made, it is now possible to compare the results calculated in the Excel model with the results extracted from TERMIS.

Excel model						
				Nord	Syd	
		1	2	3	4	Total
Heat loss	W/m	18,77	16,27	15,42	16,27	
frictionsgradient	Pa/m	21,15	49,82	90,61	17,94	
Temperature supply	°C	75,00	74,96	74,90	74,96	
Temperature Return	°C	34,99	34,99	35,00	35,00	
supply pressure	mvs	83,70	72,01	67,04	71,77	
velocity	m/s	1,04	1,47	1,55	0,88	

Figure 6.4: This figure shows all the results calculated in the Excel model for the pipeline network to Vodskov with the four set of pipes in the system.

Senario 1 SP Termis						
				Nord	Syd	
		1	2	3	4	Total
Heat loss	W/m	29,27	25,63	25,6	21,69	
frictionsgradient	Pa/m	43,95	123,09	48,74	176,55	
Temperature	°C	75	74,9	74,8	74,8	
Temperature Return	°C	34,99	35,00	35,00	35,00	
supply pressure	mvs	83,7	76,9	60,4	74,8	
velocity	m/s	1,33	1,88	1,66	1,17	

Figure 6.5: This figure shows the results extracted from the TERMIS model made for the pipeline network with the four set of pipes in the system.

From figure 6.4 and 6.5 it can be seen that the numbers calculated in the Excel model, varies a bit from the numbers made in TERMIS. The numbers calculated for the velocity and supply pressure seems to be the most consistent on getting as close as possible to the numbers from TERMIS, which satisfying, as the numbers calculated in TERMIS is not given by any formulas. This indicates that it might be the correct formulas there have been used in the Excel model, but it can not be said with any certainty. The frictional gradient seems to be the result that deviates the most from the TERMIS results. This indicates that something is not correct in that equation.

Sensitivity analysis of the Excel model

Excel model						
				Nord	Syd	
		1	2	3	4	Total
Heat loss	W/m	18,77	16,27	15,42	16,27	
frictionsgradient	Pa/m	34,46	81,70	103,50	31,64	
Temperature supply	°C	75,00	74,96	74,90	74,96	
Temperature Return	°C	34,99	34,99	35,00	35,00	
supply pressure	mvs	83,70	67,46	61,78	67,21	
velocity	m/s	1,33	1,88	1,66	1,17	

Figure 6.6: This figure shows the numbers calculated in the Excel model for the pipeline network in Vodskov with the four set of pipes in the network but using the same velocity as in TERMIS.

Excel model						
				Nord	Syd	
		1	2	3	4	Total
Heat loss	W/m	18,77	16,27	15,42	16,27	
frictionsgradient	Pa/m	29,13	68,48	83,42	26,62	
Temperature supply	°C	75,00	74,96	74,90	74,96	
Temperature Return	°C	34,99	34,99	35,00	35,00	
supply pressure	mvs	83,70	69,32	64,83	69,07	
velocity	m/s	1,22	1,72	1,49	1,07	

Figure 6.7: This figure shows the numbers calculated in the Excel model for pipeline network in Vodskov with the four set of pipes in the network but using the same mass flow as in TERMIS.

Excel model						
				Nord	Syd	
		1	2	3	4	Total
Heat loss	W/m	18,77	16,27	15,42	16,27	
frictionsgradient	Pa/m	34,46	81,70	103,50	31,64	
Temperature supply	°C	75,00	74,96	74,90	74,96	
Temperature Return	°C	34,99	34,99	35,00	35,00	
supply pressure	mvs	83,70	67,46	61,78	67,21	
velocity	m/s	1,33	1,88	1,66	1,17	

Figure 6.8: This figure shows the numbers calculated in the Excel model for the pipeline network with the four set of pipes in the network but with a combination of the velocity and mass flow as in TERMIS.

Figure 6.6, 6.7 and 6.8 are showing the results after implementing the changes in the Excel model which can be seen in figure 6.4. In order to show how the Excel model compare to the TERMIS model, the Excel model have to use some of the same numbers as TERMIS in order to recreate the same results as in TERMIS.

Figure 6.6 shows the results after changing the velocity used in the Excel model to the same velocity used in TERMIS. The modified Excel model shows an increase in the frictional gradient and a change in the supply pressure in the form of a decrease. Due to the Excel model is set up so the velocity is calculated on the behalf of the mass flow, it makes sense that only changing the velocity would not give the right results.

Figure 6.7 shows the results after changing the mass flow used in the Excel model to the same mass flow used in TERMIS. The result in the Excel model after the modification to the mass flow, shows a change in the velocity which is getting closer to the TERMIS results. The frictional gradient increases as well, but the increase is not as high as when using the same velocity as in TERMIS. Changing the mass flow will have a greater impact on the model than changing only the velocity. It also shows that the velocity is dependent on the mass flow as mention earlier in this section. The change in supply pressure also changes with the change in mass flow, but not as much as when changing the velocity.

Figure 6.8 shows the results after changing both the velocity and the mass flow in the Excel model, to the same numbers as in TERMIS. The results after changing these two parameters gives more or less the same results as shown in figure 6.6 where only the velocity was changed. The frictional gradient gives the same result as when only changing the velocity. The supply pressure shows the same tendency as the frictional gradient. The change made in the Excel model with the result of the velocity and mass flow from TERMIS, indicates that the Excel model is lacking at some points compared to TERMIS. The Excel model can not recreate the same results as TERMIS even though it uses the same values as TERMIS for the velocity and mass flow.

Validation of the TERMIS results

After making a sensitivity analysis on the Excel model, it will make good sense to try to validate the TERMIS results with the formulas used in the Excel model. In theory it should be possible to create the same results by using the results from the TERMIS model. The calculations that will be validated is the velocity and mass flow. In the TERMIS model both the velocity and mass flow is given, which makes them a good point of origin for the validation process. To calculate the velocity equation 5.14 can be used. The calculation will be based on pipe one from TERMIS.

$$v_{flow} = \frac{99.752[kg/s]}{990.1[kg/m^3] * \pi * (\frac{0.3239[m]}{2})^2} = 1.22[m/s] \quad (6.18)$$

The calculation made in equation 6.18 gave a different result than expected. The results from TERMIS states that the number after the calculation should have been 1.33 [m/s] and not 1.22 [m/s] as calculated. This calculation indicates that something is not right in the calculation, either the equation used is wrong or the numbers used in the calculation is wrong. The next step will be to try and calculate the mass flow in order to see if the same thing occur and gives a different result than expected. The mass flow will be calculated by using equation 5.14 and rewriting it so it is the mass flow, that will be calculated and not the velocity flow.

$$\dot{m} = \frac{1.33[m/s] * \pi * 990.1[kg/m^3] * (0.3239^2[m])}{4} = 108.50[kg/s] \quad (6.19)$$

This calculation also gave a different result than expected. The results from TERMIS states that the mass flow is 99.752 [kg/s] and not 108.50 [kg/s] as calculated. The calculation likewise indicates that something is not right in the way the calculations is made. It must be assumed that TERMIS is providing the right results, and there is something wrong with the used equation or numbers. If the calculation are unable produce the same results as TERMIS, then it is very hard to validate the Excel model and thereby compare it to TERMIS.

If it is the numbers used in the equation that is the problem then there are only two numbers that it can be. It is either the used density of water or the diameter of the pipe that is incorrect. As the density of water is set to be used at 45°C and not 75°C it can be considered a minor error in the calculation, but the change in value is negligible, which means that it must be the diameter that is the root of the problem.

For example when using the diameter of a Ø323 pipe, it is not stated whether it is the full diameter or the inner diameter of the pipe. If it is assumed that it is the full diameter that is given, it is necessary to calculate the what the inner diameter would be in order to recreate the results from TERMIS. This can be done by isolating for the diameter in equation 5.14 and adding the values from TERMIS to it. The equation will then look like the following:

$$D_{inner} = \frac{2 * \sqrt{99.752[kg/s]} * \sqrt{1.33[m/s] * \pi * 990.1[kg/m^3]}}{1.33[m/s] * \pi * 990.1[kg/m^3]} = 0.311[m] \quad (6.20)$$

Equation 6.20 gives an inner diameter of 0.311 [m] which verifies the speculation of there is a difference between the full diameter and the inner diameter when using an Ø323 pipe. The difference consist of 13.34 [mm] and gives a material thickness of 6.67 [mm] to the steel pipe. Considering the rather large dimensions of the pipe, it is not an unrealistic material thickness. By using the calculated inner diameter of the pipe instead of Ø323, the results from TERMIS regarding the velocity and mass flow can be recreated.

$$v_{flow} = \frac{99.752[kg/s]}{990.1[kg/m^3] * \pi * \left(\frac{0.311[m]}{2}\right)^2} = 1.33[m/s] \quad (6.21)$$

$$\dot{m} = \frac{1.33[m/s] * \pi * 990.1[kg/m^3] * (0.311^2[m])}{4} = 99.752[kg/s] \quad (6.22)$$

Excel model with new inner diameter

After proving that in order to validate the results from TERMIS, the diameter must be changed. The diameter used earlier in the model was the full diameter and not the inner diameter which was just proved, and by changing this, it would be interesting to see what kind of impact that would have on the Excel model. Furthermore it would be interesting to see the values of the mass flow when changing it to the values used in TERMIS just as was done in the sensitivity analysis.

Excel model						
				Nord	Syd	
		1	2	3	4	Total
Heat loss	W/m	16,62	14,62	13,67	14,65	
frictionsgradient	Pa/m	26,25	62,47	88,42	26,74	
Temperature supply	°C	75,00	74,96	74,90	74,96	
Temperature Return	°C	34,99	34,99	35,00	35,00	
supply pressure	mvs	83,70	70,23	65,42	69,96	
velocity	m/s	1,14	1,61	1,49	1,05	

Figure 6.9: This figure shows the values calculated in the Excel model after changing the diameter to the inner diameter.

Excel model						
				Nord	Syd	
		1	2	3	4	Total
Heat loss	W/m	16,62	14,62	13,67	14,65	
frictionsgradient	Pa/m	35,94	85,38	109,24	33,04	
Temperature supply	°C	75,00	74,97	74,91	74,97	
Temperature Return	°C	34,99	34,99	35,00	35,00	
supply pressure	mvs	83,70	66,94	60,93	66,69	
velocity	m/s	1,33	1,88	1,66	1,17	

Figure 6.10: This figure shows the values calculated in the Excel model after changing the diameter to the inner diameter and with the use of the mass flow from TERMIS.

Figure 6.9 shows the new results for the model with the same four sets of pipes. After changing the value for the diameter, the Excel model showed some more promising signs for the velocity compared to the TERMIS results. The Excel model is still not able to recreate the exact same results as TERMIS, but the accuracy of the result has improved. The supply pressure seems to be higher throughout the network than it was before, but it makes sense that changing the diameter and making the pipe smaller will have an impact on the pressure. The frictional gradient has increased as well along with change in diameter. The frictional gradient is based on the pressure in the pipe, therefore a change in frictional gradient is to be expected. The heat loss which also is dependent on the diameter of the pipe has decreased, resulting in the Excel model lose less heat than before. Compared to the heat loss results in TERMIS, the heat loss in the Excel model is still too low.

Figure 6.10 shows the Excel model with the implementation of the mass flow from TERMIS. By using the mass flow from TERMIS it can be seen that the velocity is matching the TERMIS model. As the velocity is dependent on the mass flow, it makes good sense that it shows the right result with the use of mass flow from TERMIS. The mass flow also have an impact on the supply pressure which is decreasing with the change. This deviates further from the TERMIS results in pipe two and four but is really close in pipe three. The frictional gradient has increased along with the decrease in supply pressure, or the increase in loss of pressure.

TERMIS vs energyPRO

The calculations made in the Excel model is intended to show with rough calculation, that it is possible to recreate the same results as TERMIS, without any specific knowledge of how the calculations in TERMIS is made. If the equation used in the Excel model were able to recreate all of the results from TERMIS it would be possible to combine these equations to a already existing modeling tool such as energyPRO. The modeling tools, energyPRO and TERMIS, are both designed to make calculations on energy systems, but they have different areas of expertise. TERMIS is very focused on planning and design purposes, like setting up pipeline networks in new areas, where it is necessary to calculate how big the pipes needs to be and how many pumps are needed to make sure that the future

consumers are supplied by hot water. EnergyPRO as a modelling tool is more focused on the technical and financial analysis of simple or complex energy systems. Where each of these tools lacks expertise, the other one excels. It would therefore make good sense for energyPRO to look into the possibility of adopting the networks calculation made in TERMIS. In a more user friendly point of view, it would be a good idea to make the pipeline networks visually, for example in a GIS format, TERMIS utilises this as well. It makes it easier for the user to see, visually, where the problems in a system would be and thereby easier for them to locate it, instead of looking at raw numbers like in Excel for example.

6.3 A combination of the Excel models

In order to demonstrate how the pipeline network and temperature levels models can be combined into one coherent model, an example is used where energyPRO forms the foundation of the combined model. This example is based on the combined heat demand from Vodskov syd and nord in the period from October 18th at 13 o'clock till October 19th to 14 o'clock. For this example it is assumed that the model, at any time, can supply the consumers with a minimum temperature level of 60°C. The heat pump in this example have a capacity of 8 MW and a COP factor at 4. The heat pump is not allowed to run at partial load.

The heat pump produces heat at 80°C and is sent to Vodskov as well as the thermal energy storage in a charging situation. The heat going to the thermal energy storage is sent in at the top of the storage and the colder water at the bottom, is sent to the heat pump to get heated. The water can also be tapped from the middle of the storage tank where it will be warmer. This is however depend on the spot marked prices on electricity, when it will be best to do so. The produced heat that is not going to the thermal energy storage is sent to Vodskov. For this example the supply temperature to the town is only 60°C instead of the 80°C which is produced at the heat pump. In order to lower the temperature to the 60°C, the return temperature of 35°C is shunted into the hot water in order to mix it to 60°C. The return water from the town is sent back to the heat pump where it is mixed with the cold water from the thermal energy storage before entering the heat pump. In situations where the heat pump is turned off, the heat is supplied by the thermal energy storage. The figure 6.11 illustrates how the system could look like.

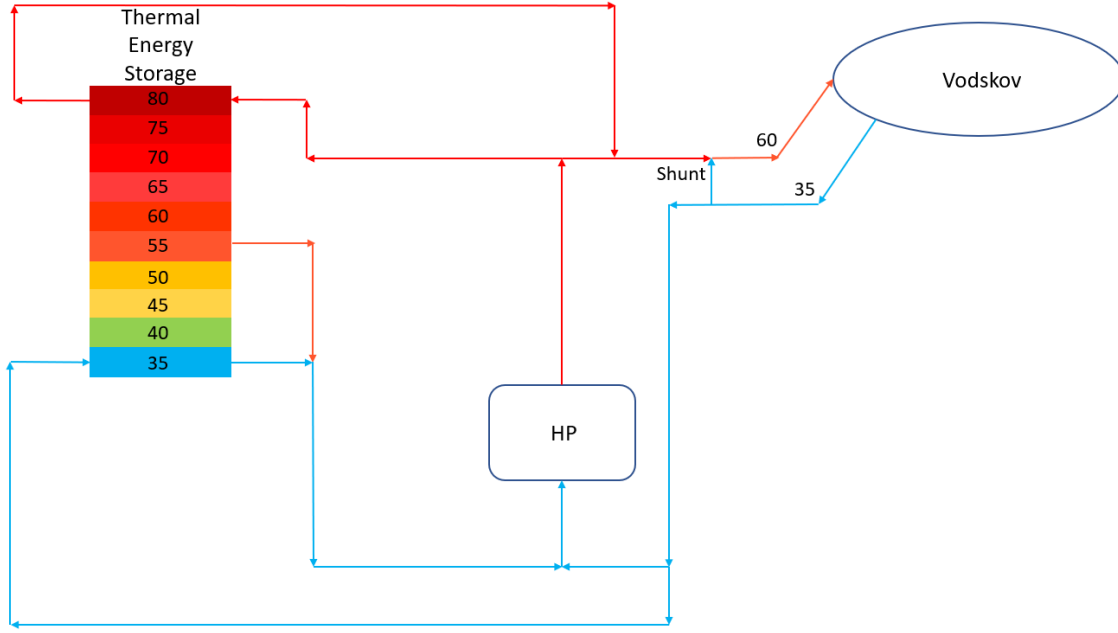


Figure 6.11: Flow diagram of the combined system

The chosen time period illustrates a charging situation where the heat pump covers the heating demand and the excess heat is sent into the thermal energy storage. The mass flow from the heat pump and into the heat network is dependent on the heat demand from the consumers. The mass flow from the heat pump into the storage can then be calculated by the difference between the heat pump capacity and the heat demand multiplied by 1,000, divided by the specific heat capacity of water divided by the temperature difference inside of the storage. Which equals a loading flow into node 1 at 20.1 [kg/s] in the first hour of the calculation. The loading flow differentiates as the heat demand develops over the chosen time period. The development of the temperature inside the thermal energy storage can be seen in figure 6.12.

	Abværk	Heat Pump	Loading flow	Node	1	2	3	4	5	6	7	8	9	10	11	12	13	14	15
	[MW]	[MW]	In node 1 [kg/s]	m_{Mass} [kg/s]															
Start på tidskridt					80.0	80.0	80.0	35.0	35.0	35.0	35.0	35.0	35.0	35.0	35.0	35.0	35.0	35.0	35.0
18/10/2019 13:00	4.2463	8.0000	19.9	19.9	80.0	80.0	80.0	46.7	35.0	35.0	35.0	35.0	35.0	35.0	35.0	35.0	35.0	35.0	35.0
18/10/2019 14:00	4.2463	8.0000	19.9	19.9	79.9	79.9	79.9	55.8	38.0	35.0	35.0	35.0	35.0	35.0	35.0	35.0	35.0	35.0	35.0
18/10/2019 15:00	4.2463	8.0000	19.9	19.9	79.9	79.9	79.9	61.7	42.5	35.8	35.0	35.0	35.0	35.0	35.0	35.0	35.0	35.0	35.0
18/10/2019 16:00	4.2463	8.0000	19.9	19.9	79.9	79.9	79.8	66.4	47.5	37.5	35.1	34.9	34.9	34.9	34.9	34.9	34.9	34.9	34.9
18/10/2019 17:00	4.2463	8.0000	19.9	19.9	79.9	79.8	79.8	69.9	52.4	40.1	35.7	35.0	34.9	34.9	34.9	34.9	34.9	34.9	34.9
18/10/2019 18:00	3.4039	8.0000	24.4	24.4	79.9	79.8	79.8	73.0	58.0	44.0	37.1	35.2	34.9	34.9	34.9	34.9	34.9	34.9	34.9
18/10/2019 19:00	3.4039	8.0000	24.4	24.4	79.9	79.8	79.7	75.1	62.7	48.4	39.3	35.8	35.0	34.9	34.9	34.9	34.9	34.9	34.9
18/10/2019 20:00	3.4039	8.0000	24.4	24.4	79.9	79.8	79.7	76.6	66.7	53.0	42.2	36.9	35.2	34.9	34.9	34.9	34.9	34.9	34.9
18/10/2019 21:00	3.4039	8.0000	24.4	24.4	79.9	79.8	79.7	77.5	69.8	57.3	45.6	38.6	35.8	35.0	34.9	34.9	34.9	34.9	34.9
18/10/2019 22:00	3.4039	8.0000	24.4	24.4	79.9	79.8	79.7	78.2	72.2	61.3	49.3	40.8	36.6	35.2	34.9	34.9	34.9	34.9	34.9
18/10/2019 23:00	3.4039	8.0000	24.4	24.4	79.9	79.8	79.7	78.6	74.1	64.7	53.1	43.5	38.0	35.7	35.0	34.9	34.8	34.8	34.8
19/10/2019 00:00	3.9406	8.0000	21.5	21.5	79.9	79.8	79.7	78.9	75.3	67.3	56.4	46.2	39.5	36.3	35.2	34.9	34.8	34.8	34.8
19/10/2019 01:00	3.9406	8.0000	21.5	21.5	79.9	79.8	79.7	79.1	76.3	69.5	59.4	49.0	41.4	37.2	35.5	35.0	34.8	34.8	34.8
19/10/2019 02:00	3.9406	8.0000	21.5	21.5	79.9	79.7	79.6	79.2	77.0	71.4	62.2	51.9	43.5	38.3	35.9	35.1	34.9	34.8	34.8
19/10/2019 03:00	3.9406	8.0000	21.5	21.5	79.9	79.7	79.6	79.3	77.6	73.0	64.8	54.8	45.9	39.8	36.6	35.3	34.9	34.8	34.8
19/10/2019 04:00	3.9406	8.0000	21.5	21.5	79.9	79.7	79.6	79.3	78.0	74.2	67.1	57.6	48.3	41.5	37.5	35.7	35.0	34.8	34.8
19/10/2019 05:00	3.9406	8.0000	21.5	21.5	79.9	79.7	79.6	79.4	78.4	75.3	69.0	60.2	50.9	43.4	38.6	36.2	35.2	34.9	34.8
19/10/2019 06:00	4.9172	8.0000	16.3	16.3	79.9	79.7	79.6	79.4	78.5	75.9	70.3	62.1	52.9	45.0	39.6	36.7	35.4	34.9	34.8
19/10/2019 07:00	4.9172	8.0000	16.3	16.3	79.8	79.7	79.6	79.4	78.7	76.4	71.5	63.8	54.8	46.6	40.7	37.3	35.6	35.0	34.8
19/10/2019 08:00	4.9172	8.0000	16.3	16.3	79.8	79.7	79.6	79.4	78.8	76.9	72.5	65.4	56.7	48.4	42.0	38.0	36.0	35.1	34.8
19/10/2019 09:00	4.9172	8.0000	16.4	16.4	79.8	79.7	79.6	79.4	78.9	77.2	73.4	66.9	58.5	50.1	43.3	38.8	36.4	35.3	34.9
19/10/2019 10:00	4.9172	8.0000	16.4	16.4	79.8	79.7	79.6	79.4	79.0	77.6	74.2	68.3	60.3	51.9	44.8	39.8	36.9	35.5	34.9
19/10/2019 11:00	4.9172	8.0000	16.4	16.4	79.8	79.7	79.5	79.4	79.0	77.8	74.9	69.5	62.0	53.7	46.3	40.8	37.5	35.8	35.0
19/10/2019 12:00	4.9172	8.0000	16.4	16.4	79.8	79.7	79.5	79.4	79.1	78.0	75.5	70.6	63.6	55.4	47.8	42.0	38.2	36.1	35.2
19/10/2019 13:00	4.9172	8.0000	16.5	16.5	79.8	79.7	79.5	79.4	79.1	78.2	76.0	71.6	65.1	57.2	49.5	43.2	39.0	36.6	35.4
19/10/2019 14:00	4.9172	8.0000	16.6	16.6	79.8	79.7	79.5	79.4	79.1	78.4	76.4	72.5	66.4	58.8	51.1	44.6	39.9	37.1	35.6

Figure 6.12: Temperature distribution in a chosen charging situation.



Figure 6.13: An excerpt from energyPRO. The area between the dotted lines is the chosen time period.

Figure 6.13 illustrates how the users of energyPRO can see the development of the storage when it is being charged. The only indication of what is available in the storage is the amount of MWh and not what temperature levels are available. If the calculations of how to calculate the temperature levels where to be implemented in for example energyPRO, it would give the user a better understanding of what temperatures are actually available inside of the storage. Furthermore it would be possible for energyPRO to use these different temperature levels to optimise the energy production, thereby choosing which energy producing units should be producing or be used as a booster, depending on what temperatures are available, as also mentioned in the example in the last paragraph in section 6.1.

		Heat loss	frictionsgradient	Temperature supply	Temperature Return	supply pressure	velocity	Mass flow
Time/hour	pipe	W/m	Pa/m	°C	°C	mvs	m/s	kg/s
1	1	14,00	5,91	60,18	34,97	83,70	0,54	40,44
	2	12,32	14,03	60,11	34,99	77,15	0,76	40,44
	3	11,53	19,84	60,00	35,00	76,37	0,71	13,94
	4	12,35	6,00	60,11	35,00	76,90	0,50	26,50
2	1	14,00	5,91	60,18	34,97	83,70	0,54	40,44
	2	12,32	14,03	60,11	34,99	77,15	0,76	40,44
	3	11,53	19,84	60,00	35,00	76,37	0,71	13,94
	4	12,35	6,00	60,11	35,00	76,90	0,50	26,50

Figure 6.14: A 2 hour cut from the 26 hour model showing the different calculated results for the pipeline network

The figure 6.14 shows the values for the pipeline network of the four pipes on a hourly basis. The results is calculated from the heat consumption given from the energyPRO model in the 26 hour time period. As mention, this a charging situation where the heat produced by the heat pump is divided between the heat consumption from the town of Vodskov and the thermal energy storage. In the hours where the heat consumption is the same, the results stays the same. The supply temperature has been set to be supplied at 60°C, due to the small amount of heat loss in the system, it is not necessary to have a higher supply temperature in order to supply the consumers with water at 60°C as promised. As the

heat consumption in these given hours is not nearly as high as the heat consumption at its peak hour, the mass flow and velocity are so low that the pipeline network in no way is overloaded. This example demonstrates that a more detailed temperature level modes of the thermal energy storage and a pipeline network model can be combined. The fully detailed hourly model in the pipeline network can be found in Appendix A.2.

Discussion 7

The following discussion will expand on some of the challenges there are with the existing energy modeling tools regarding thermal energy storage and pipeline networks as well as addressing some of the challenges when simplifying the calculations. This discussion will therefore primarily focus on the implementation of the temperature level calculation as well as the pipeline network calculation into an already existing energy modeling tool.

Thermal energy storage vs. energy modeling tools

It is common practice in most energy modeling tools to calculate the rate of heat loss from the thermal energy storage with an average or overall U-value [Cruickshank, 2009]. One of the issues by using an average or overall U-value is that the different variations of the thermal energy storage geometry is not taken into consideration [Cruickshank, 2009]. This is also true for the inlet and outlet ports, these ports can act as thermal conduits through the insulation and thereby increase the heat loss from the thermal energy storage tank [Cruickshank, 2009]. But one of the main issues in many of the energy modeling tools, is that the thermal energy storage is modelled as a two dimensional storage. This means that the energy modeling tools is only working with two temperature levels inside of the storage, one temperature at the top of storage and one temperature at the bottom of the storage. Figure 7.1 is a snapshot from the energy modeling tool, energyPRO, where all of the storage inputs can be seen. EnergyPRO does have the possibility to adjust the calculation of the heat loss, U-value, in order to accommodate for the geometry of the specific energy storage. As can be seen on top of the figure, energyPRO only have the possibility of using two temperatures, one at the top and one at the bottom of the storage.

Varmelager

Volumen [V]
172248.8 m³

Temperatur i toppen af lageret [Tt]
90.00 °C

Temperatur i bunden af lageret [Tb]
40.00 °C

Udnyttelsesgrad
100.0 %

Lagerkapacitet:
9980.00 MWh per 01/01/2019

Lagerindhold ved beregningsstart 01/01/2019 00:00: 0 MWh
Ønsket lagerindhold per 01/01/2020 00:00: 900 MWh

Minimum lagerkapacitet i % af lagerkapacitet
0.0 % 0.00 MWh

☒ **Lagertab**

Lagerets højde [h] 79.00 m Lager radius [Radius] 26.34 m Isoleringstykkelse [s] 300.00 mm Varmedningsevne [Lambda] 0.0370 W/(m*K)

Omgivende temperatur [Ta]
<Konstant> 20.00 °C

Formel for varmetab ved fuldt lager ☐ Brugerdefineret

$$(\text{Lambda} * 1000 / \text{s}) * 2 * \pi * (\text{h} * \text{Radius} + \text{Radius}^2) * (\text{Tt}(_) - \text{Ta}(_)) / 10^6$$
 MW

Formel for varmetab ved tomt lager

$$(\text{Lambda} * 1000 / \text{s}) * 2 * \pi * (\text{h} * \text{Radius} + \text{Radius}^2) * (\text{Tb}(_) - \text{Ta}(_)) / 10^6$$
 MW

☐ Drift begrænset til periode

Kommentarer:

Ok Annuller

Figure 7.1: An illustration of the storage options available in energyPRO.

These kind of assumption or simplification will lead to incorrect outcomes of the heat loss and in the temperature distribution within the energy storage. Resulting in the energy modeling tools not fully demonstrating the flexibility a thermal energy storage could provide to the modelled energy system. The energy modeling tools are often used on a specific energy system in order to analyse how the energy system can be optimised. This can be done by either changing the production or what kind of energy producing unit should have priority based on for example fuel prices, or by investing in a thermal energy storage both with or without a solar combination. Then it is a bit contradictory that many of the energy modeling tools are not capable of doing a more correct optimising of the energy system due to simplifications in regards to the calculation of heat loss, U-value, and or only being capable of calculating with an inlet temperature and an outlet temperature.

This results in the energy modeling tool not being able to optimise the energy system as much as possible because of these simplifications. If the energy modeling tool were able to take the temperature levels inside of the thermal energy storage into consideration it would have the means necessary in order to optimise the energy system even further. By being able to calculate the temperature levels inside of the thermal energy storage the energy modeling tool could also calculate more precisely when it would be most optimal to charge or to discharge the storage.

An example could be: If the heat demand exceeds the current supply of heat provided by

a natural gas fired motor running at full capacity, then there are a number of ways of how to deliver the heat. Depending on the heat capacity of the storage and the temperatures at the inlet and outlet ports it could be possible to use the heat at the top of the storage and send that directly out into the heat network. If this is not possible then the heat can be produced either by the heat pump or by solar collectors, whereas with the current system in energy modeling tools such as energyPRO, it is only possible to use the temperature at the top and at the bottom of the storage. The heat pump could then only use the temperature of the water at the bottom of the storage, and the temperature of that water would influence the COP factor. If the energy modeling tools were able to calculate and utilise all of the temperature levels inside of the storage, then it would be possible for the heat pump to use water at a higher temperature and thereby increase its COP factor. The solar collectors on the other hand could be of little to no help, as a booster, as long as the energy modeling tools only are able to use the bottom temperature of the thermal energy storage. This could indicate that the solar collectors are more limited in the energy production than what is actually true. By being able to use the temperature at the middle of the storage, solar collectors could just as well as heat pumps, be considered as a valid booster option. The use of solar collectors as a booster option are however dependent on weather conditions and are therefore more limited than that of heat pumps.

When modeling an energy system with the implementation of solar collectors, the solar collectors are often used to heat the cold water from the bottom of the storage and send that out to the consumers, or send the heated water back into the storage. This is also what gives the highest efficiency of the solar collectors [Arcon-Sunmark, 2019]. But by being able to calculate the temperature levels inside of the storage, there would be periods where the solar collectors could use the heated water in the middle of the storage and warm that up to the supply temperature and send that out to the consumers, just like the example used earlier for the booster option. Depending on the heat demand, the solar collectors could be used to cover the demand, instead of running the natural gas motor or boiler.

Pipeline Network

The analysis showed that in general the needed equation for making a pipeline network model can be found and used to mixed satisfaction. The problem with trying to recreate the results from TERMIS, with the Excel model is that, TERMIS is set up with a more user friendly interface, where the values are put into different black boxes. This makes it somewhat difficult to know what kinds of equation have been used in the calculation. The equations used in the Excel model are based on different text books that covers the subject about heat transfer, fluid mechanics and thermodynamics. The equations used in the Excel model are potentially more general and basic compared to the equations used in TERMIS. This is potentially why some of the equations used in the Excel model can not replicate the exact values as in TERMIS.

The Excel model takes its starting point in the actual pipe sizes and length that is dug into the ground between Vodskov and Rærup, which forms the basis of the case system. The Excel model includes the elevation of the pipes from Rærup to Vodskov, which have an effect of the pressure since the pressure is dependent on that. The elevation values have been taken directly from TERMIS in order for the input values for the case system to

be as close as possible to the values from TERMIS. This should ensure that the values calculated would be close to each other, but as shown in section 6.2 the velocity seems be off, compared to the results from TERMIS. The most likely reason for this would be that the heat consumption in Vodskov do not match in terms of what they actually use. The value used for the heat consumption should be the most precise value, but it where not possible to extract the heat demand from TERMIS. This is due to the circumstances of the lockdown caused by COVID-19. It was not possible to go to Aalborg Forsyning and extract more information from the TERMIS simulation of the case system. By rewriting equation 5.12 the TERMIS value for the heat consumption can be found. The result from this calculation gives that the heat consumption should be 1.2 MW higher than the value given by Aalborg Forsyning. The heat consumption is more or less the entire foundation of all of the calculation so a difference in this number does not sets the best conditions for recreating the results from TERMIS. A reason for the heat consumption being relatively higher compared to TERMIS could be because of the model is a bit oversized to ensure that there is enough heat supplied to the town in case of expanding the town, or to supply extra heat if the weather should get colder than what is expected in the TERMIS simulation.

When trying to compare the numbers between the Excel model and the TERMIS model, the velocity number is however relatively close to the results from TERMIS. This may be because of the velocity is mostly depended on one variable, the mass flow rate, as the rest of the variables must be more or less the same, due to they are common table values. It can therefore also be argued from this calculation forward, the values will start to diverge more from the TERMIS results.

The supply and return temperature seems to be very close to result of TERMIS. The difference in supply and return temperature between the Excel model and the TERMIS model, is so small it is almost negligible. The reason here would be that the heat loss in both TERMIS and Excel is also very low and would only have a minor impact on the total heat loss.

The heat loss in the Excel model is calculated to be lower than the heat loss calculated in TERMIS. It could be because of TERMIS is more elaborate in terms of the numbers for the loss of heat in the different pipes, where the Excel model are more simple. The thermal conductivity used in the TERMIS model is not known, which could lead to a difference in the values for the use of the heat loss calculation. Due to the low value of the thermal conductivity the value should not change much before the Excel calculation would be even closer to the TERMIS results.

The supply pressure is set to be the same in pipe one in order to establish a base pressure for the Excel model. The TERMIS model have been set up there will be an increase in pressure after a certain point. This is due to a pump in the model in order to ensure that the heat will get out to the consumers. In order to simplify this, the pressure have been assumed to be the same in the Excel model and the pump have been set to be located at the heat plant in order to make the model for this case more simple to set up. The pump is not that interesting due to it is more or less just a black box where the pressure can be increased by the user. The focus have been put on the pipes instead and trying to understand the losses there will be and how the pressure is behaving throughout the network. The Excel model is showing the same tendencies as the TERMIS model but the

pressure seems to be a bit lower in the Excel model than in the TERMIS model. Again it is not known how the pressure loss is calculated in the TERMIS model and if it is considering more losses to the pressure than what have been done in the Excel model. The difference between the values are within a low margin.

The last number of the calculation is the frictional gradient. This is where the biggest discrepancy between the two models are. The numbers calculated in the Excel model seems to be a factor of two or three times lower than the frictional gradient numbers from the TERMIS model. In pipe three where the value in the TERMIS model is getting lower, the value in the Excel model increasing rapidly. This indicates that something is wrong in the way that the frictional gradient have been calculated in the Excel model.

The sensitivity analysis of the Excel model illustrated that more of the calculated results in the Excel model seems to be diverging from the results in TERMIS. By performing the sensitivity analysis is a good way for testing the Excel model. By changing the velocity to the same as in TERMIS for the Excel model showed that the frictional gradient is dependent on the velocity. Furthermore the velocity in the Excel model is dependent on the mass flow, which was demonstrated when that parameter was changed to show the affects on the model. The intention was to get as close as possible to the TERMIS results, and by changing the mass flow to the mass flow from TERMIS, it showed that the Excel results was getting closer, but still inside a reasonable error of margin. When the material thickness of the pipe was taken into consideration when making the calculation, it was possible to recreate the same velocity by using the mass flow from TERMIS. The last part of the sensitivity analysis were where both parameters was changed at the same time. This showed however mostly the same results, as if only the velocity was changed. The sensitivity analysis clearly shows that some calculation are done differently compared to TERMIS and this Excel model is only able to show the same result in velocity when using the same mass flow as in TERMIS. Even tough the same values are used as in TERMIS, the current state of the Excel model is not able to recreate the results as in TERMIS.

As mentioned in section 6.2 the different energy modeling tools have their different strength and weaknesses. Excel as a energy modeling tool is a bit different than energyPRO and TERMIS in that regards, that Excel is entirely raw data based, where the user provides the formulas and decide what needs to be calculated, where as energyPRO and TERMIS have a interface, where the user is not required to provide the formulas as they are implemented in the program. This is one of the reasons why it can be hard to replicate the results from TERMIS, due to the calculation black box. Excel has the ability to show some of the calculations, that can be made in either energyPRO or TERMIS at the same time. The Excel model demonstrates that it is possible to replicate some of the results an in TERMIS therefore making it a possibility for more research to be done to fully replicate the results of TERMIS and potentially incorporate it in another energy modeling, potentially energyPRO. If this where to be done it would likewise be a good idea to implement a map overview, for example in a GIS format, in order to visualise potential problems in the pipeline network. With a format such as Excel it is easily overlooked if there is a wrong number, but with a map format with color indication on the pipes it makes it easier to determine which and where the pipes in question are.

Combined model

The example used for the combined model is only considering a time step in energyPRO where the thermal energy storage is being charged. This does illustrate how the temperature as well as the stratification is developing, but it does not show how the storage would develop in a scenario where it would be charged and discharged multiple times. If a scenario were used with both charge and discharge cycles, it would be possible to illustrate a more realistic behaviour of the temperature levels inside of the thermal energy storage.

Due to the minimal heating loss throughout the chosen pipeline network as well as the commitment to supply the consumers with a constant minimum temperature of 60°C, 60.3°C is chosen as the supply temperature for the combined model. This may not seem as the obvious choice since the heat pump is producing heat at 80°C. In order to get the supply temperature at 60.3°C, the water coming from the heat pump is being shunted with the return water from Vodskov as illustrated in figure 6.11. If this is the correct choice regarding the supply temperature is a matter of optimisation of the energy system. Due to the flow in the pipeline network is dependent on the supply temperature, changes in supply temperature can either increase or decrease the flow in the pipeline network.

Data verification

All of the calculations made in this thesis is based on theories and equations gathered through research. In order to verify the calculated results regarding the distribution of the temperature levels inside of the energy storage, a real experiment should be conducted. By conducting a real life experiment in a smaller scale but over the same time period as used in the different examples, would help to validate the calculations made in this thesis.

The Excel calculations made in this thesis are done in such a way that it should replicate the same values as the values calculated in TERMIS. This would aid in validating the equations used in the thesis, if they are comparable to the value from TERMIS.

If the equations used in this thesis could be verified by experiments and are within a reasonable margin of error, could pave the way for integrating the calculation used in this thesis into an already existing energy modeling tool, which are not able to calculate the losses in pipeline networks and so on, or a energy modeling tool that are not able to make a more optimised energy system model in combination with a thermal energy storage.

Conclusion 8

The purpose of this thesis was to analyse the strength and weaknesses of existing energy modeling tools and evaluate improvement opportunities in order to handle the challenges posed by the future energy system towards 2030. The increasing capacity of the heating sector being electrified, a more versatile and flexible energy system is needed. This is due to energy producing units based on electricity should produce when the electricity price is low, even though the heating demand is satisfied. Which is why thermal energy storage could play a significant role in reaching the 2030 goals and facilitate the energy system of the future. The future energy system therefore demands energy modeling tools that can fully utilise the potential of the thermal energy storage as well as combining the system with the pipeline network in order to analyse if the existing pipeline network can accommodate the intended energy system. This is why the research question for this thesis is:

"What limitations does the current energy modeling tools have, and how can the individual strength of the modeling tools be combined into one?"

The purpose of the two different areas of investigation was to investigate how the temperature levels inside of a thermal energy storage could be calculated and how the stratification would develop both in a isolated perspective as well as in a charging situation. Furthermore it was investigated which equation is used in TERMIS in order to validate if it where possible to recreate the results from TERMIS by the use of multiple thermodynamics equations.

The results from the analysis of replicating the results from TERMIS indicates that some of the equation used in the thesis Excel model, is the same as in TERMIS, since the velocity results was recreated when the same mass flow as in TERMIS was used. It was however not possible to recreate the same values for the calculated mass flow, heat loss, supply pressure or the pressure gradient. The discrepancy in mass flow is most likely due to the heating demand was not updated in TERMIS when the values were extracted, since the heating demand used in the Excel model is based on the heating demand informed by Aalborg Forsyning. The heating loss as well as the pressure gradient deviates significantly from what is calculated in the thesis. This indicates that the correct equations for calculating these are not used. This could also be true for the pressure drop but since the results does not deviate as much, it is uncertain what the error is. Based on the overall results from the calculated model it is possible to replicate some of the results from TERMIS and thereby the possibility of coupling these values into another energy modeling tool that can use these values in combination with a energy system. It is however necessary to correct the

equation used in this thesis regarding the calculation of the heating loss and the frictional pressure gradient.

The results regarding the temperature levels indicates that through a number of calculation it is possible to calculate the development of the temperature levels inside of a thermal energy storage, both in an isolated perspective and in a charging situation. This kind of calculation needs to be implemented in either an already existing energy modeling tool or in a new developed energy modeling tool. Energy modeling tools needs to be prepared for the challenges that comes with the planning and designing of the future energy system. The possibility to model and fully utilise the advantages that comes along by implementing a thermal energy storage must be a high criteria. If this becomes a reality then the energy system would be able to utilise the different temperature levels inside of the thermal energy storage. This would result in more optimisation possibilities as well as, different technologies can be valid booster options. This would create more flexibility in the operation strategy of the energy system.

The fact is that the future energy system will consist of a high share of fluctuating energy sources and in order to create an energy system that can manage the intermittency in energy production, the energy modeling tools for making it a reality must be ready.

Future research 9

The chapter will present the topics that is outside of the boundaries of this thesis, as well as what was not possible to implement in the thesis due to the time frame. The topics that will be mentioned could be relevant for further research in order to further investigate how to make one one coherent energy modeling tool.

In this thesis, two separate Excel models was made highlighting different areas, pipeline network in a district heating context, and the stratification of the temperature levels in a thermal energy storage. The model focusing on the stratification made it possible to start utilising different temperatures levels inside of the thermal energy storage, instead of only working with a fixed top and bottom temperature.

The intention of this thesis was to establish the basis for the combined model, therefore an optimisation of the case system have not been covered in this thesis. It would be interesting to see how the energy system would look like, when trying to optimise the energy system. The energy system is supplying the town of Vodskov with 60°C but the heat pump is supplying the thermal energy storage 80°C. The 80°C is mixed with the cold return water to reach 60.3°C in order to supply the consumers with 60°C. It would be interesting to see which temperature would be the most optimal temperature to supply Vodskov with, considering that the heat pump will continue to supply the system with 80°C water.

It would also be interesting to make a feasibility study and thereby optimise the energy system with that in mind. The heat pump could start using the heat from the middle of the thermal energy storage instead of the cold water at the bottom in order to increase the COP factor on the heat pump. This will have an effect on the stratification process in the thermal energy storage as well. One of the optimisation possibilities could be for the heat pump to determine when to use the temperature from the middle of the thermal energy storage and when it should use the temperature from the bottom of the thermal energy storage. This would properly be controlled by the electricity spot market prices, and what other renewable energy source is connected to the energy system.

Bibliography

- Aage B. Lauritsen, 2015.** et. al. Aage B. Lauritsen. *Varme staabi*. 7. Praxis - Nyt Teknisk Forlag, 2015. ISBN:978-87-571-2854-3.
- Aalborg Forsyning, 2019.** Aalborg Forsyning. *Interview and general information at internship, Michael*), 2019.
- Abdulrahman Dahash, 2019.** Michele Bianchi Janetti Wolfgang Streicher Abdulrahman Dahash, Fabian Ochs. *Advances in seasonal thermal energy storage for solar district heating applications: A critical review on large-scale hot-water tank and pit thermal energy storage systems*, 2019. URL <https://doi.org/10.1016/j.apenergy.2019.01.189>. Accessed: 26-03-2020.
- Aitkaliyev, 2017.** Bauyrzhan Aitkaliyev. *District Heating and Cooling Analysis*, 2017. URL <https://www.theseus.fi/handle/10024/129875>. Accessed: 14-05-2020.
- Anlæg, 2014.** Aktive Energi Anlæg. *Solvarmeanlæg til Dronninglund*, 2014. URL <https://aea.dk/portfolio-items/dronninglund-fjernvarmedamvarmelager/?fbclid=IwAR1733G5G6sI8GYSIZuehcYAFNaGgaHtizUW6JKt7Jow24p1tWmuYhsxkto>. Accessed: 18-05-2020.
- Arcon-Sunmark, 2019.** Arcon-Sunmark. *Sæsonlagring*. Intern information fra praktikophold, 2019.
- calculation blogspot, 2013.** Excel calculation blogspot. *Solving the Colebrook-White Equation with Excel*, 2013. URL <http://excelcalculations.blogspot.com/2011/04/solving-colebrook-white-equation-with.html>. Accessed: 29-05-2020.
- Christoph Bott, 2019.** Peter Bayer Christoph Bott, Ingo Dressel. *State-of-technology review of water-based closed seasonal thermal energy storage systems*, 2019. URL <https://doi.org/10.1016/j.rser.2019.06.048>. Accessed: 27-03-2020.
- Cruickshank, 2009.** Cynthia Ann Cruickshank. *Evaluation of a stratified multi-tank thermal storage for solar heating applications*, Queen's University, 2009.
- Electric, 2020.** Schneider Electric. *TERMIS Simulation Modes*, 2020. URL <http://7t.dk/products/termis/Product-Information/termis-simulation-modes.aspx>. Accessed: 14-05-2020.
- Energistyrelsen, 2019.** Energistyrelsen. *Basisfremskrivning 2019. Energi- og klimafremskrivning frem til 2030 under fravær af nye tiltag*, Energistyrelsen, 2019.
- Euroheat, 2016.** Euroheat. *Smart Energy Systems and 4th Generation District Heating*, 2016. URL <https://www.euroheat.org/events/other-events/2nd-international-conference-smart-energy-systems-4th-generation-district-heating/>. Accessed: 02-06-2020.

- Fjernvarme, 2020.** Dansk Fjernvarme. *Fjernvarmeselskaberne kan levere 44 procent af den nødvendige CO₂-reduktion i 2030*, 2020. URL <https://www.danskfjernvarme.dk/viden/groen-varme/gr%C3%B8n-varme-til-alle>. Accessed: 05-05-2020.
- Geoser, 2019.** Geoser. *Product information*, 2019. URL <https://www.environmental-expert.com/products/geoser-geonet-646864>. Accessed: 22-04-2020.
- Hegazy, 2007.** Adel. A Hegazy. *Effect of inlet design on the performance of storage-type domestic electrical water heaters*, 2007. URL <https://doi.org/10.1016/j.apenergy.2006.09.014>. Accessed: 03-04-2020.
- international, 2020.** EMD international. *Welcome to energyPRO*, 2020. URL <https://www.emd.dk/energypro/>. Accessed: 13-05-2020.
- Jensen, 2014.** Morten Vang Jensen. *Seasonal pit heat storages - Guidelines for materials & construction*, PlanEnergi, 2014.
- Klima, n.d.** Energi-og Forsyningsministeriet Klima. *Klimaindsatsen i Danmark*, n.d. URL <https://kefm.dk/klima-og-vejr/klimaindsatsen-i-danmark/>. Accessed: 05-05-2020.
- Lee, 2010.** Kun Sang Lee. *A review on Concepts, Applications, and Models of Aquifer Thermal Energy Storage Systems*, 2010. URL <https://doi.org/10.3390/en3061320>. Accessed: 01-04-2020.
- Li, 2015.** Gang Li. *Sensible heat thermal storage energy and exergy performance evaluations*, 2015. URL <https://doi.org/10.1016/j.rser.2015.09.006>. Accessed: 02-04-2020.
- Liang Zhang, 2015.** Jiachen Mao Xu Tang Zhengwei Li Jianguo Shi Liang Zhang, Peng Xu. *A low cost seasonal solar soil heat storage system for greenhouse heating: Design and pilot study*, 2015. URL <https://doi.org/10.1016/j.apenergy.2015.07.036>. Accessed: 01-04-2020.
- Martin Bloemendal, 2015.** Frans van de Ven Martin Bloemendal, Theo Olsthoorn. *Combining climatic and geo-hydrological preconditions as a method to determine world potential for aquifer thermal energy storage*, 2015. URL <https://doi.org/10.1016/j.scitotenv.2015.07.084>. Accessed: 01-04-2020.
- Newton, 1995.** Brian J. Newton. *Modeling of solar storage tanks*, University of Wisconsin-madison, 1995.
- Nina Kanstrup Kjaer, 2011.** Nina Kanstrup Kjaer. *Dataindsamling, Bearbejdning og Formidling*, 2011. URL <http://forlaget94.dk/cms/wp-content/uploads/F94-DOSAP-2013-K1-Prove2.pdf>. Accessed: 08-01-2020.
- Olesen, 2012.** Georgi K. Pavlov & Bjarne W. Olesen. *Thermal energy storage—A review of concepts and systems for heating and cooling applications in buildings: Part*

- 1—*Seasonal storage in the ground*, 2012. URL <https://www-tandfonline-com.zorac.aub.aau.dk/doi/full/10.1080/10789669.2012.667039>. Accessed: 01-04-2020.
- PlanEnergi, 2011.** NIRAS GG-Construction Teknologisk Institut SOLITES PlanEnergi, Dronninglund Fjernvarme. *SUNSTORE 3 - Fase 1 - Projektering og udbud*, 2011. URL https://energiteknologi.dk/sites/energiteknologi.dk/files/slutrappporter/slutrapport_incl._bilag_1_12042011_1824.pdf. Accessed: 18-05-2020.
- RegneRegler, n.d.** RegneRegler. *Rumfanget af en pyramidestub*, n.d. URL <https://www.regneregler.dk/pyramidestub-rumfang>. Accessed: 18-05-2020.
- Robert K. Yin, 2009.** Robert K. Yin. *Case Study Research: Design and Methods*, 2009. URL https://books.google.dk/books?id=FzawIAdilHkC&pg=PA24&hl=da&source=gbv_toc_r&cad=4#v=onepage&q&f=false. Accessed: 12-05-2020.
- Toolbox, n.d.** The Engineering Toolbox. *Thermal Conductivity of selected Materials and Gases*, n.d. URL https://www.engineeringtoolbox.com/thermal-conductivity-d_429.html. Accessed: 28-04-2020.
- Y. A. Cengel, 2012.** et. al. Y. A. Cengel. *Fundamentals of thermal-fluid sciences*. 4. McGraw-Hill, 2012. ISBN:978-007-132511-0.

Appendix A

A.1 Appendix A.1

Temperaturlag		1	2	3	4	5	6	7	8	9	10	11	12	13	14	15
	Døgn fra start															
Starttemperatur	0.0	80.0	80.0	80.0	80.0	80.0	80.0	80.0	40.0	40.0	40.0	40.0	40.0	40.0	40.0	40.0
	0.5	79.5	79.5	79.5	79.5	79.5	79.5	79.5	39.9	39.8	39.8	39.8	39.8	39.8	39.8	39.8
	1.0	79.1	79.1	79.1	79.1	79.1	79.1	79.0	39.7	39.6	39.6	39.6	39.6	39.6	39.6	39.6
	1.5	78.6	78.6	78.6	78.6	78.6	78.6	78.5	39.6	39.4	39.4	39.4	39.4	39.4	39.4	39.4
	2.0	78.2	78.2	78.2	78.2	78.2	78.2	77.9	39.4	39.2	39.2	39.2	39.2	39.2	39.2	39.2
	2.5	77.7	77.7	77.7	77.7	77.7	77.7	77.4	39.3	39.0	39.0	39.0	39.0	39.0	39.0	39.0
	3.0	77.3	77.3	77.3	77.3	77.3	77.3	76.9	39.1	38.8	38.8	38.8	38.8	38.8	38.8	38.8
	3.5	76.8	76.8	76.8	76.8	76.8	76.8	76.4	39.0	38.6	38.6	38.6	38.6	38.6	38.6	38.6
	4.0	76.4	76.4	76.4	76.4	76.4	76.4	76.0	38.8	38.4	38.4	38.4	38.4	38.4	38.4	38.4
	4.5	75.9	75.9	75.9	75.9	75.9	75.9	75.5	38.7	38.2	38.2	38.2	38.2	38.2	38.2	38.2
	5.0	75.5	75.5	75.5	75.5	75.5	75.5	75.0	38.5	38.0	38.0	38.0	38.0	38.0	38.0	38.0
	5.5	75.1	75.1	75.1	75.1	75.1	75.1	74.5	38.4	37.8	37.8	37.8	37.8	37.8	37.8	37.8
	6.0	74.6	74.6	74.6	74.6	74.6	74.6	74.0	38.2	37.6	37.6	37.6	37.6	37.6	37.6	37.6
	6.5	74.2	74.2	74.2	74.2	74.2	74.2	73.6	38.1	37.4	37.4	37.4	37.4	37.4	37.4	37.4
	7.0	73.8	73.8	73.8	73.8	73.8	73.8	73.1	38.0	37.2	37.2	37.2	37.2	37.2	37.2	37.2
	7.5	73.4	73.4	73.4	73.4	73.4	73.4	72.6	37.8	37.1	37.1	37.1	37.1	37.1	37.1	37.1
	8.0	73.0	73.0	73.0	73.0	73.0	72.9	72.2	37.7	36.9	36.9	36.9	36.9	36.9	36.9	36.9
	8.5	72.5	72.5	72.5	72.5	72.5	72.5	71.7	37.5	36.7	36.7	36.7	36.7	36.7	36.7	36.7
	9.0	72.1	72.1	72.1	72.1	72.1	72.1	71.2	37.4	36.5	36.5	36.5	36.5	36.5	36.5	36.5
	9.5	71.7	71.7	71.7	71.7	71.7	71.7	70.8	37.2	36.3	36.3	36.3	36.3	36.3	36.3	36.3
	10.0	71.3	71.3	71.3	71.3	71.3	71.3	70.3	37.1	36.1	36.1	36.1	36.1	36.1	36.1	36.1
	10.5	70.9	70.9	70.9	70.9	70.9	70.9	69.9	37.0	36.0	36.0	36.0	36.0	36.0	36.0	36.0
	11.0	70.5	70.5	70.5	70.5	70.5	70.5	69.4	36.8	35.8	35.8	35.8	35.8	35.8	35.8	35.8
	11.5	70.1	70.1	70.1	70.1	70.1	70.1	69.0	36.7	35.6	35.6	35.6	35.6	35.6	35.6	35.6
	12.0	69.7	69.7	69.7	69.7	69.7	69.7	68.6	36.5	35.4	35.4	35.4	35.4	35.4	35.4	35.4
	12.5	69.3	69.3	69.3	69.3	69.3	69.3	68.1	36.4	35.3	35.2	35.2	35.2	35.2	35.2	35.2
	13.0	68.9	68.9	68.9	68.9	68.9	68.9	67.7	36.3	35.1	35.1	35.1	35.1	35.1	35.1	35.1
	13.5	68.5	68.5	68.5	68.5	68.5	68.5	67.3	36.1	34.9	34.9	34.9	34.9	34.9	34.9	34.9

Figure A.1: The temperature levels in the beginning of the half-yearly calculation.

168.0	16.3	16.3	16.3	16.3	16.2	16.0	15.1	12.9	11.9	11.7	11.7	11.7	11.7	11.7	11.7	11.7
168.5	16.2	16.2	16.2	16.2	16.2	16.0	15.0	12.9	11.9	11.7	11.7	11.7	11.7	11.7	11.7	11.7
169.0	16.2	16.2	16.2	16.2	16.1	15.9	15.0	12.8	11.9	11.7	11.6	11.6	11.6	11.6	11.6	11.6
169.5	16.1	16.1	16.1	16.1	16.1	15.9	14.9	12.8	11.9	11.7	11.6	11.6	11.6	11.6	11.6	11.6
170.0	16.1	16.1	16.1	16.1	16.0	15.8	14.9	12.8	11.8	11.6	11.6	11.6	11.6	11.6	11.6	11.6
170.5	16.0	16.0	16.0	16.0	16.0	15.8	14.8	12.7	11.8	11.6	11.6	11.6	11.6	11.6	11.6	11.6
171.0	16.0	16.0	16.0	16.0	15.9	15.7	14.8	12.7	11.8	11.6	11.5	11.5	11.5	11.5	11.5	11.5
171.5	15.9	15.9	15.9	15.9	15.9	15.7	14.8	12.7	11.8	11.6	11.5	11.5	11.5	11.5	11.5	11.5
172.0	15.9	15.9	15.9	15.9	15.8	15.6	14.7	12.7	11.8	11.5	11.5	11.5	11.5	11.5	11.5	11.5
172.5	15.8	15.8	15.8	15.8	15.8	15.6	14.7	12.6	11.7	11.5	11.5	11.5	11.5	11.5	11.5	11.5
173.0	15.8	15.8	15.8	15.8	15.7	15.5	14.6	12.6	11.7	11.5	11.5	11.5	11.5	11.5	11.5	11.5
173.5	15.7	15.7	15.7	15.7	15.7	15.5	14.6	12.6	11.7	11.5	11.4	11.4	11.4	11.4	11.4	11.4
174.0	15.7	15.7	15.7	15.7	15.6	15.4	14.5	12.5	11.7	11.4	11.4	11.4	11.4	11.4	11.4	11.4
174.5	15.6	15.6	15.6	15.6	15.6	15.4	14.5	12.5	11.6	11.4	11.4	11.4	11.4	11.4	11.4	11.4
175.0	15.6	15.6	15.6	15.6	15.5	15.3	14.4	12.5	11.6	11.4	11.4	11.4	11.4	11.4	11.4	11.4
175.5	15.5	15.5	15.5	15.5	15.5	15.3	14.4	12.5	11.6	11.4	11.3	11.3	11.3	11.3	11.3	11.3
176.0	15.5	15.5	15.5	15.5	15.4	15.2	14.4	12.4	11.6	11.4	11.3	11.3	11.3	11.3	11.3	11.3
176.5	15.4	15.4	15.4	15.4	15.4	15.2	14.3	12.4	11.5	11.3	11.3	11.3	11.3	11.3	11.3	11.3
177.0	15.4	15.4	15.4	15.4	15.3	15.1	14.3	12.4	11.5	11.3	11.3	11.3	11.3	11.3	11.3	11.3
177.5	15.3	15.3	15.3	15.3	15.3	15.1	14.2	12.4	11.5	11.3	11.3	11.3	11.3	11.3	11.3	11.3
178.0	15.3	15.3	15.3	15.3	15.2	15.0	14.2	12.3	11.5	11.3	11.2	11.2	11.2	11.2	11.2	11.2
178.5	15.2	15.2	15.2	15.2	15.2	15.0	14.1	12.3	11.5	11.3	11.2	11.2	11.2	11.2	11.2	11.2
179.0	15.2	15.2	15.2	15.2	15.2	14.9	14.1	12.3	11.4	11.2	11.2	11.2	11.2	11.2	11.2	11.2
179.5	15.1	15.1	15.1	15.1	15.1	14.9	14.1	12.3	11.4	11.2	11.2	11.2	11.2	11.2	11.2	11.2
180.0	15.1	15.1	15.1	15.1	15.1	14.9	14.0	12.2	11.4	11.2	11.2	11.2	11.2	11.2	11.2	11.2
180.5	15.1	15.1	15.1	15.0	15.0	14.8	14.0	12.2	11.4	11.2	11.1	11.1	11.1	11.1	11.1	11.1
181.0	15.0	15.0	15.0	15.0	15.0	14.8	13.9	12.2	11.4	11.2	11.1	11.1	11.1	11.1	11.1	11.1
181.5	15.0	15.0	15.0	15.0	14.9	14.7	13.9	12.1	11.3	11.1	11.1	11.1	11.1	11.1	11.1	11.1
182.0	14.9	14.9	14.9	14.9	14.9	14.7	13.9	12.1	11.3	11.1	11.1	11.1	11.1	11.1	11.1	11.1
182.5	14.9	14.9	14.9	14.9	14.8	14.6	13.8	12.1	11.3	11.1	11.1	11.1	11.1	11.1	11.1	11.1

Figure A.2: The temperature levels at the end of the half-yearly calculation.

The temperature levels between the beginning and the end of the half-yearly calculation can be found in the subjoined ZIP-files in the Excel document called: Løsning af lager differentiaaligningen, in the tab called: Temperatur (uden flow).

A.2 Appendix A.2

		Heat loss	frictionsgradient	Temperature supply		Temperature Return	supply pressure	velocity	Mass flow
Time/hour	pipe	W/m	Pa/m	°C	°C		mvs	m/s	kg/s
1	1	14,00	5,91	60,18	34,97		83,70	0,54	40,44
	2	12,32	14,03	60,11	34,99		77,15	0,76	40,44
	3	11,53	19,84	60,00	35,00		76,37	0,71	13,94
	4	12,35	6,00	60,11	35,00		76,90	0,50	26,50
2	1	14,00	5,91	60,18	34,97		83,70	0,54	40,44
	2	12,32	14,03	60,11	34,99		77,15	0,76	40,44
	3	11,53	19,84	60,00	35,00		76,37	0,71	13,94
	4	12,35	6,00	60,11	35,00		76,90	0,50	26,50
3	1	14,00	5,91	60,18	34,97		83,70	0,54	40,44
	2	12,32	14,03	60,11	34,99		77,15	0,76	40,44
	3	11,53	19,84	60,00	35,00		76,37	0,71	13,94
	4	12,35	6,00	60,11	35,00		76,90	0,50	26,50
4	1	14,00	5,91	60,18	34,97		83,70	0,54	40,44
	2	12,32	14,03	60,11	34,99		77,15	0,76	40,44
	3	11,53	19,84	60,00	35,00		76,37	0,71	13,94
	4	12,35	6,00	60,11	35,00		76,90	0,50	26,50
5	1	14,00	5,91	60,18	34,97		83,70	0,54	40,44
	2	12,32	14,03	60,11	34,99		77,15	0,76	40,44
	3	11,53	19,84	60,00	35,00		76,37	0,71	13,94
	4	12,35	6,00	60,11	35,00		76,90	0,50	26,50
6	1	14,01	3,78	60,23	34,96		83,70	0,43	32,36
	2	12,33	8,98	60,14	34,98		77,88	0,61	32,36
	3	11,54	12,70	60,00	35,00		77,51	0,57	11,15
	4	12,36	3,84	60,14	35,00		77,63	0,40	21,21
7	1	14,01	3,78	60,23	34,96		83,70	0,43	32,36
	2	12,33	8,98	60,14	34,98		77,88	0,61	32,36
	3	11,54	12,70	60,00	35,00		77,51	0,57	11,15
	4	12,36	3,84	60,14	35,00		77,63	0,40	21,21
8	1	14,01	3,78	60,23	34,96		83,70	0,43	32,36
	2	12,33	8,98	60,14	34,98		77,88	0,61	32,36
	3	11,54	12,70	60,00	35,00		77,51	0,57	11,15
	4	12,36	3,84	60,14	35,00		77,63	0,40	21,21

Figure A.3

9	1	14,01	3,78	60,23	34,96	83,70	0,43	32,36
	2	12,33	8,98	60,14	34,98	77,88	0,61	32,36
	3	11,54	12,70	60,00	35,00	77,51	0,57	11,15
	4	12,36	3,84	60,14	35,00	77,63	0,40	21,21
10	1	14,01	3,78	60,23	34,96	83,70	0,43	32,36
	2	12,33	8,98	60,14	34,98	77,88	0,61	32,36
	3	11,54	12,70	60,00	35,00	77,51	0,57	11,15
	4	12,36	3,84	60,14	35,00	77,63	0,40	21,21
11	1	14,01	3,78	60,23	34,96	83,70	0,43	32,36
	2	12,33	8,98	60,14	34,98	77,88	0,61	32,36
	3	11,54	12,70	60,00	35,00	77,51	0,57	11,15
	4	12,36	3,84	60,14	35,00	77,63	0,40	21,21
12	1	14,00	5,08	60,20	34,97	83,70	0,50	37,51
	2	12,32	12,07	60,12	34,99	77,43	0,71	37,51
	3	11,53	17,06	60,00	35,00	76,81	0,66	12,93
	4	12,35	5,16	60,12	35,00	77,18	0,46	24,58
13	1	14,00	5,08	60,20	34,97	83,70	0,50	37,51
	2	12,32	12,07	60,12	34,99	77,43	0,71	37,51
	3	11,53	17,06	60,00	35,00	76,81	0,66	12,93
	4	12,35	5,16	60,12	35,00	77,18	0,46	24,58
14	1	14,00	5,08	60,20	34,97	83,70	0,50	37,51
	2	12,32	12,07	60,12	34,99	77,43	0,71	37,51
	3	11,53	17,06	60,00	35,00	76,81	0,66	12,93
	4	12,35	5,16	60,12	35,00	77,18	0,46	24,58
15	1	14,00	5,08	60,20	34,97	83,70	0,50	37,51
	2	12,32	12,07	60,12	34,99	77,43	0,71	37,51
	3	11,53	17,06	60,00	35,00	76,81	0,66	12,93
	4	12,35	5,16	60,12	35,00	77,18	0,46	24,58
16	1	14,00	5,08	60,20	34,97	83,70	0,50	37,51
	2	12,32	12,07	60,12	34,99	77,43	0,71	37,51
	3	11,53	17,06	60,00	35,00	76,81	0,66	12,93
	4	12,35	5,16	60,12	35,00	77,18	0,46	24,58
17	1	14,00	5,08	60,20	34,97	83,70	0,50	37,51
	2	12,32	12,07	60,12	34,99	77,43	0,71	37,51
	3	11,53	17,06	60,00	35,00	76,81	0,66	12,93
	4	12,35	5,16	60,12	35,00	77,18	0,46	24,58

Figure A.4

18	1	14,00	7,94	60,16	34,97	83,70	0,62	46,88
	2	12,32	18,85	60,10	34,99	76,46	0,88	46,88
	3	11,53	26,65	60,00	35,00	75,28	0,82	16,16
	4	12,35	8,06	60,10	35,00	76,21	0,58	30,72
19	1	14,00	7,94	60,16	34,97	83,70	0,62	46,88
	2	12,32	18,85	60,10	34,99	76,46	0,88	46,88
	3	11,53	26,65	60,00	35,00	75,28	0,82	16,16
	4	12,35	8,06	60,10	35,00	76,21	0,58	30,72
20	1	14,00	7,94	60,16	34,97	83,70	0,62	46,88
	2	12,32	18,85	60,10	34,99	76,46	0,88	46,88
	3	11,53	26,65	60,00	35,00	75,28	0,82	16,16
	4	12,35	8,06	60,10	35,00	76,21	0,58	30,72
21	1	14,00	7,94	60,16	34,97	83,70	0,62	46,88
	2	12,32	18,85	60,10	34,99	76,46	0,88	46,88
	3	11,53	26,65	60,00	35,00	75,28	0,82	16,16
	4	12,35	8,06	60,10	35,00	76,21	0,58	30,72
22	1	14,00	7,94	60,16	34,97	83,70	0,62	46,88
	2	12,32	18,85	60,10	34,99	76,46	0,88	46,88
	3	11,53	26,65	60,00	35,00	75,28	0,82	16,16
	4	12,35	8,06	60,10	35,00	76,21	0,58	30,72
23	1	14,00	7,94	60,16	34,97	83,70	0,62	46,88
	2	12,32	18,85	60,10	34,99	76,46	0,88	46,88
	3	11,53	26,65	60,00	35,00	75,28	0,82	16,16
	4	12,35	8,06	60,10	35,00	76,21	0,58	30,72
24	1	14,00	7,94	60,16	34,97	83,70	0,62	46,88
	2	12,32	18,85	60,10	34,99	76,46	0,88	46,88
	3	11,53	26,65	60,00	35,00	75,28	0,82	16,16
	4	12,35	8,06	60,10	35,00	76,21	0,58	30,72
25	1	14,00	7,94	60,16	34,97	83,70	0,62	46,88
	2	12,32	18,85	60,10	34,99	76,46	0,88	46,88
	3	11,53	26,65	60,00	35,00	75,28	0,82	16,16
	4	12,35	8,06	60,10	35,00	76,21	0,58	30,72
26	1	14,00	7,94	60,16	34,97	83,70	0,62	46,88
	2	12,32	18,85	60,10	34,99	76,46	0,88	46,88
	3	11,53	26,65	60,00	35,00	75,28	0,82	16,16
	4	12,35	8,06	60,10	35,00	76,21	0,58	30,72

Figure A.5

A.3 Appendix A.3

Disclaimer fra Studieleder og Studienævnsmænd

Corona og dets konsekvens med nedlukning af universitetet siden 13 marts 2020 har selvsagt haft indflydelse på hvilke aktiviteter det har været mulige at igangsætte og udføre som en del af projektarbejdet. Konkret har det ikke været muligt at udføre aktiviteter der ikke har kunnet foregå online, dvs. følgende aktiviteter har ikke været mulige: værkstedsaktiviteter, opmålingsaktiviteter, on-site etnografiske studier eller inddragelsesaktiviteter on-site. Ved bedømmelse af projekter i forårssemestret 2020 bedes dette tages i betragtning.

Herefter tilføjes de studerendes egne refleksioner på hvilke udfordringer Corona har haft for deres projekt, samt hvordan de har imødekommet dem.

Corona nedlukningen har haft visse indflydelser på vores projekt. Dette har blandt andet haft en indflydelse på nøjagtigheden af vores beregninger, hvir vi skulle eftervise resultaterne fra TERMIS. Efter nedlukningen har det ikke længere været muligt at komme ud på Aalborg Forsyning, hvor TERMIS licens filerne er. Det betyder at det ikke har været muligt at indhente flere data end hvad vi allerede havde indhentet inden nedlukningen. De allerede indhentede data var dog nok til at lave en nogenlunde fyldestgørende validering af resultaterne, men på en bekostning af tiden brugt derpå. Havde det været muligt stadig at

kunne anvende TERMIS havde vi bedre og hurtigere kunne fremskaffe de nødvendige data samt data som ville have været 'nice-to-have'. I forbindelse med validering af TERMIS beregninger har det været nødvendigt at tilegne sig kendskab til fjernvarmerør og dets egenskaber, her havde vi et tiftigt møde med Logstor sammen med vores vejleder hvor vi luftede tanken om de ville være sparringspartner i denne henseende samt vi kunne komme ned og besøge virksomheden og få en rundtur hvor vi skulle se og snakke om fjernvarmerørene, hvilket de gerne ville. Efter nedlukningen har Logstor blandt andet været nødsaget til at prioritere deres egne arbejdsopgaver og ikke haft ressourcer til hverken virksomheds besøg eller sparring omkring hvordan de beregner varmetab i rørene eller hvordan de beregner friktionsgradienten. Varmetabet samt friktionsgradienten er nogle af de værdier som vi ikke har kunne beregne tilfredsstillende sammenlignet med værdierne fra TERMIS. Hvis ikke nedlukningen havde været en spillende faktor så havde vi haft de rigtigt forudsætninger for at kunne beregne disse korrekt. Ligeledes havde det været muligt at tilegne os konkret viden fra Logstor eller Aalborg Forsyning omkring godstykkelser på rørene, og om hvordan disse tages i betragtning når der beregnes på rørene. Vi brugte lang tid på at analysere hvorfor vores resultater var forskellige i forhold til TERMIS. Vi afprøvede i sidste ende at fratrække godstykkelsen på diameteren på røret, hvilket gav os nogle sammenlignelige resultater med TERMIS. Vi erfarede ud fra dette at selvom størrelsen på rørene er opgivet som Ø273, så er det ikke en diameter som man kan bruge direkte i sine beregninger da godstykkelsen på røret skal trækkes fra først. Dette tog lang tid at gennemskue, og ville være noget vi kunne have forhindret ved at have haft mulighed for at anvende Logstor som sparringspartner. Ydermere skulle vi have haft et møde med Danfoss sammen med de ansatte som arbejde med det nye Energis. Nogle af disse personer har været med til at udvikle TERMIS programmet og de kunne have været med til at give os et bedre indblik i, hvilke formler TERMIS anvender samt hvilke forudsætninger TERMIS tager i betragtning når den laver net modellen. Udover dette var det også planen at vi skulle lave den samme beregning for Rærup til Vodskov i Energis som vi har lavet i TERMIS, og også eftervise resultaterne fra Energis med vores Excel model.

Corona nedlukningen har betydet at vores processer har taget meget længere tid i forhold til hvad det burde have taget, hvis vi havde haft de forudsætninger som vi havde sat os i begyndelsen af projekt perioden. Vi har ikke kunne nå at lave alt det arbejde som vi ville grundet den ekstra tid brugt på at analysere hvorfor vores model ikke gav de samme resultater som TERMIS. Som nævnt tidligere dette kunne vi mere eller mindre have undgået hvis vi havde haft muligheden for at fortsætte det tætte samarbejde med Aalborg Forsyning samt samarbejdet med Logstor. Dette har resulteret i at den endelige sammenkobling af vores model ikke er lige så kompleks og dynamisk som først planlagt. Vi har forsøgt at anvende tiden bedst muligt og arbejdet under de forudsætninger og begrænsninger som denne nedlukning forårsagede, hvilket har betydet en mere forsimplet model og flere antagelser.

Udover de mere projekt relaterede problematikker har nedlukningen også haft en effekt på hvordan det har været muligt at udføre gruppearbejde. Grundet nedlukningen har det ikke været tilladt for de studerende at sidde sammen og lave gruppearbejde og ligeledes fraråede Staten befolkningen om at omgås andre end dem fra egen husholdning. Dette har betydet at vi har skulle arbejde hver for sig og kun komminkere via digitale medier, hvilket er noget af en anderledes arbejdsgang end den ellers vante arbejdsgang med fysisk

tilstedeværelse og sparring. Der må derfor også tilskrives en hvis faktor for forstyrrelse i ens eget hjem da forudsætninger for ens arbejde ikke kan være det samme som når man sidde på lokalerne som står til de studerendes rådighed af universitetet.